CHALMERS
UNIVERSITY OF TECHNOLOGY

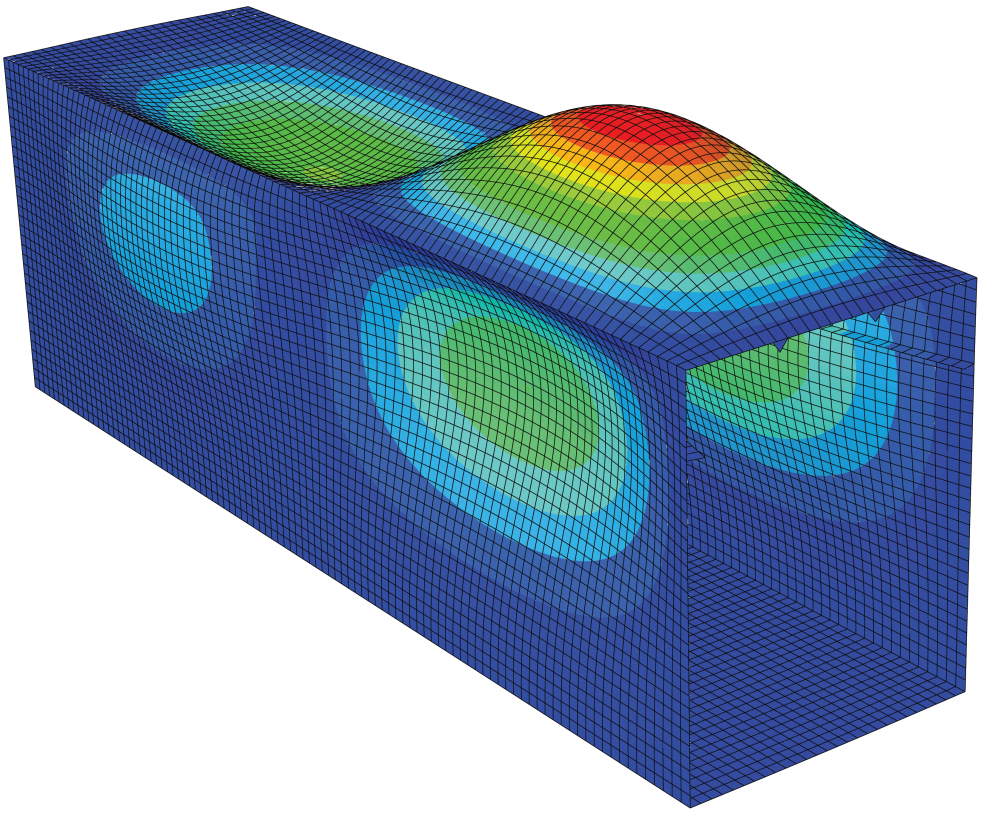

Steel Design of Plated Structural Elements

A comparison of the effective width method and the reduced stress method

Master's thesis in Master Programme Structural Engineering and Building Technology

JOHAN AHLSTRAND

ELLEN JOHANSSON

DEPARTMENT OF ARCHITECTURE AND CIVIL ENGINEERING

CHALMERS UNIVERSITY OF TECHNOLOGY
Gothenburg, Sweden 2021
www.chalmers.se

Master's thesis ACEX30

Steel Design of Plated Structural Elements

A comparison of the effective width method and the reduced stress method

JOHAN AHLSTRAND

ELLEN JOHANSSON

CHALMERS
UNIVERSITY OF TECHNOLOGY

Department of Architecture and Civil Engineering
Division of Structural Engineering
Lightweight Structures
Chalmers University of Technology
Gothenburg, Sweden 2021

Steel Design of Plated Structural Elements
A comparison of the effective width method and the reduced stress method
JOHAN AHLSTRAND
ELLEN JOHANSSON

Examensarbete ACEX30
Instutitionen för arkitektur och samhällsbyggnadsteknik
Chalmers tekniska högskola, 2021

Department of Architecture and Civil Engineering
Division of Structural Engineering
Lightweight Structures
Chalmers University of Technology
SE-412 96 Gothenburg
Telephone +46 31 772 1000

Cover: A 3D model of one geometric beam section that is analysed in the parametric study.

Typeset in LaTeX
Department of Architecture and Civil Engineering
Gothenburg, Sweden 2021

Steel Design of Plated Structural Elements
A comparison of the effective width method and the reduced stress method
JOHAN AHLSTRAND
ELLEN JOHANSSON
Department of Architecture and Civil Engineering
Chalmers University of Technology

Abstract

There are two methods described in Eurocode 1993-1-5 that are used for capacity controls on members in cross-section class 4. The methods are called *the effective width method* and *the reduced stress method*. The aim of this thesis is to investigate if the capacity varies depending on which of the two methods is used and see in what design situation one or the other method provide a higher capacity.

A parametric study of two box-beam sections is performed. The beams are a longitudinally stiffened box beam and an unstiffened box beam, where the height and width are kept constant as the thicknesses of the web and flange vary as well as the distance between transverse stiffeners. All variations of the two box beams are investigated with both methods from Eurocode 1993-1-5 and three different loading combinations. The loading situations on the beams are either solely moment or shear force or a combination of both moment and shear force. An FE-analysis is performed to obtain the buckling mode which is used in the calculations of the reduced stress method.

The results show that the reduced stress method is generally more conservative than the effective width method. However, there are a few geometric variations and loading situations where the reduced stress method results in a higher capacity. A low slenderness difference between flange and web yields a higher capacity for the reduced stress method and for an unstiffened beam and for a stiffened beam there are a lot of factors that impact the capacity when solely moment is considered. The lack of stress redistribution in the reduced stress method is a big disadvantage in order for it to result in the same capacity as the effective width method.

Keywords: Effective width method, Reduced stress method, Longitudinal stiffeners, Steel plates, Eurocode 1993-1-5, Finite Element Method

Design av plåtbalkar
En jämförelse av effektiva tvärsnittsmetoden och reducerade spänningsmetoden
JOHAN AHLSTRAND
ELLEN JOHANSSON
Instutitionen för arkitektur och samhällsbyggnad
Chalmers tekniska högskola

Sammanfattning

Det finns två metoder i Eurocode 1993-1-5 som beskriver hur kapaciteten beräknas för plåtbalkar i tvärsnittsklass 4, det är den *effektiva tvärsnittsmetoden* och den *reducerade spänningsmetoden*. Syftet med det här arbetet är att undersöka om och hur kapaciteten av plåtbalkar varierar beroende på vilken av de två metoderna som används samt att se i vilka designsituationer som den ena eller andra metoden ger en högre kapacitet.

En parametrisering av två lådbalksegment utförs. Det ena balksegmentet är avstyvat i längsgående riktning och det andra är oavstyvat. Höjden och bredden av tvärsnittet hålls konstant och det är liv- och flänstjocklekarna som varierar samt längden på segmentet mellan två vertikala avstyvningar. Alla kombinationer av geometrier och tre olika lastfall studeras med hjälp av de två metoderna. Lastfallen som undersöks är bara tvärkraft, bara moment och en kombination av de två. En FE-analys har gjorts för att få fram bucklingsmoden som används i beräkningarna för den reducerade spänningsmetoden.

Resultaten visar att den reducerade spänningsmetoden generellt sett är mer konservativ än den effektiva tvärsnittsmetoden. Det finns geometrier och lastkombinationer som resulterar i en högre kapacitet för den reducerade spänningsmetoden. En låg skillnad mellan slankheten av flänsen och livet ger en högre kapacitet för den reducerade spänningsmetoden för en oavstyvad plåtbalk och för en avstyvad plåtbalk är det många faktorer som påverkar kapaciteten när endast moment är beaktat. Att inte kunna omfördela krafter mellan plåtfälten är i slutändan en stor nackdel för den reducerade tvärsnittsmetoden för att kunna ge lika bra kapacitet som den effektiva tvärsnittsmetoden.

Nyckelord: Effektiva tvärsnittsmetoden, reducerade spänningsmetoden, längsgående avstyvare, stålplåt, Eurocode 1993-1-5, finita elementmetoden

Acknowledgements

This Master's Thesis was performed in order to compare, understand and see in what design situation which of the two methods described in Eurocode 1993-1-5, for assessing the buckling capacity of thin-walled steel plates, yields higher capacity. The thesis was written during the spring of 2021 and the project was carried out at the Division of Structural Engineering and Building Technology at Chalmers University of Technology.

We would like to thank our supervisor Emanuel Trolin at Norconsult for his great guidance and support during the whole project. We would also like to thank Mozhdeh Amani for her feedback and help. Finally, a big thank you goes out to our examiner Mohammad Al-Emrani for his valuable feedback.

Johan Ahlstrand & Ellen Johansson, Gothenburg, June 2021

Contents

List of Figures

List of Tables

Nomenclature

Lowercase greek letters

α	Aspect ratio [-]
α_e	Imperfection factor [-]
α_{cr}	Critical load amplifier [-]
$\alpha_{ult.k}$	Ultimate load amplifier [-]
$\bar{\eta}_1$	Utilisation factor of the plastic moment [-]
$\bar{\eta}_3$	Utilisation factor of the web for shear [-]
$\bar{\lambda}_c$	Relative column slenderness [-]
$\bar{\lambda}_p$	Relative plate slenderness [-]
$\bar{\lambda}_w$	Shear panel slenderness [-]
$\beta_{A.c}$	Ratio between local effective area and gross area [-]
χ_c	Column reduction factor [-]
χ_v	Shear reduction factor [-]
χ_w	Contribution from the web to the shear buckling resistance [-]
η	Factor [-]
η_1	Utilisation factor for normal force and moment [-]
η_3	Utilisation factor for shear [-]
γ_{M0}	Factor [-]
γ_{M1}	Factor [-]
ν	Poisson's ratio [-]
ϕ	Angle between shear stress field and x-axis [deg]
ψ	Stress ratio [-]
ρ	Reduction factor for plate buckling [-]
ρ_c	Global reduction factor [-]
$\sigma_{cr.c}$	Critical column stress [MPa]
$\sigma_{cr.p}$	Critical plate buckling stress [MPa]
$\sigma_{cr.sl.c}$	Critical column stress at stiffener's level [MPa]
$\sigma_{cr.sl.p}$	Critical plate buckling stress at stiffener's level [MPa]
$\sigma_{cr.sl}$	Critical stress at stiffener's level [MPa]
$\sigma_{x.Ed}$	Design stress in longitudinal direction [MPa]
$\sigma_{z.Ed}$	Design stress in transverse direction [MPa]
τ	Shear stress [MPa]
τ_u	Ultimate shear resistance [MPa]
τ_{cr}	Critical elastic shear buckling stress [MPa]
τ_{cr}	Critical shear buckling stress [MPa]
τ_{Ed}	Design shear stress [MPa]
ε	Strain [-]
φ	Factor [-]
ξ	Weighting factor for plate and column-like buckling [-]

Uppercase latin letters

A_c	Gross area in the compression

zone [m^2]

$A_{c.eff.loc}$ Effective area of one longitudinal stiffener and adjacent subpanels [m^2]

$A_{c.eff}$ Effective area in the compression zone [m^2]

$A_{sl.1}$ Area of one longitudinal stiffener and adjacent subpanels' area [m^2]

E Modulus of elasticity [GPa]

G Shear modulus [GPa]

I Moment of inertia [m^4]

$I_{sl.1}$ Moment of inertia of one longitudinal stiffener and adjacent subpanels [m^4]

M_{el} Elastic moment [Nm]

$M_{f.Rd}$ Moment resistance in flange [Nm]

M_{pl} Plastic moment [Nm]

P_{cr} Critical buckling load of a column [N]

S First moment of area [m^3]

U Utilisation in the reduced stress method [-]

$V_{b.Rd}$ Total shear resistance [N]

$V_{bw.Rd}$ Shear resistance in web [N]

W_{eff} Effective elastic section modulus [m^3]

N Normal force [N]

Lowercase latin letters

$\bar{b}$ Width of member according to Eurocode 1993-1-1 Table 5.2 or distance from stiffener to the neutral axis [m]

a Length of a plate or distance between transverse stiffeners [m]

a_c Factor [m]

b_1 Distance from the top of a fictive column to the buckle [m]

b_2 Distance from the bottom of a fictive column to the buckle [m]

b_c Height of the compression zone [m]

b_f Width of flange [m]

$b_{edge.eff}$ Effective width of the edge part of a subpanel [m]

b_{edge} Width of edge part of a subpanel [m]

b_{eff} Effective width [m]

$b_{inf.eff}$ Effective width of a subpanel adjacent to and above a stiffener [m]

b_{inf} Width of a subpanel adjacent to and above a stiffener [m]

$b_{sup.eff}$ Effective width of a subpanel adjacent to and below a stiffener [m]

b_{sup} Width of a subpanel adjacent to and below a stiffener [m]

e Largest distance from the respective centroids pf the plate or stiffener to the neutral axis of the effective column [m]

f_y Yield stress [MPa]

h_w Height of the web [m]

h_{sl} Length of stiffener [m]

i Radius of gyration [m]

k_σ Buckling coefficient due to normal stresses [-]

k_τ Buckling coefficient due to shear stresses [-]

$k_{\tau.st}$ Shear buckling coefficient for the stiffener [-]

t_f Thickness of flange [m]

t_w Thickness of web [m]

t_{sl} Thickness of stiffener [m]

x_{tp} Centre of gravity [m]

1

Introduction

In today's society every new construction aims to be as material efficient as possible. For this to be possible the designing engineer needs to have knowledge on which method is suitable to use for the structural calculations. In steel structure design, there are two methods described in Eurocode 1993-1-5 for designing thin-walled steel plates. Both methods described can be used to design plate elements but there is no indication in Eurocode 1993-1-5 on when one method results in too conservative values. The decision on which method that is used is mainly dependant on the country's national guidelines, personal preferences of the designer and how the finite element model is constructed.

This thesis examines whether there are any differences in the results depending on which method is used. If there are any clear scenarios when one method yields less conservative results compared to the other in terms of utilisation for loads such as bending moment and shear force and geometry of the cross-section is examined.

1.1 Background

The design of thin steel plates in Europe is performed with Eurocode 1993-1-5. The standard includes two different design procedures for assessing the capacity regarding the local buckling of thin plates. The two methods that are used to determine the capacity are the *effective width method* and the *reduced stress method*. Both methods reduce the capacity with respect to buckling if the structural member is in cross-section class 4 (CSC4). If a member is in CSC4, local elastic buckling can occur for forces corresponding to less than the elastic limit. In order to consider this buckling effect, the members are modified to be regarded as having a lower cross-section class. This is done by reducing the area or stresses that have an impact of the capacity for the two methods respectively.

The effective width method reduces the cross-sectional area that is used in calculations and thus the capacity for the cross-section is decreased. For the reduced stress method, the maximum allowable stress is put to the lowest critical buckling stress in the whole section and this stress is used to calculate the capacity of the structure.

Different countries are used to different methods. In Sweden the effective width

method is the most common method. Boverket (Boverkets Författningssamling, 2011, p. 88) even recommends in *Boverkets föreskrifter och allmänna råd om tillämpning av europeiska konstruktionsstandarder (2011:10)* that the reduced stress method should not be used in Swedish structural engineering design. However, it is still used in other European countries, mainly in Germany and Austria (Kuhlmann et al., 2021, p. 9). Why Sweden do not use the reduced stress method is unclear.

The company *Norconsult* have during the last few years used the reduced stress method when constructing large complex box girder bridges in Norway. However, when performing a finite element method (FEM) buckling analysis on larger structures it has been noted that the obtained buckling strength differs compared to hand calculations with varying transverse stiffener spacing. Transverse stiffeners are used to increase the stability against buckling in the longitudinal direction of the beam by placing them in the span to reduce the buckling length. The variations that were noted were that at a certain interception point the buckling strength increases with a longer distance between transverse stiffeners in the FEM buckling analysis, which does not correspond to the theory in Eurocode where the strength only decreases with increasing distance between vertical stiffeners.

Since material efficiency is an important criterion in the construction industry, it is important to realise the advantages and disadvantages of the two methods. With an indication of when one method results in less conservative values compared to the other it yields an efficient material use while still achieving all the safety requirements.

1.2 Aim and objectives

The main aim of this Master's Thesis is to understand and see in what design situation which of the two methods, effective width method and reduced stress method, yields higher capacity so the design can be as efficient as possible.

The objectives to fulfil the aims are:

- Perform a parametric study of a box beam
- Compare the effective width method with the reduced stress method for a parametrised box beam
- Analyse the influence of the distance between two transverse stiffeners

1.3 Limitations

- The Master's Thesis will be limited to Eurocode 1993-1-5: Plated structural elements.
- Geometric limitation is limited to a section of a box beam between two trans-

verse stiffeners. The section can have longitudinal stiffeners in both the upper flange and the webs. Complex geometries are not considered. This is done to better focus the Master's Thesis towards the comparisons of the different methods and parametrisation.

- Only welded sections are regarded since the focus is on cross-sections for larger structures where rolled sections are not as common.
- Different cross-sections are analysed, where the thicknesses and length of the members vary, and the longitudinal stiffeners' position and proportion are kept constant.
- The forces acting on the section are limited to shear force and bending moment. They are acting on the section simultaneously and with alternating magnitudes for different analyses. No transverse forces are assumed to act on the section.

1.4 Method

The project is divided into a literature part and a calculation part using the theory gathered to better understand the calculations. In the literature part Eurocode 1993-1-5 is examined. The differences between the effective width method and the reduced stress method are thoroughly investigated.

Thereafter parametrised hand calculation for the effective width method is performed using Mathcad. This is done for a few different parametrised cross-sections. The cross-section has longitudinal stiffeners with set positions in the upper flange and the webs. A cross-section containing no longitudinal stiffeners is also studied.

The next step is to perform FE-modelling with parametrisation to receive the critical buckling load, with respect to shear and normal stresses, that is used in the reduced stress method. This is done for the same cross-sections as the hand calculations in the effective width method. The FE-model is computed as individual parts, web and flange, and made as 2D panels for the parametric study. A 3D beam section between two transverse stiffeners is also modelled for one specific case.

When the FE-analysis is completed, hand calculations are performed using the buckling mode obtained from the FE-analysis to receive the results for the reduced stress method for the same cross-sections as for the effective width method.

The results from the two different methods are compared and conclusions of which method yields the less conservative result are made. A discussion of what the main differences are and why there are differences follows the results.

2

Theory

The theory chapter covers general behaviour and stress distribution of a beam, what a stiffener is and its effect on a structure. This is followed by a description of buckling in form of column-like plate buckling and plate buckling. The two methods that are compared in this thesis are described in detail. In the section for the effective width method the calculations are described for an unstiffened beam first followed by a longitudinally stiffened beam. Finally, the reduced stress method calculations are described followed by a brief description of other instability phenomena.

2.1 Steel beam behaviour

This section describes typical beam behaviour and material properties for steel as well as a description regarding shear and bending stress distribution for a beam cross-section. Finally, cross-section classes are described.

Structural beams come in many shapes such as I-beams, T-beams and box beams and are used in a variety of settings. There exist many standard dimensions to choose from when designing but an advantage when using steel beams is that it is also possible to accommodate the beam dimensions to the requirements of the structure. The steel beams are either welded together or rolled sections. It is often desired to use a material efficient design with a sufficient capacity to transfer the acting forces to the foundation, for this slender beams are commonly used. Al-Emrani and Åkesson (2020) states that flanges are designed to resist bending moment and the web the shear force.

2.1.1 Material

The most common material for steel beams is structural steel but aluminium profiles also exist. The structural steel that is used in construction can have different yielding limits, which is described in the steel name. For example, S355 means that the yielding stress is 355 MPa. However, there are some other material properties that remain the same for all structural steel that is used in the Eurocode calculations. These are elastic and shear modulus and Poisson's ratio for the elastic stage which are stated in Eurocode 1993-1-1 (2005):

Modulus of elasticity, E = 210 GPa

Poisson's ratio in elastic stage, $\nu = 0.3$

Shear modulus, $G = \dfrac{E}{2 \cdot (1 + \nu)} = 81$ GPa

2.1.2 Stress distribution

The effects of bending moment and shear force on the cross-section of a steel beam depends on the size of the forces. The behaviour and changes in stress distribution are described in sections 2.1.2.1 and 2.1.2.2. Section 2.1.2.1 describes the influence of bending moment on the cross-section and Section 2.1.2.2 describes the shear force's influence.

2.1.2.1 Bending moment influence on the cross-section

Bending moment acts on the cross-section and deformation is primarily resisted by the capacity of the flanges. When the bending moment increases, the flanges reach their capacity and the stresses correspond to the yielding stress. For further increased moment, the stresses increase until the whole section reaches yielding stress and the cross-section is thus plasticised (Al-Emrani et al., 2013, p. S52). Figure 2.1 illustrates how the stress distribution changes with increasing bending moment.

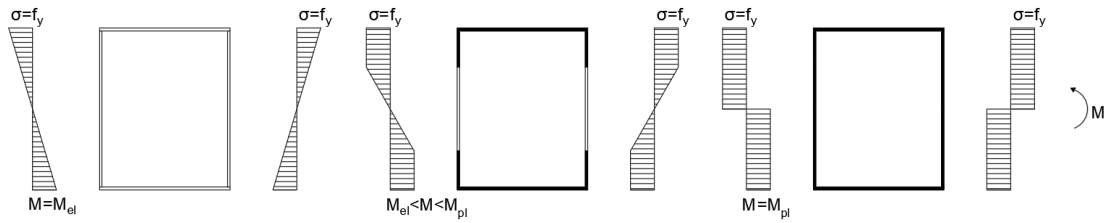

Figure 2.1: *The impact on stress distribution of the cross-section for increasing bending moment.*

2.1.2.2 Shear force influence on the cross-section

The shear force is primarily resisted by the web. The reason why the contribution from the flanges can be neglected is that the shear stresses in the flanges are often very small (Al-Emrani and Åkesson, 2020, p. 127). The shear stress is calculated by equation 2.1 and the stress distribution can be seen in Figure 2.2 where V is the shear force, S is the first moment of area of the cross-section part outside where the shear stresses are calculated, I the moment of inertia for the cross-section and t the web thickness.

$$\tau = \frac{V \cdot S}{I \cdot t} \tag{2.1}$$

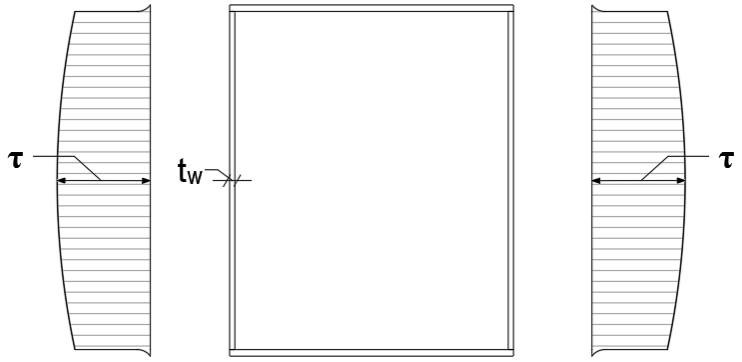

Figure 2.2: *Shear stress distribution on the web of a box beam.*

2.1.3 Cross-section classes

To consider the slenderness of different structural members Eurocode 1993-1-1 (2005) has defined four cross-section classes (CSC). With higher slenderness there is an increased risk that the member will be influenced by local buckling. The lower the CSC for the member is, the higher the bending capacity is. Cross-section class 1 has enough rotational capacity for plastic analysis to be performed, for cross-section class 2 there is plastic capacity but plastic redistribution is not allowed and for worse classes local buckling makes the rotational capacity decrease further (Al-Emrani and Åkesson, 2020, p. 81-83).

Members in cross-section class 4 are considered to be thin-walled meaning that the slenderness is high and buckling occurs even before the outmost fibre has reached yielding. Cross-section class 4 members are reduced with respect to global and local buckling. Local buckling can occur before the elastic moment is reached (Al-Emrani and Åkesson, 2020, p.81-83). To account for buckling Eurocode 1993-1-5 (2006) offers two different methods, the effective width method and the reduced stress method. To determine the cross-section class for a specific member the geometries are evaluated based on what steel class is used, if it is an outstand or internal element and if it is evaluated for compression, bending or a combination of both. The slenderness ratio is calculated by dividing the length of the member with the thickness of the same member, then compared to Table 5.2 in Eurocode 1993-1-1 (2005).

2.2 Stiffeners

This section provides information about the impact stiffeners have on a beam and what type of stiffeners there is to choose from. There exists both longitudinal and transverse stiffeners, the longitudinal are located horizontally along the beam and the transverse are vertically located.

2.2.1 Longitudinal stiffeners

According to Al-Emrani and Åkesson (2020) a longitudinal stiffener is a structural element that can be attached to a structure to increase the capacity of a thin-walled plate. The longitudinal stiffener reduces the amount of free spacing between the flanges that is subjected to compression. Instead of increasing the plate's thickness, stiffeners can be used to achieve the same results of increased moment and shear capacity. There exist several different types of stiffeners that are explained further. Stiffeners can be placed in such a way that they counteract the expected buckle zones (Al-Emrani and Åkesson, 2020). For example if the buckle is more likely to occur in the web, in the flange or both, the placement of the stiffener can vary, see Figure 2.3 for respective placement of the stiffeners.

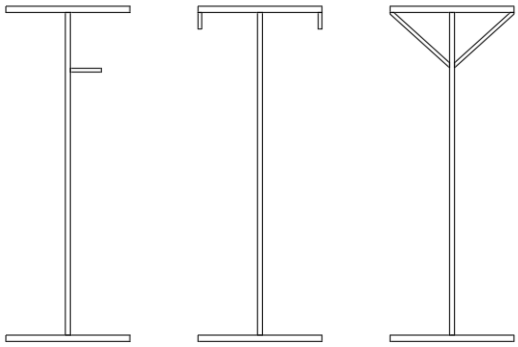

Figure 2.3: *Placements of longitudinal stiffeners. Leftmost beam resists web buckling, middle beam resists flange buckling and rightmost beam resist both web and flange buckling. Adapted with permission from (Al-Emrani and Åkesson, 2020).*

2.2.1.1 Different types of stiffeners

There are different types of stiffeners that are being used for different reasons and applications. The types of stiffeners are generally divided into open stiffeners and closed stiffeners, see Figure 2.4, where flat, angled and tee stiffeners are classified as open stiffeners since it has one part welded whilst a closed stiffener has two parts welded. Examples of closed stiffeners are V-shaped and trapezoidal stiffener (Hendy and Iles, 2015). What type of stiffener that is preferred depends on the requirements of bending stiffness and torsional rigidity (Hendy and Iles, 2015).

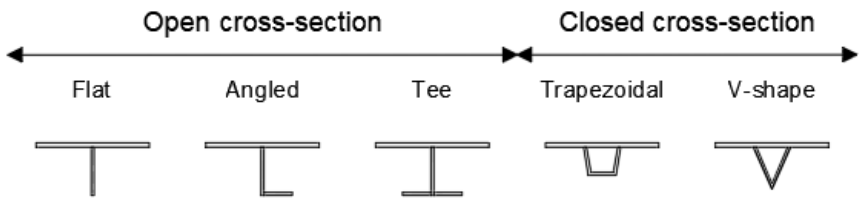

Figure 2.4: *Different types of stiffeners.*

2.2.1.2 Stiffeners' effect on the stress distribution

Al-Emrani and Åkesson (2020) states that stiffeners affect how the stress is distributed, under the assumption that the stiffener is sufficiently strong. The part above the stiffener remains in compression, but when assessing the risk of buckling above the stiffener the buckling length is reduced to only the part above the stiffener as well. However, when looking at the part below the stiffener the buckling length is the length between the bottom flange up to the stiffener (Al-Emrani and Åkesson, 2020, p.84). When increasing the thickness of the bottom flange, the neutral axis is lowered, and the stress distribution changes. The compression zone increases and there might be a need for longitudinal stiffeners to deal with the compressive stresses by increasing the capacity and thus the cross-section is restrained from buckling. When the stiffener is added, the neutral axis moves slightly towards the stiffener. Figure 2.5 show the stress distribution for an unstiffened beam and for a beam with shifted stress distribution that requires a stiffener in the web.

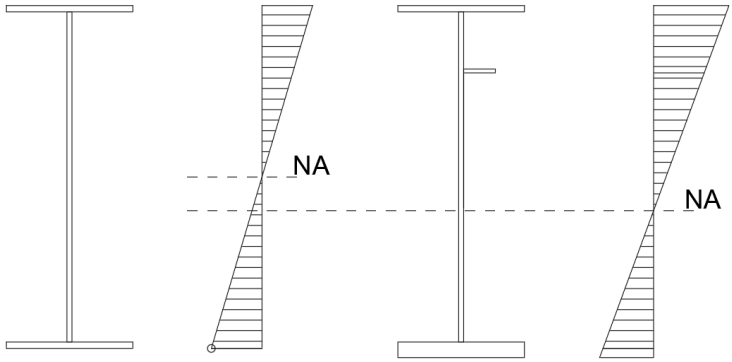

Figure 2.5: *Stress distribution differences for a beam with a thin bottom flange versus a thick flange and a stiffener.*

2.2.2 Transverse stiffeners

The structure can also be stiffened in the transverse direction. The purpose of the transverse stiffeners is to increase shear capacity, provide support for longitudinal stiffeners and increase stiffness against a vertical concentrated load. The distance between two transverse stiffeners is the length of the web and flange panels. The transverse stiffener is required to be sufficiently strong and not buckle. The deflection is also limited to not exceed the smallest value between the height of the web divided by 300 or distance between transverse stiffeners divided by 300 (Al-Emrani and Åkesson, 2020, p.103-104).

2.3 Local buckling

This section describes the phenomena of local buckling. Further the local buckling is divided into plate buckling (due to normal force, moment or shear force) and column-like buckling. Also, the buckling of longitudinal stiffeners is briefly described.

Local buckling occurs when a structural member deforms due to a load. This happens when the element is slender and the critical buckling load is lower than the yielding load. There are several different ways an element can buckle. It can be a column that deforms laterally due to a compressive load or it can be a plate that deforms due to shear force or bending (Al-Emrani and Åkesson, 2020). When buckling occurs the structural member's capacity depends on the type of buckling and if there is any post-critical load capacity. Buckling can occur long before actual failure should happen. When assessing the structural member the initial imperfection as well as the residual stresses have quite a substantial effect on the buckling strength. However, the initial imperfections and residual stresses do not influence the ultimate load-carrying capacity in the same extent (Al-Emrani and Åkesson, 2020, p. 69-71).

2.3.1 Plate buckling

Plate buckling is a type of buckling that can occur in plates. Usually if the plate is thin-walled, slender and loaded with bending, shear or axial compression forces in plane the plate can experience out-of-plane buckling according to Al-Emrani and Åkesson (2020, p. 55). The difference between column-like buckling and plate buckling is that the plate should be supported on at least three edges to be considered a plate, and that the plate can account for post-critical strength after buckling has occurred before the ultimate capacity is reached. Another difference is that the width of the panel "b" governs the buckling strength rather than the distance between transverse stiffeners "a", which is used for column-like plate buckling, see Figure 2.6 for what "a" and "b" is. Compare equation 2.2 with equation 2.5 to see what parameter impacts the critical stress σ_{cr}. Furthermore, the buckling coefficient k_σ is used in the calculations for the plate buckling. The boundary and loading condition both influence the value of k_σ according to Al-Emrani and Åkesson (2020, p. 63) but for illustrative purposes Figure 2.7 show only a plate that is simply supported on all four edges but with varying types of loading conditions. For fixed edges the buckling factor k_σ increases. Figure 2.7 show that it is in the compressive zone that buckling can occur. For an axial compressive force, this means the whole width experience buckling but for bending forces the buckling only occurs in the part of the plate that is subjected to compression. The buckling coefficient k_σ can be obtained from Figure 2.8 where ψ is the stress ratio. The figure only show how to consider internal elements and for outstand elements Eurocode 1993-1-5 (2006, Table 4.2) should be used.

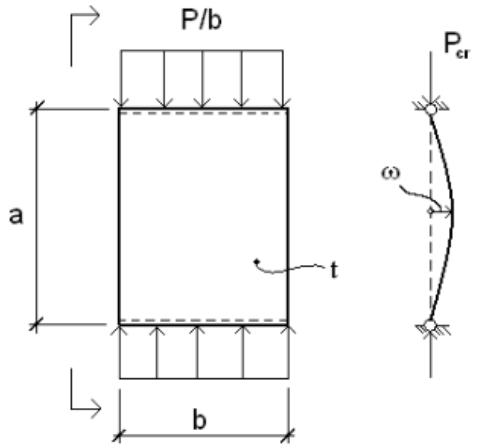

Figure 2.6: *The distance between transverse stiffeners "a" and width of plate visualised subjected to a critical load P_{cr} (Al-Emrani and Åkesson, 2020).*

$$\sigma_{cr.p} = k_\sigma \cdot \frac{\pi^2 \cdot E}{12 \cdot (1 - \nu^2) \cdot (\frac{b}{t})^2} \tag{2.2}$$

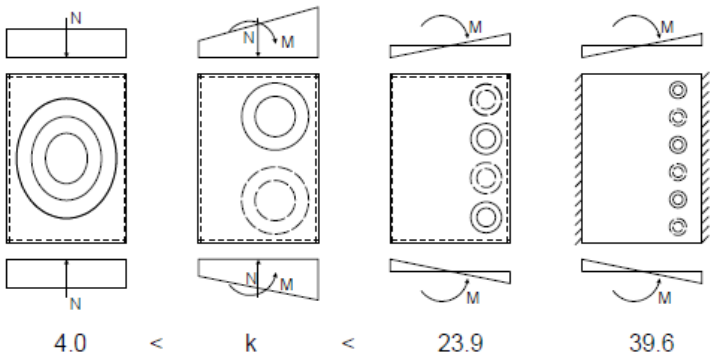

Figure 2.7: *Loading condition's influence on the buckling of a plate. Rightmost figure shows fixed edge influence on the buckling coefficient (Al-Emrani and Åkesson, 2020).*

Stress distribution (compression positive)	Effective width b_{eff}
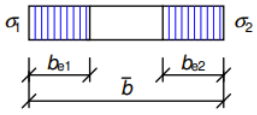	$\psi = 1$: $b_{eff} = \rho\ \bar{b}$ $b_{e1} = 0{,}5\ b_{eff}$ $b_{e2} = 0{,}5\ b_{eff}$
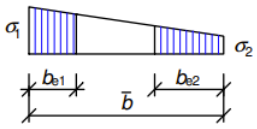	$1 > \psi \geq 0$: $b_{eff} = \rho\ \bar{b}$ $b_{e1} = \frac{2}{5-\psi} b_{eff}$ $b_{e2} = b_{eff} - b_{e1}$
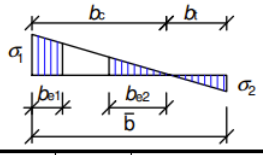	$\psi < 0$: $b_{eff} = \rho\ b_c = \rho\ \bar{b} / (1-\psi)$ $b_{e1} = 0{,}4\ b_{eff}$ $b_{e2} = 0{,}6\ b_{eff}$

$\psi = \sigma_2/\sigma_1$	1	$1 > \psi > 0$	0	$0 > \psi > -1$	-1	$-1 > \psi > -3$
Buckling factor k_σ	4,0	$8{,}2 / (1{,}05 + \psi)$	7,81	$7{,}81 - 6{,}29\psi + 9{,}78\psi^2$	23,9	$5{,}98\ (1 - \psi)^2$

Figure 2.8: *Internal compression elements (Eurocode 1993-1-5, 2006, Table 4.2).*

Another type of loading is the shear that can cause buckling with a 45° angle from the applied load (Al-Emrani and Åkesson, 2020, p. 64), as can be seen in Figure 2.9. For shear buckling Eurocode 1993-1-5 Annex A.3 (2006) suggests another coefficient, k_τ to be used when calculating shear buckling stresses, τ_{cr} which can be seen in equation 2.3. The equation is the same as equation 2.2 but for shear stresses the plate width is annotated d instead of b (Al-Emrani and Åkesson, 2020, p. 64).

$$\tau_{cr} = k_\tau \cdot \frac{\pi^2 \cdot E}{12 \cdot (1 - \upsilon^2) \cdot (\frac{d}{t})^2} \tag{2.3}$$

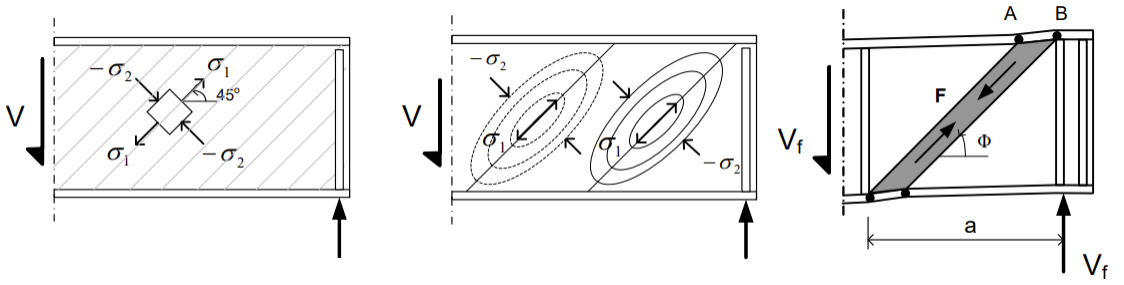

Figure 2.9: *Shear buckling on a web plate. Stresses and buckling modes are shown (Al-Emrani and Åkesson, 2020).*

When the plate is loaded in shear, in the direction of the buckle a tension field occur that is anchored in the flanges. When the plate is loaded to the ultimate load, plastic hinges are formed in the flanges. When the flanges are subjected to bending and shear, the capacity to anchor the tension field in the flanges is reduced

(Al-Emrani and Åkesson, 2020, p. 139-141). Scandella et al. (2020, p. 1) states that when a girder is stiffened, the post-critical strength is increased and the shear capacity is larger than for the linear elastic assumptions. Scandella et al. (2020) further compares the theory behind the equations for shear capacity and concludes that to determine the ultimate capacity consideration of plastic hinges is critical (Scandella et al., 2020, p. 15-16).

There are some local effects that are not considered here. These are web crippling and web buckling due to transverse concentrated loads. When the web is very slender there is a risk of local deformations due to these effects and a reduction of the capacity is needed (Al-Emrani and Åkesson, 2020, p. 117-118).

2.3.1.1 Post-critical strength of plate buckling

For plate buckling, the phenomenon of post-critical strength occurs when the plate reaches the critical buckling stress and this was first proven in 1960 by Basler et al. (1960, p. 18). When the plate has buckled, it can still carry some load before it fails, this reserve capacity, the post-critical strength occurs for plates subjected to axial compressive forces, bending moments and shear forces (Al-Emrani and Åkesson, 2020, p. 65). The plate can continue to carry loads around the buckle through the edges that are parallel to the applied load as can be seen in Figure 2.10. The ultimate capacity is determined by the size of the effective width of the edges that contribute to the post-critical strength. This is accounted for in Eurocode 1993-1-5 Table 4.1 and 4.2 (2006).

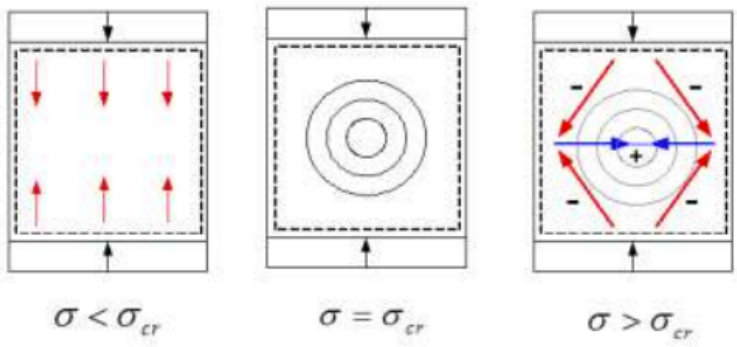

Figure 2.10: *Illustration of how the post-critical strength works for a plate that experience loading after buckling. Negative forces are compression (Al-Emrani and Åkesson, 2020).*

2.3.2 Column-like plate buckling

Column-like plate buckling is when a plate is loaded in the same way a column is loaded. The plate is only restricted by two edge supports so that when it is modelled in two dimensions it acts similar to a column. To calculate the critical load for a column equation 2.4 could be used, as stated in the book *Steel Structures* (Al-Emrani and Åkesson, 2020).

$$P_{cr} = \frac{\pi^2 \cdot EI}{a^2} \cdot \frac{1}{1-\nu^2} \tag{2.4}$$

The main difference in calculating the critical column load for a plate versus a regular column is the second term of equation 2.4. This part takes into account that it is a plate and not a column that buckles and that it has another dimension. In column-like plate buckling the length of the plate element a is used instead of the buckling length L_{cr}, but it is comparable since a is the length of the plate that is checked against buckling, see Figure 2.6. In column-like buckling there is no additional loading capacity after the element has reached critical loading. The critical stress for column-like buckling can be calculated by dividing the critical load P_{cr} with the width b and the thickness t of the element and also utilising that $I = \frac{b \cdot t^3}{12}$, see equation 2.5 for the stress calculation.

$$\sigma_{cr.c} = \frac{P_{cr}}{b \cdot t} = \frac{\pi^2 \cdot E}{12 \cdot (1-\nu^2)(\frac{a}{t})^2} \tag{2.5}$$

2.3.2.1 Buckling of longitudinal stiffeners

The longitudinal stiffeners are in theory considered to act as a rigid nodal line in order for the structure to utilise the stiffeners full capacity. In the book *Steel Structures* (Al-Emrani and Åkesson, 2020, p. 90) it is explained what is needed to fulfil the requirement of "a rigid nodal line" for a stiffener. The stiffener should not buckle locally nor globally. Meaning that the stiffener should be in CSC 1-3 and that the stiffener with adjacent effective parts of the plate cannot buckle due to column-like or torsional buckling (Al-Emrani and Åkesson, 2020, p. 90). If global buckling needs to be accounted for the area of the stiffeners is reduced. This is done with a reduction factor called ρ_c. In Section 2.4 this factor and how it is used is explained further.

2.4 Effective width method

The effective width method is the first of the two methods described in Eurocode 1993-1-5 (2006) regarding calculations of the structural capacity for thin-walled plate elements. It can be used for both unstiffened and stiffened elements. First the unstiffened case is described followed by the stiffened case that is based on the unstiffened. The stiffened case addresses a longitudinally stiffened beam.

This section aims to describe the effective width method, how the equations are used and how plate and column-like buckling are accounted for in this method along with shear and moment resistance and interaction of them both.

2.4.1 Unstiffened plate buckling

In Section 2.1.3 it is stated that if a structural member is in cross-section class 4, the width has to be reduced to account for local buckling. This reduction applies for plate buckling and if shear lag needs to be considered an interaction check is performed (Johansson et al., 2007, p. 42), see Section 2.4.5. The cross-sectional class check is found in Table 5.2 in Eurocode 1993-1-1 (2005). The reduction of the width of the member is done according to Table 4.1 or 4.2 in Eurocode 1993-1-5 (2006) where the type of stress distribution and location of the member in the global geometry is considered. The effective width b_{eff} is calculated as the reduction factor ρ times the length of the part in compression as can be seen in Figure 2.8.

The reduction factor ρ is obtained from equation 2.6 where $\bar{\lambda}_p$ is the relative plate slenderness which is calculated using equation 2.7. The direct stress distribution ψ can be obtained from Figure 2.8. Equation 2.6 only applies for internal members of the cross-section that needs to be reduced, for both unstiffened or stiffened plates. For outstand members, see Eurocode 1993-1-5 (2006, Table 4.2). Johansson et al. (2007) states that the calculations for the critical plate buckling stress $\sigma_{cr.p}$ differs depending on how many stiffeners the plate has. For unstiffened plates the equation for the relative plate slenderness can be simplified to that of equation 2.7. The strain ε is related to the yield strength of the steel and since structural steel usually have a yield strength of at least 235 MPa (Eurocode 1993-1-1, 2005, Table 3.1), it is this value the strain is related to such as $\varepsilon = \sqrt{235/f_y}$. Further, the buckling factor k_σ for unstiffened plates is obtained by the methods presented in Section 2.3.1 and $\bar{b}$ can be found in Figure 2.8. The constant 28.4 comes from equation 2.2 and uses the steel's material properties to retrieve the value of the constant (Beg et al., 2010, p. 33).

$$\rho = \begin{cases} 1 & \text{if } \bar{\lambda}_p \leq 0.5 + \sqrt{0.085 - 0.055\psi} \\ \dfrac{\bar{\lambda}_p - 0.055 \cdot (3+\psi)}{\bar{\lambda}_p^2} \leq 1 & \text{if } \bar{\lambda}_p > 0.5 + \sqrt{0.085 - 0.055\psi} \end{cases} \tag{2.6}$$

$$\bar{\lambda}_p = \sqrt{\frac{f_y}{\sigma_{cr.p}}} = \frac{\bar{b}/t}{28.4 \cdot \varepsilon \cdot \sqrt{k_\sigma}} \tag{2.7}$$

The flanges' and web's effective areas $A_{c.eff}$ are separately calculated as the gross area A_c in the compression zone times the reduction factor ρ in equation 2.8. Then the effective cross-section properties such as area, moment of inertia and section modulus are summarised in order to calculate the capacity of the beam.

$$A_{c.eff} = \rho \cdot A_c \tag{2.8}$$

If the aspect ratio between the height b and width a of the plate suffice the condition $\dfrac{a}{b} > 1$, then there is no need to consider column-like buckling and also no need to

check plate and column interaction for the unstiffened plate (Eurocode 1993-1-5, 2006, Section 4.4). Shear resistance is also needed in order for shear capacity to be checked along with moment and shear interaction. These calculations are described further in Section 2.4.6 and 2.4.7.

2.4.2 Stiffened plate buckling

A stiffened plate is a plate that has some form of stiffeners attached to it. Here the influence of longitudinal stiffeners is described by showing how the calculations change from an unstiffened plate. The stiffened plate can have a combined effect of plate and column-like buckling, meaning that reduction factors for both types need to be calculated. In this section the plate buckling is described.

In Eurocode 1993-1-5 (2006) the calculations for plate buckling differs slightly depending on whether the plate is unstiffened, has one, two or multiple stiffeners in the longitudinal direction. It is the calculation for the relative slenderness $\bar{\lambda}_p$ that is influenced by the number of stiffeners. For stiffened plates the critical stress $\sigma_{cr.p}$ is changed and a factor called $\beta_{A.c}$ is added in equation 2.9.

$$\bar{\lambda}_p = \sqrt{\frac{\beta_{A.c} \cdot f_y}{\sigma_{cr.p}}} \tag{2.9}$$

When a stiffened cross-section is assessed the parts in between stiffeners are considered as unstiffened plates, these are called subpanels. The calculations for the subpanels are performed in the same way as for an unstiffened plate, see Section 2.4.1. These calculations aim to find the reduction factor and thus the effective widths of the subpanel that are in CSC4. The effective widths are the widths that can be accounted for in the cross-section when checking the plate's capacity against local buckling.

When considering a stiffened plate element, global buckling should also be taken into account. The area that accounts for this is $A_{c.eff.loc}$, which is the area of the subpanels adjacent to the stiffeners and the area of the stiffeners. This area is already reduced due to local buckling. $A_{c.eff.loc}$ is reduced with the global reduction factor ρ_c. The effective area of a stiffened element $A_{c.eff}$ is calculated in equation 2.10 where the first term considers both local and global buckling and the second term consider local buckling of the subpanels that are not adjacent to a stiffener, $b_{edge.eff} \cdot t$.

$$A_{c.eff} = \rho_c \cdot A_{c.eff.loc} + \Sigma b_{edge.eff} \cdot t \tag{2.10}$$

The $\beta_{A.c}$-factor used in the relative plate slenderness calculations in equation 2.9 derives from the ratio between the effective area of the stiffened section $A_{c.eff.loc}$ compared to the gross area of the same section A_c in the compression zone, see equation 2.11 (Johansson et al., 2007, p. 47-48). For the case of two stiffeners in

the compressive zone, Figure 2.11 illustrates what is meant by $A_{c.eff.loc}$ and A_c. As can be seen A_c is not the whole area of the compressive zone but rather the area in connection to the stiffeners and the subpanels in between them. $A_{c.eff.loc}$ is only the area of the stiffeners and the effective part of the adjacent web. For example the effective width is $b_{i.eff.inf} = \rho \cdot b_{i.inf}$. The width of the different parts such as edge part, inferior and superior parts of the subpanels are calculated with respect to if the whole of the subpanel is in the compressive zone or if the subpanel is both in the compressive and tensile zone (Eurocode 1993-1-5, 2006, Section A.1-A.2). If the member is subjected to linearly distributed stresses, the widths can be calculated with the help of Table 2.1. For uniformly distributed stresses the widths of the adjacent parts of the subpanel are calculated as $0.5 \cdot b_i$.

$$\beta_{A.c} = \frac{A_{c.eff.loc}}{A_c} \tag{2.11}$$

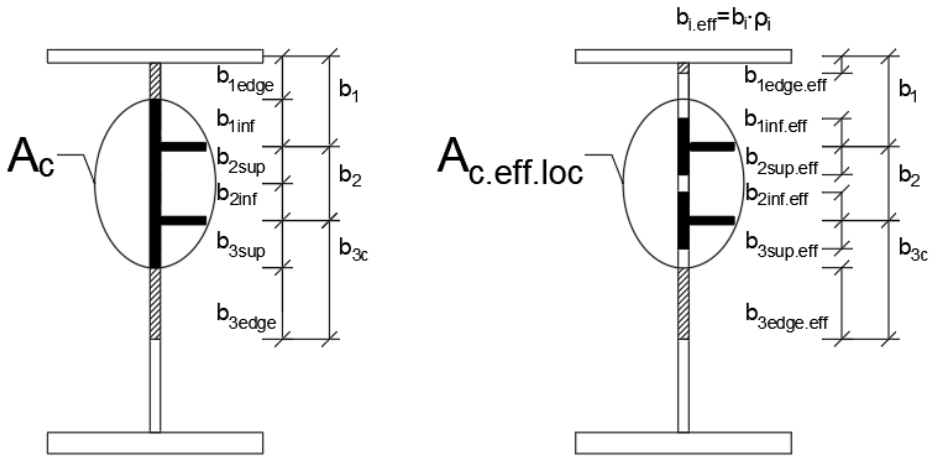

Figure 2.11: *Definition of $A_{c.eff.loc}$ and A_c for a plate with two stiffeners in the compressive zone. Adapted from Eurocode 1993-1-5, 2006.*

Table 2.1: *Determination of the contributing part of the subpanel adjacent to the stiffener for linearly distributed stresses (Eurocode 1993-1-5, 2006).*

Width	**Gross width**	**Effective width**	**Condition for ψ_i**
$b_{1.inf}$	$\frac{3-\psi_1}{5-\psi_1}b_1$	$\frac{3-\psi_1}{5-\psi_1}b_{1.eff}$	$\psi_1 = \frac{\sigma_{cr.sl.1}}{\sigma_{cr.p}} > 0$
$b_{2.sup}$	$\frac{2}{5-\psi_2}b_2$	$\frac{2}{5-\psi_2}b_{2.eff}$	$\psi_2 = \frac{\sigma_2}{\sigma_{cr.sl.1}} > 0$
$b_{2.inf}$	$\frac{3-\psi_2}{5-\psi_2}b_2$	$\frac{3-\psi_2}{5-\psi_2}b_{2.eff}$	$\psi_2 > 0$
$b_{3.sup}$	$0.4b_{3c}$	$0.4b_{3c.eff}$	$\psi_3 = \frac{\sigma_3}{\sigma_2} < 0$

2.4.2.1 Influence of multiple stiffeners

When the plate has three or more stiffeners the stiffness contribution from them on the cross-section can be regarded as distributed along the plate so the subpanels between the stiffeners are irrelevant. This is called *smeared stiffeners* according to Johansson et al. (2007, p. 44). When the plate has multiple stiffeners the plate can be regarded as an orthotropic plate and for equivalent orthotropic plates the effects of local plate buckling can be neglected (Johansson et al., 2007, p. 46-48).

The critical stress $\sigma_{cr.p}$ can be calculated with the buckling factor k_σ multiplied with an equivalent stress σ_E. The buckling factor is dependent on the stiffeners' distribution and amount. Calculating the buckling factor is more demanding for orthotropic plates. It requires consideration to the area of the subpanels and the stresses in the edges of the plate panel, compared to only boundary conditions and load distribution as for the case of the unstiffened plate (Johansson et al., 2007). Stated by Beg et al. (2010, p. 38) the buckling factor can be obtained from computer simulations, simplified analytical expressions, which are found in Eurocode 1993-1-5 (2006, Section A.1-A.2) or by extracting the value from charts. The most common charts are those made by Klöppel (Johansson et al., 2007, p. 136). There are different charts depending on if the stiffeners are considered as smeared or discretely spaced (Beg et al., 2010, p. 38).

2.4.2.2 Influence of one or two stiffeners

According to Eurocode 1993-1-5 (2006, Section A.2) there is a simplified method for calculating the elastic plate buckling stress $\sigma_{cr.p}$ for the case of plates with only one or two stiffeners. There are three cases to regard when having two stiffeners in the compressive zone, see Figure 2.12. The first two cases considers one of the stiffeners

rigid enough so that only the other stiffener buckles, Case 1 and 2 in Figure 2.12. The third case regards simultaneous buckling of both stiffeners and the two stiffeners are lumped together to one in this calculation method (Eurocode 1993-1-5, 2006, Section A.2).

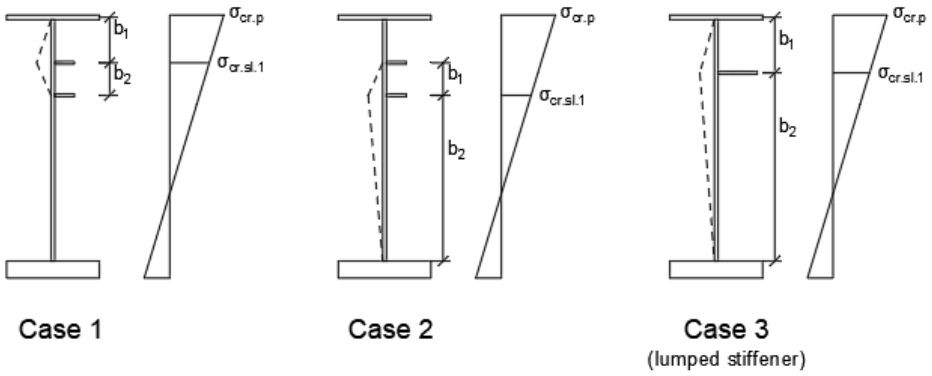

Figure 2.12: *The three cases of how two stiffeners can buckle. Adapted from Eurocode 1993-1-5, 2006, Section A.2.*

As can be seen in Figure 2.12 the stiffeners' critical stress $\sigma_{cr.sl}$ is marked for where the stiffener buckles. Eurocode 1993-1-5 (2006, Section A.2.2) states that for plates with one stiffener, the behaviour can be seen as Case 3 with lumped stiffeners but with the area $A_{sl.1}$ and moment of inertia $I_{sl.1}$ for one stiffener with adjacent parts of the subpanel. Thus the critical stress of the stiffener is received from equation 2.12 which is dependent on the distance between the transverse stiffeners "a". When there are two stiffeners, all three cases needs to be checked and the case that results in the smallest critical stiffener's stress $\sigma_{cr.sl}$ is governing. The stiffeners' critical stress is then used to interpolate the most stressed point in the plate $\sigma_{cr.p}$. This stress is then used to calculate the relative slenderness $\bar{\lambda}_p$ in equation 2.9. Further the reduction factor ρ due to plate buckling can be obtained from equation 2.6 (Eurocode 1993-1-5, 2006).

$$\sigma_{cr.sl.p} = \begin{cases} \dfrac{1.05 \cdot E}{A_{sl.1}} \cdot \dfrac{\sqrt{I_{sl.1} \cdot t^3 \cdot b}}{b_1 \cdot b_2} & \text{if } \ a \geq a_c \\ \dfrac{\pi^2 \cdot E \cdot I_{sl.1}}{A_{sl.1} \cdot a^2} \cdot \dfrac{E \cdot t^3 \cdot b \cdot a^2}{4 \cdot \pi^2 \cdot (1-\nu^2) \cdot A_{sl.1} \cdot b_1^2 \cdot b_2^2} & \text{if } \ a < a_c \end{cases} \tag{2.12}$$

Where $a_c = 4.33 \sqrt[4]{\dfrac{I_{sl.1} \cdot b_1^2 \cdot b_2^2}{t^3 \cdot b}}$

and $A_{sl.1}$ and $I_{sl.1}$ is dependent on which of the three cases in Figure 2.12 is calculated. The area is calculated with regards to which stiffener is set to buckle and

its adjacent parts of the web. The widths for the adjacent parts are received from Table 2.1. For the lumped stiffener, the areas for Case 1 and Case 2 are added, the same applies for the moment of inertia (Eurocode 1993-1-5, 2006, Section A.2.2).

2.4.3 Column-like plate buckling calculations

It is required to calculate the reduction factor due to column-like plate buckling for stiffened plates. However, for unstiffened plates column-like buckling can be disregarded for aspect ratios a/b greater than one (Eurocode 1993-1-5, 2006, Section 4.4).

Column-like plate buckling of a stiffened plate is calculated where the same area of the stiffener and adjacent area of the subpanels is used as for the plate buckling scenario. However, instead of calculating the plate buckling reduction factor ρ, a column reduction factor, χ_c, is calculated. When combining the equations 2.13, 2.14 and 2.15 the reduction factor can be calculated.

$$\chi_c = \frac{1}{\varphi + \sqrt{\varphi^2 - \bar{\lambda}_c^2}} \tag{2.13}$$

$$\varphi = 0.5[1 + \alpha_e(\bar{\lambda}_c - 0.2) + \bar{\lambda}_c^2] \tag{2.14}$$

$$\alpha_e = \alpha + \frac{0.09}{i/e} \tag{2.15}$$

For an unstiffened plate that requires column-like buckling reduction the same equations are used but with $\alpha_e = 0.21$. For a stiffened plate the coefficient α is dependent on which buckling curve that is used and can be found in Eurocode 1993-1-1 (2005, Section 6.3.1.2). If a closed stiffener is used a smaller reduction can be utilised due to less residual stresses, i.e. $\alpha = 0.34$ instead of $\alpha = 0.49$, which corresponds to buckling curve b and c respectively. Johansson et al. (2007, p. 53-54) states that the coefficient e is the largest distance from the centroid of either the stiffener $x_{tp.sl}$ or the adjacent part of the subpanels $x_{tp.w}$ to the combined centroid $x_{tp.w+sl}$, see Figure 2.13. The radius of gyration can be calculated as $i = \sqrt{\frac{I_{sl,1}}{A_{sl,1}}}$. The stiffener's area with adjacent contributing part of the subpanels $A_{sl.1}$, is calculated with Table 2.1, and $I_{sl.1}$ is the second moment of area of the same section.

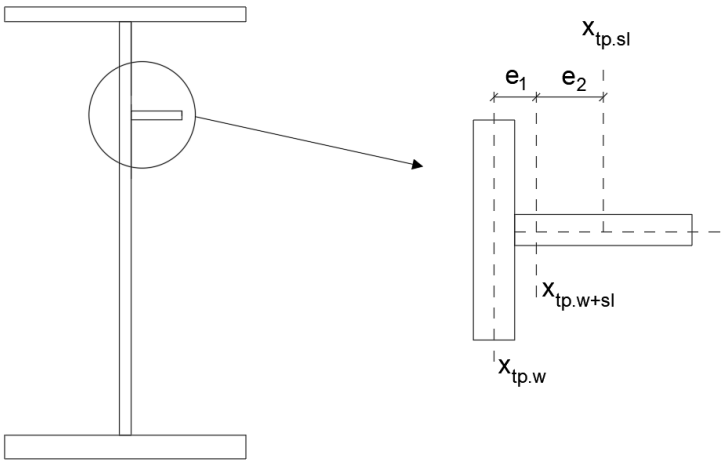

Figure 2.13: *Distance to the combined centroid of part of the web and a stiffener.* $x_{tp.w}$ *is the centroid of the adjacent part of the web and* $x_{tp.sl}$ *is the centroid of the stiffener and* $x_{tp.w+sl}$ *is the combined centroid.*

The slenderness can be calculated according to equation 2.16 where the reduction factor $\beta_{A.c}$ can be calculated according to equation 2.17. The area for this ratio is the area of one stiffener including adjacent parts of the subpanel. $A_{sl.eff.loc}$ is the effective area and $A_{sl.1}$ is the gross area for one stiffener.

$$\bar{\lambda}_c = \sqrt{\frac{\beta_{A.c} \cdot f_y}{\sigma_{cr.c}}} \tag{2.16}$$

$$\beta_{A.c} = \frac{A_{sl.eff.loc}}{A_{sl.1}} \tag{2.17}$$

The critical column stress $\sigma_{cr.c}$ is determined as explained in equation 2.5 if there are no stiffeners. However, if the cross-section contains stiffeners the critical stress for the stiffeners $\sigma_{cr.sl.c}$ needs to be calculated according to equation 2.18. When $\sigma_{cr.sl.c}$ is obtained, a critical column stress $\sigma_{cr.c}$ for the top of the plate can be calculated according to equation 2.19 where b_c is the height of the compressive zone and $\bar{b}$ is the distance from the stiffener to the neutral axis (Johansson et al., 2007). This stress is then used to calculate the relative slenderness $\bar{\lambda}_c$ and reduction factor χ_c.

$$\sigma_{cr.sl.c} = \frac{\pi^2 \cdot E \cdot I_{sl.1}}{A_{sl.1} \cdot a^2} \tag{2.18}$$

$$\sigma_{cr.c} = \sigma_{cr.sl.c} \cdot \frac{b_c}{\bar{b}} \tag{2.19}$$

2.4.4 Plate and column-like buckling interaction

Plate and column-like buckling interaction needs to be considered since the reality of the stiffened plate's behaviour is probably somewhere in between the two extremes, only plate buckling or only column-like buckling. An interpolation is made according to equation 2.20 to consider the effect of both column-like plate buckling as well as plate buckling (Eurocode 1993-1-5, 2006, Section 4.5.4).

$$\rho_c = \xi(2 - \xi)(\rho - \chi_c) + \chi_c \tag{2.20}$$

$$\xi = \frac{\sigma_{cr.p}}{\sigma_{cr.c}} - 1 \quad \text{but} \quad 0 \leq \xi \leq 1 \tag{2.21}$$

It can be seen in equation 2.21 that the critical plate buckling stress $\sigma_{cr.p}$ is limited to not be larger than two times the critical column-like buckling stress $\sigma_{cr.c}$. However, if that is the case then column-like buckling is deemed irrelevant and the final reduction factor is equal to the reduction factor for the plate buckling, $\rho_c = \rho$ (Johansson et al., 2007, p. 54-55). The interpolation is visualised in Figure 2.14. In the figure it can be seen that there are three stages that can occur depending on the value of ξ from equation 2.21. If $\xi > 1$ the plate buckling is determining the reduction factor. For $\xi \leq 0$ it is the column-like buckling that determines the reduction. However, if ξ is somewhere in between zero and one equation 2.20 can be used to determine the combined reduction factor ρ_c.

The weighted reduction factor ρ_c reduces the area of the stiffener and adjacent part of the subpanels to account for the fact that the stiffener is not rigid enough and that the cross-sectional capacity cannot be calculated utilising the whole section. The use of ρ_c is seen in equation 2.10.

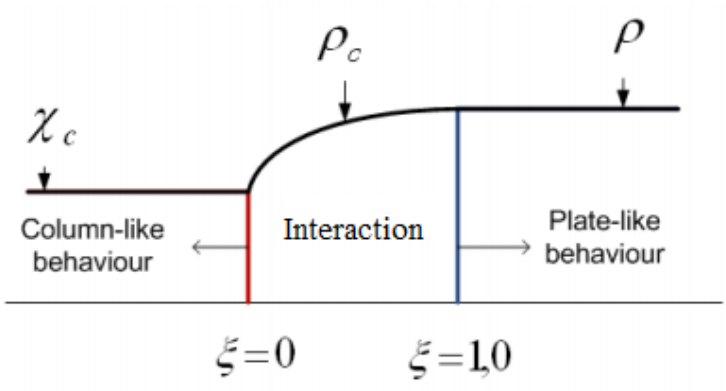

Figure 2.14: *Visualisation of the plate and column-like buckling interaction. The interaction occurs between 0 and 1 for ξ (Al-Emrani and Åkesson, 2020).*

2.4.5 Capacity control of the cross-section

When the cross-section is reduced with respect to local and global buckling, the effective area is calculated as seen in equation 2.8 for the unstiffened case and equation 2.10 for the stiffened case. The effective area $A_{c.eff}$ and moment of inertia I_{eff} is used in the capacity controls of the cross-section.

If the cross-section is subjected to uniaxial bending, equation 2.22 should be used. However, if it is only subjected to a moment, and no axial force, then the maximum compressive stress is controlled to make sure it does not exceed the yielding stress according to equation 2.23. The maximum compressive stress $\sigma_{x.Ed}$ is decided by the design moment M_{Ed} and the elastic section modulus W_{eff}. The elastic section modulus is in turn decided by the second moment of area I_{eff} and the distance v between the centre of gravity and the fibre for which the stress is checked, as seen in equation 2.24 (Johansson et al., 2007). From equation 2.23 the utilisation of the cross-section is obtained with respect to applied bending moment. If axial forces are present equation 2.22 is used instead to receive the same result but these forces are disregarded in this thesis.

$$\eta_1 = \frac{N_{Ed}}{(f_y \cdot A_{c.eff})/\gamma_{M0}} + \frac{M_{Ed} + N_{Ed} \cdot e_N}{(f_y \cdot W_{eff})/\gamma_{M0}} \leq 1 \tag{2.22}$$

$$\eta_1 = \frac{M_{Ed}}{(f_y \cdot W_{eff})/\gamma_{M1}} \leq 1 \tag{2.23}$$

$$W_{eff} = \frac{I_{eff}}{v} \tag{2.24}$$

2.4.6 Resistance to shear

In this section the shear capacity of a thin-walled slender plate is described. How the calculations differ between an unstiffened plate and a stiffened plate is also described.

2.4.6.1 Shear resistance of an unstiffened plate

According to Johansson et al. (2007, p. 59-60) panels that are slender have quite large shear resistance even post-buckling. Eurocode 1993-1-5 is using a method called *rotated stress field* which should yield a less conservative assumption of the post-buckling capacity of shear compared to other well-known methods that are used for the same purpose. In the rotated stress field method the principle stresses can be calculated according to the two equations 2.25 and 2.26, the angle of the stress field ϕ described in the equations can be seen in Figure 2.9. The rotated stress field makes the assumption that there are no membrane stresses in the transverse direction (Höglund, 1997, p. 15). The stresses σ_1 and σ_2 are principle stresses that occur due to the shear force τ.

$$\sigma_1 = \frac{\tau}{\tan\phi} \tag{2.25}$$

$$\sigma_2 = -\tau \cdot \tan\phi \tag{2.26}$$

The compressive stress will stay the same as the shear buckling stress even after buckling. This assumption results in membrane stresses according to equation 2.27 (Höglund, 1997). It utilises the criterion for yielding from von Mises, $\sigma_1^2 - \sigma_1\sigma_2 + \sigma_2^2 = f_y^2$, the yield strength can be expressed in terms of $\bar{\lambda}_w$ which can be seen in equation 2.28. $\bar{\lambda}_w$ is the shear panel slenderness and is calculated according to equation 2.29.

$$\sigma_2 = -\tau \tag{2.27}$$

$$\frac{\tau_u}{f_y/\sqrt{3}} = \frac{1}{\bar{\lambda}_w^2}\sqrt{\sqrt{3 \cdot \bar{\lambda}_w^4 - \frac{3}{4}} - \frac{1}{2}} \tag{2.28}$$

$$\bar{\lambda}_w = \sqrt{\frac{f_y/\sqrt{3}}{\tau_{cr}}} = 0.76 \cdot \sqrt{\frac{f_y}{\tau_{cr}}} \tag{2.29}$$

τ_u mentioned in equation 2.28 is the ultimate shear resistance, and τ_{cr} mentioned in equation 2.29 is the stress for elastic shear buckling when the panel is a perfect shear panel. By combining equation 2.29 and 2.30 the slenderness of the shear panel slenderness $\bar{\lambda}_w$ can be written as equation 2.31.

$$\tau_{cr} = k_\tau \cdot \sigma_E = k_\tau \cdot \frac{\pi E}{12(1-\nu^2)}\left(\frac{t}{h_w}\right)^2 \tag{2.30}$$

$$\bar{\lambda}_w = \frac{h_w}{37.4 \cdot t \cdot \varepsilon\sqrt{k_\tau}} \tag{2.31}$$

When the shear buckling coefficient k_τ is determined it is dependent on how the plate is transversely stiffened and if the stiffeners can be considered rigid or not. The reduction factor χ_w is also dependent on the rigidity, see Table 2.2. If the plate is stiffened with two rigid transverse stiffeners and simply supported, equation 2.32 can be used to calculate k_τ. If the plate is not rigid the shear buckling coefficient can be decided by an applicable design chart (Johansson et al., 2007, p. 67).

Table 2.2: *χ_w depends on if the stiffener can be considered rigid or non-rigid (table adapted from Table 5.1 Eurocode 1993-1-5).*

Condition for $\bar{\lambda}_w$	**Rigid end post**	**Non-rigid end post**
$\bar{\lambda}_w < 0.83/\eta$	η	η
$0.83\eta \leq \bar{\lambda}_w < 1.08$	$0.83/\bar{\lambda}_w$	$0.83/\bar{\lambda}_w$
$\bar{\lambda}_w \geq 1.08$	$1.37/(0.7+\bar{\lambda}_w)$	$0.83/\bar{\lambda}_w$

$$k_\tau = \begin{cases} 5.34 + \dfrac{4.0}{\alpha^2} & \text{if } \alpha \geq 1.0 \\ \\ 4.0 + \dfrac{5.34}{\alpha^2} & \text{if } \alpha < 1.0 \end{cases} \tag{2.32}$$

Höglund (1997) states that if plastic hinges are formed in the flanges it does not affect the shear resistance of the web. In equation 2.33 the distance between the plastic hinges are calculated (Höglund, 1997, p. 21). This is calculated with regards to the plastic moment of the flanges $M_{pl.f}$ and the web $M_{pl.w}$ in equation 2.34. Based on the rotated stress field theory the shear resistance of the flanges can be regarded and thus increasing the total shear resistance $V_{b.Rd}$ according to equation 2.35. However, this can only occur when the flanges have enough capacity to first handle the bending moment. The shear resistance of the web $V_{bw.Rd}$ is calculated in equation 2.36.

$$c = a\left(0.25 + 1.6\frac{M_{pl.f}}{M_{pl.w}}\right) = a\left(0.25 + \frac{1.6 \cdot b_f \cdot t_f^2 \cdot f_y}{t \cdot h_w^2 \cdot f_y}\right) \tag{2.33}$$

$$M_{pl.f} = \frac{b_f \cdot t_f^2 \cdot f_y}{4}, \qquad M_{pl.w} = \frac{t \cdot h_w^2 \cdot f_y}{4} \tag{2.34}$$

$$V_{b.Rd} = V_{bw.Rd} + V_{bf.Rd} \leq \frac{\eta f_y h_w t}{\sqrt{3}\gamma_{M1}} \tag{2.35}$$

$$V_{bw.Rd} = \frac{\chi_w f_y h_w t}{\sqrt{3}\gamma_{M1}} \tag{2.36}$$

The contribution from the flanges to the shear force $V_{bf.Rd}$ is calculated according to equation 2.37. The contribution is reduced based on how much smaller the design moment is compared to the moment capacity of the flanges, equation 2.38. Then

finally the contribution of the flanges can be added to the resistance for the web to receive the total shear resistance according to equation 2.35 which is checked against the design shear force, see equation 2.39. However, the additional shear resistance from the flanges is generally quite small in comparison to the shear resistance of the web.

$$V_{bf.Rd} = \frac{b_f \cdot t_f^2 \cdot f_y}{c\gamma_{M1}} \left(1 - \left(\frac{M_{Ed}}{M_{f.Rd}}\right)^2\right) \tag{2.37}$$

$$M_{f.Rd} = \frac{M_{f.k}}{\gamma_{M0}} = min\left(h_f \cdot A_{f.Top}\frac{f_y}{\gamma_{M0}}, h_f \cdot A_{f.Bot}\frac{f_y}{\gamma_{M0}}\right) \tag{2.38}$$

$$\eta_3 = \frac{V_{Ed}}{V_{b.Rd}} \leq 1 \tag{2.39}$$

2.4.6.2 Shear resistance of a stiffened plate

The main difference in the calculation of the shear resistance between a stiffened plate and an unstiffened plate is how the shear buckling coefficient k_τ is calculated. In equation 2.40 several possibilities are presented to calculate the shear buckling coefficient. However, if the plate is rigid the shear buckling coefficient can be decided by either an applicable design chart or by performing an eigenvalue analysis (Johansson et al., 2007, p. 67).

$$k_\tau = \begin{cases} 5.34 + 1.36\sqrt[3]{\gamma} & \textbf{if} \text{ the plate is long and longitudinally stiffened} \quad (a) \\ 5.34 + \dfrac{4}{\alpha^2} + \dfrac{3.45 \cdot \gamma^{3/4}}{\alpha^2} * & \textbf{if } \alpha \geq 3 \textbf{ and} \text{ more than two longitudinal stiffeners } \textbf{but } k_\tau \geq \text{equation 2.40}(a) \quad (b) \\ 4.1 + \dfrac{6.3 + 0.05\gamma}{\alpha^2} + 1.44\sqrt[3]{\gamma} * & \textbf{if} \text{ one or two longitudinal stiffeners } \textbf{and } \alpha < 3 \quad (c) \\ 5.34 + 4 \cdot \dfrac{h_w}{a} + k_{\tau.st} & \textbf{if} \text{ rigid transverse stiffeners } \textbf{and } \alpha \geq 1.0 \quad (d) \\ 4 + 5.34 \cdot \dfrac{h_w}{a} + k_{\tau.st} & \textbf{if} \text{ rigid transverse stiffeners } \textbf{and } \alpha < 1.0 \quad (e) \\ 4.1 + \dfrac{6.3 + 0.18\dfrac{I_{sl}}{t^3 h_w}}{\alpha} + 2.2\sqrt[3]{\dfrac{I_{sl}}{t^3 h_w}} & \textbf{if} \text{ one or two longitudinal stiffeners } \textbf{and } \alpha < 3 \quad (f) \end{cases} \tag{2.40}$$

* Equations used for closely spaced transverse stiffeners.

The shear buckling coefficient in equation 2.40 requires the relative flexural stiffness out of plane γ and the shear buckling coefficient for the stiffeners $k_{\tau.sl}$ which are obtained from equations 2.41 and 2.42. The aspect ratio α is the distance between the stiffeners "a" and height of the web h_w (Johansson et al., 2007, p. 67-69).

$$\gamma = \frac{12(1-\nu^2)I_{sl}}{h_w t^3} = 10.92 \cdot \frac{I_{sl}}{h_w t^3} \tag{2.41}$$

$$k_{\tau.st} = 9\left(\frac{h_w}{a}\right)^2 \sqrt[4]{\left(\frac{I_{sl}}{t^3 h_w}\right)^3} \text{ but not less than } \frac{2.1}{t}\sqrt[3]{\frac{I_{sl}}{h_w}} \tag{2.42}$$

After the shear buckling coefficient, k_τ is calculated the shear capacity for the stiffened plate can be calculated in the same way that it was calculated for an unstiffened plate in Section 2.4.6.1.

2.4.7 Moment and shear interaction

Depending on how the cross-section looks and the individual capacities of the flange and web there might be reason to include interaction effects between the elements, e.g. the web can contribute to the moment capacity. Eurocode 1993-1-1 (2005) describes moment and shear interaction for sections in cross-section class 1 and 2. The cross-sections are not prone to buckle and it is the plasticity that governs the capacity of the sections. However, when using the effective width method, it is members in cross-section class 3 and 4 that are considered. These members will buckle before yielding is reached so it is the buckling capacity that governs the moment and shear interaction. The interaction with respect to buckling capacity is described in Eurocode 1993-1-5 (2006, Section 7.1).

Before checking the moment and shear interaction, it is necessary to determine whether interaction has an impact or whether it can be neglected. If the flange's capacity M_f is less than the applied moment M_{Ed} the moment and shear interaction has an impact on the flanges. If the design force V_{Ed} is greater than half of the capacity of the web $V_{bw.Rd}$ the interaction has an impact on both web and flange. Figure 2.15 show how the interaction check can be interpreted graphically. If the acting forces are within the marked area, interaction according to equation 2.43 is required. Interaction can occur for applied moments greater than M_f or shear forces greater than V_{bw} but is not critical to consider if not the requirements in equation 2.43 are fulfilled. Interaction that has an impact (marked area in Figure 2.15) works in such way that the design moment and axial forces, if there are any, are reduced to account for shear forces to be carried in the flanges as well as the web (Eurocode 1993-1-5, 2006, Section 7.1).

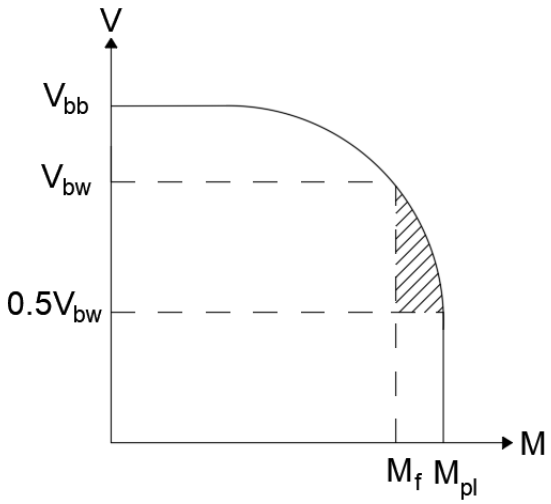

Figure 2.15: *Moment and shear interaction graph. In the marked area the interaction has an impact on the structural capacity. Adapted from Al-Emrani and Åkesson, 2020.*

$$\bar{\eta}_1 + (1 - \frac{M_{f.Rd}}{M_{pl.Rd}})(2\bar{\eta}_3 - 1)^2 \leq 1 \quad \text{for} \quad \bar{\eta}_1 \geq \frac{M_{f.Rd}}{M_{pl.Rd}} \quad \text{and} \quad \bar{\eta}_3 > 0.5 \tag{2.43}$$

where $\bar{\eta}_1 = \frac{M_{Ed}}{M_{pl.Rd}}$ and $\bar{\eta}_3 = \frac{V_{Ed}}{V_{bw.Rd}}$

Johansson et al. (2007, p. 95) states that the interaction equation is based on plastic resistance coming from studies analysing the bending resistance due to shear influence. It is further stated that regarding interaction for sections where buckling governs, there are no useful theories to describe the interaction and therefore the theory of plasticity is used in combination with test data from empirical studies on the subject (Johansson et al., 2007, p. 94-96).

Johansson et al. (2007, p. 95-97) describes that the reason for why interaction can be disregarded for values below $0.5 \cdot V_{bw.Rd}$ is due to computer simulations and studies performed. The studies' aim was to determine the influence of shear when considering moment and shear interaction for a CSC3 or CSC4 girder. The simulations conclude that small shear forces have little or no influence on the interaction. However, the simulations' results are not comparable with the design rules in Eurocode 1993-1-5 (2006). It is stated by Johansson et al. (2007, p. 97) that these simulations along with another separate study that uses Eurocode 1993-1-5 gives reliability on the design rules given, and that the design rules even are on the conservative side when compared to the simulations' results (Johansson et al., 2007, p. 96-97).

2.4.8 Necessity of capacity control for a cross-section

Buckling will not occur in every part of a plate. It is more likely for a buckle to arise in a central region of the plate than close to a support. This means that every section in a bridge girder for example might not need to be checked.

Eurocode 1993-1-5 (2006, Section 7.1) states that interaction, equation 2.43, does not apply in regions close to the supports with vertical stiffeners. In regions closer to the support than half of the web height $h_w/2$ or $0.4a$ (a is the length of the panel), it is deemed unlikely for buckles to occur since the buckles that do occur have a peak in more central parts of the plate and thus the stresses close to the supports are irrelevant and so is the buckling control there (Johansson et al., 2007, p. 97). Eurocode 1993-1-5 does not give any guidance on how to account for this statement when the section has longitudinal stiffeners but Johansson et al. (2007, p. 97) and Beg et al. (2010, p. 111) both declares that in engineering practice half of the height for the longest subpanel should be used when longitudinal stiffeners are present.

The statement that buckling control is irrelevant close to the supports have a significant influence on the design of a structure. This means that over a mid-support where the applied moment is at its largest, the buckling capacity of the girder does not need to be checked. This in turn results in the girder being able to fully utilise its cross-sectional capacity since the part can be regarded as to not be in CSC4 due

to the lack of buckling risk (Beg et al., 2010, p. 49).

2.5 Reduced stress method

The reduced stress method is an alternative method for calculating thin-walled structural elements' capacity. The method is described in Eurocode 1993-1-5 (2006) but in less detail than the reduced section method. The Eurocode used is from 2006 and Simon-Talero and Caballero (2010) states in 2010 that it is first then that the reduced stress method is researched in more detail. Therefor if there are any relevant findings in the reduced stress method theory, these are not accounted for in Eurocode 1993-1-5 (2006). This section describes what the reduced stress method is, how the calculations are performed and aids to give further knowledge to the equations and assumptions stated in Eurocode 1993-1-5 (2006).

For structural elements that are slender and might experience a risk of elastic buckling, the reduced stress method can be used instead of the effective width method. The stresses are reduced so that the capacity is regarded with respect to the section that first experience buckling. Beg et al. (2010, p. 160-161) describes that for cross-sections composed of more than one element, it is the lowest critical buckling stress in any part of the plate element that governs the whole cross-section's capacity. It is assumed that this stress is the largest stress that can act anywhere in the section before it buckles.

2.5.1 Reduced stress calculations

The calculations for this method can be divided into three categories. The design stresses in longitudinal (x) and transverse (z) direction, $\sigma_{x.Ed}$ and $\sigma_{z.Ed}$, as well as shear stresses, τ_{Ed} needs to be obtained together with the reduction factors $\rho_{c.x}$, $\rho_{c.z}$ and χ_v in order to calculate the utilisation factor of the structure. The design stresses are obtained from an FE-software by retrieving the buckling mode and multiplying it with the applied stress, resulting in the critical buckling stress of the member. One panel, web or flange, is calculated at the time. The most critical panel then decides the whole structure's capacity.

2.5.1.1 Slenderness factor

First the plate slenderness $\bar{\lambda}_p$ is determined by equation 2.44. The slenderness is then used to calculate the plate buckling reduction factors for both longitudinal and transverse stresses as well as the column-like buckling reduction factor. The slenderness is dependent on the critical and ultimate load amplifiers α_{cr} and $\alpha_{ult.k}$. The load amplifier α_{cr} is determined by the individual critical load amplifiers $\alpha_{cr.i}$ where i is the x- or z-direction. These factors are calculated as the critical stress $\sigma_{cr.i}$ divided by the design stress $\sigma_{i.Ed}$. The critical stress is calculated in the same way as for the effective width method, see equation 2.12. The stress ratios ψ_i are also calculated in the same way as the effective width method. The critical load amplifier due to shear stress $\alpha_{cr.\tau}$ is also needed and is calculated in the same way as for the

normal stresses. The critical stress is calculated as for an unstiffened plate times the shear buckling coefficient k_τ, see equation 2.30. The total critical load amplifier α_{cr} is calculated in equation 2.45 (Eurocode 1993-1-5, 2006, Section 10). The total critical load amplifier can also be obtained through FE-analysis and compared to the value that is calculated by hand, where the FE-value is less conservative and thus is used since the whole reduced stress method is very conservative as it is. Further the value of the load amplifier $\alpha_{ult.k}$ can be obtained by utilising the von Mises criterion, see equation 2.46.

$$\bar{\lambda}_p = \sqrt{\frac{\alpha_{ult.k}}{\alpha_{cr}}} \tag{2.44}$$

$$\alpha_{cr} = \frac{1}{\frac{1+\psi_x}{4\cdot\alpha_{cr.x}} + \frac{1+\psi_z}{4\cdot\alpha_{cr.z}} + \sqrt{\left(\frac{1+\psi_x}{4\cdot\alpha_{cr.x}} + \frac{1+\psi_z}{4\cdot\alpha_{cr.z}}\right)^2 + \frac{1-\psi_x}{2\cdot\alpha_{cr.x}^2} + \frac{1-\psi_z}{2\cdot\alpha_{cr.z}^2} + \frac{1}{\alpha_{cr.\tau}^2}}} \tag{2.45}$$

$$\alpha_{ult.k} = \sqrt{\frac{1}{\left(\frac{\sigma_{x.Ed}}{f_y/\gamma_{M1}}\right)^2 + \left(\frac{\sigma_{z.Ed}}{f_y/\gamma_{M1}}\right)^2 - \left(\frac{\sigma_{x.Ed}}{f_y/\gamma_{M1}}\right)\cdot\left(\frac{\sigma_{x.Ed}}{f_y/\gamma_{M1}}\right) + 3\cdot\left(\frac{\tau_{Ed}}{f_y/\gamma_{M1}}\right)^2}} \tag{2.46}$$

2.5.1.2 Plate and column-like buckling

To account for the plate or column-like buckling, the reduction factors for these phenomena are calculated. The reduction factors $\rho_{pc.x}$ and $\rho_{pc.z}$ for plate buckling in the longitudinal or transverse direction and column-like buckling χ_c are calculated. These reduction factors are then used to receive the global reduction factors $\rho_{c.x}$ and $\rho_{c.z}$ with the interpolation formula, equation 2.20 and equation 2.49 to obtain ξ.

In x-direction the plate reduction factor $\rho_{pc.x}$ is calculated as for the effective width method, using equation 2.6, with the slenderness from equation 2.44. However, for the transverse stresses it is not appropriate to calculate the reduction factor in the same way as for the longitudinal stresses according to Beg et al. (2010, p. 164-165). It is not justifiable to transfer the reduction factor $\rho_{pc.z}$ fully to transverse stresses which could result in unsafe results. For the reduction factor for transverse stresses it is therefore recommended to perform equations 2.47 and 2.48 to get $\rho_{pc.z}$. These equations do not allow for the same amount of post-critical reserve strength as $\rho_{pc.x}$ does. The values of $\bar{\lambda}_{p0}$ and α_p depends on what kind of stress the member is subjected to and if the section is hot rolled, welded or cold-formed. For a welded section with transverse stresses the values are; $\bar{\lambda}_{p0} = 0.8$ and $\alpha_p = 0.34$ (Eurocode 1993-1-5, 2006, Section B.1). The column-like buckling reduction factor χ_c is calculated using equation 2.13.

$$\rho_{pc.z} = \frac{1}{\varphi + \sqrt{\varphi^2 - \bar{\lambda}_p^2}} \tag{2.47}$$

$$\varphi = 0.5 \cdot (1 + \alpha_p \cdot (\bar{\lambda}_p - \bar{\lambda}_{p0}) + \bar{\lambda}_p) \tag{2.48}$$

$$\xi = \frac{\sigma_{cr.x}}{\sigma_{cr.c}} - 1 \quad 0 \leq \xi \leq 1 \tag{2.49}$$

2.5.1.3 Utilisation factor

The reduction factors $\rho_{c.x}$ and $\rho_{c.z}$ in equations 2.50 and 2.51 considers the global reduction factor that accounts for interaction between plate and column-like buckling. The shear reduction factor χ_v is calculated using Table 2.2 and is also considered in the same equations that calculate the utilisation of the structure.

The reduced stress method results in a utilisation factor U that can either be calculated according to equation 2.50 or equation 2.51. The one comparing to the minimum value of $\rho_{c.x}$, $\rho_{c.z}$ and χ_v is more conservative and does not allow for different reduction factors in different directions. The reduced stress method allows for interaction between different stress types which is regarded by utilising the von Mises criterion, $\sigma_x^2 + \sigma_z^2 - \sigma_x \cdot \sigma_z + 3\tau^2 = \sigma_{eq}^2$, as can be seen in the two equations. This also means that moment, shear and the interaction between moment and shear do not need to be checked individually (Beg et al., 2010, p.161). Another way of calculating the utilisation is by looking at only normal or shear stresses. These stresses are compared to the yield stress f_y and the reduction factor $\rho_{c.x}$, $\rho_{c.z}$ for normal stresses and χ_v for shear stresses, see equation 2.52 and 2.53. The utilisation factor used is then the maximum utilisation out of U_i, U_τ and the smallest of U_1 and U_2, where i in U_i stands for the directions x or z.

$$U_1 = \frac{\sqrt{\left(\frac{\sigma_{x.Ed}}{f_y/\gamma_{M1}}\right)^2 + \left(\frac{\sigma_{z.Ed}}{f_y/\gamma_{M1}}\right)^2 - \left(\frac{\sigma_{x.Ed}}{f_y/\gamma_{M1}}\right) \cdot \left(\frac{\sigma_{z.Ed}}{f_y/\gamma_{M1}}\right) + 3 \cdot \left(\frac{\tau_{Ed}}{f_y/\gamma_{M1}}\right)^2}}{\min(\rho_{cx}, \rho_{cz}, \chi_v)} \leq 1 \tag{2.50}$$

$$U_2 = \left(\frac{\sigma_{x.Ed}}{\rho_{cx} f_y/\gamma_{M1}}\right)^2 + \left(\frac{\sigma_{z.Ed}}{\rho_{cz} f_y/\gamma_{M1}}\right)^2 - \left(\frac{\sigma_{x.Ed}}{\rho_{cx} f_y/\gamma_{M1}}\right) \cdot \left(\frac{\sigma_{z.Ed}}{\rho_{cz} f_y/\gamma_{M1}}\right) + 3 \cdot \left(\frac{\tau_{Ed}}{\chi_v f_y/\gamma_{M1}}\right)^2 \leq 1 \tag{2.51}$$

$$U_i = \frac{\sigma_{i.Ed}}{\rho_{ci} f_y/\gamma_{M1}} \tag{2.52}$$

$$U_\tau = \frac{\tau_{Ed}}{\chi_v f_y / \sqrt{3} \gamma_{M1}} \tag{2.53}$$

2.6 Advantages of the two methods

In Eurocode 1993-1-5 (2006) there are no clear description on which method should be used when but they both have advantages to regard.

Johansson et al. (2007, p. 16) states that an advantage with the effective width method is that the iteration process to determine the neutral axis is more effective along with determining the local stiffness. The longitudinal stiffeners can be included in this method when checking the column-like buckling capacity (Johansson et al., 2007, p. 16) but they need to be in horizontal planes and not inclined for this method to consider their effects. Johansson et al. (2007, p. 63) states that the flanges need to be parallel, with a maximum inclination of 10° and that the plates should be rectangular in order for this method to be used.

Some advantages with the reduced stress method are that it is easy to use in combination with FE-analysis (Johansson et al., 2007, p. 9) and thus complex cross-sections can be regarded efficiently since the design is based on the gross cross-section (Beg, 2012, p. 304). Another advantage of the reduced stress method is its capability to deal with complex stresses, such stresses can be shear and biaxial direct stress (Johansson and Veljkovic, 2009, Beg, 2012, p. 305). It is the load amplifier $\alpha_{ult.k}$ and α_{cr} that enables further calculations, and the load amplifiers are obtained either by the FE-analysis or by numerical calculations, which can be performed in a simple step, or by hand calculations (Beg et al., 2010, p. 164). However, observe that this method results in the buckling strength to be close to the yielding strength when put to practice. This is due to the fact that no stress redistribution occur since the limit is set to that of the weakest buckling stress (Beg et al., 2010, p. 164).

2.7 Other instability phenomena that can influence the buckling behaviour

There exist several other phenomena that can influence the buckling behaviour. These behaviours include shear lag and lateral torsional (LT) buckling. Shear lag, if present needs to be considered with respect to plate buckling, and LT-buckling is a global instability phenomenon on its own.

2.7.1 Shear lag

The first step in determining the effective cross-sectional area in a beam is to check if the flange of a girder experience shear lag. According to Eurocode 1993-1-5 (2006) shear lag needs to be considered if equation 2.54 applies. Where b_0 is half of the flange length for an internal flange or the whole length of an outstand flange, and L_e

is the length between the zero moment intersection points for the bending moment (Eurocode 1993-1-5, 2006, Section 3.2). If shear lag needs to be considered, the width of the flanges is reduced according to equation 2.55 for the elastic effects and where β comes from Eurocode 1993-1-5 (2006, Section 3.2). Depending on if the control is performed in SLS or ULS different equations are used to calculate the effective width and the effective flange area. In SLS the elastic shear lag effects are regarded whereas in ULS the elastic effects are regarded along with plate buckling and elastic-plastic shear lag effects (Eurocode 1993-1-5, 2006, Section 3.3).

$$b_0 > L_e/50 \tag{2.54}$$

$$b_{eff} = \beta \cdot b_0 \tag{2.55}$$

2.7.1.1 Shear lag and plate buckling interaction

When shear lag is present and the ULS capacity is of interest, the influence of plate buckling needs to be regarded according to Eurocode 1993-1-5 (2006, Section 3.3). There are two cases, the combination of shear lag and plate buckling or elastic-plastic behaviour of the shear lag effect. The checks are only described in short since shear lag is not a main focus in this thesis.

The first case, shear lag and plate buckling interaction is considered with the help of equation 2.56. The effective area of the flange in compression $A_{c.eff}$ is obtained by plate buckling calculations of the element. The contribution of the shear lag is considered in β_{ult} that comes from Table 3.1 in Eurocode 1993-1-5 (2006, Section 3.2) where instead of using the default a_0, another equation for a_0 is used when considering interaction.

$$A_{eff} = A_{c.eff} \cdot \beta_{ult} \tag{2.56}$$

The second case, elastic-plastic effects of shear lag in ULS that limits the plastic strains are calculated using equation 2.57 where β and κ comes from Table 3.1 in Eurocode 1993-1-5 (2006, Section 3.2).

$$A_{eff} = A_{c.eff} \cdot \beta^{\kappa} \geq A_{c.eff} \cdot \beta \tag{2.57}$$

In the unstiffened case the effective area $A_{c.eff}$ of the flange that is regarded in the shear lag calculations is calculated in equation 2.8 whereas for the stiffened flange, the effective area is calculated as seen in equation 2.10.

2.7.2 Lateral-torsional buckling

Lateral-torsional (LT) buckling occurs around the weak axis of a beam. It is an instability phenomena that consists of lateral deflection of the top flange due to compression of the flange, and torsional rotation due to warping (Al-Emrani and Åkesson, 2020, p. 35-37). LT-buckling is accounted for by reducing the critical moment capacity with a factor χ_{LT}. The reduction factor can be obtained in different ways according to Eurocode 1993-1-1 (2005, Section 6.3.2). The moment capacity of the beam is reduced due to lateral-torsional buckling in equation 2.58. However, in this thesis LT-buckling is not an area of interest and the LT-buckling reduction factor χ_{LT} is seen as 1, meaning that there is no reduction due to this phenomenon.

$$M_{b.Rd} = \chi_{LT} \cdot W_y \cdot \frac{f_y}{\gamma_{M1}} \tag{2.58}$$

3

Methodology

The methodology chapter describes how the two methods, the effective width method and reduced stress method are compared. The comparisons consisted of both a geometric parametrisation and force variation evaluation.

3.1 Description of the comparisons performed

The comparison of the two methods consisted of mainly two different models. For the effective width method there were two models of a box beam. One model that had unstiffened panels and the other model that included longitudinal stiffeners in both the web and the top flange. The models are illustrated in Figure 3.1. For the reduced stress method the same models were analysed.

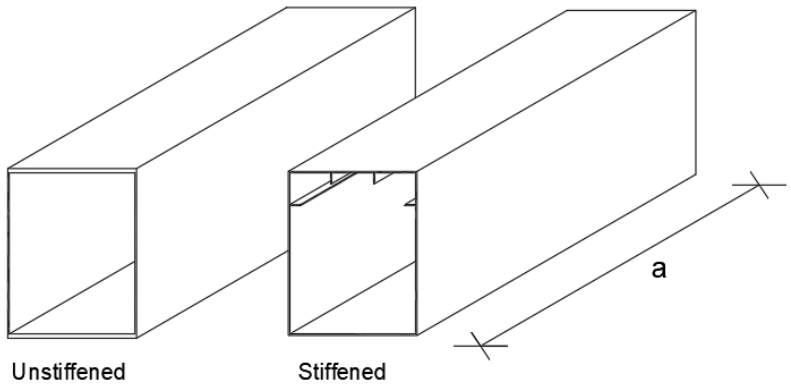

Figure 3.1: *To the left: an unstiffened box beam section. To the right a stiffened box beam section. The section is illustrated as the part between transverse stiffening, at the distance "a" from each other.*

The capacities of the two methods were calculated in order to compare the results. The effective width method was used as a baseline. The applied moment and shear forces were calculated for each case to correspond to 100 % utilisation of the cross-section, according to equations 2.23 and 2.43. The same forces were applied in the reduced stress method and the utilisation factor was calculated. The difference in

the utilisation factor were used to indicate if one method yielded higher capacity than the other.

3.1.1 Geometry

The unstiffened and stiffened models were analysed separately for the two methods. The methods were then compared for the same cross-sectional geometries for each of the models. The cross-section was also parametrised with respect to web and flange thicknesses and length between the transverse stiffeners. This was done to identify if the methods gave different results depending on the geometry. The parametrisation was performed by varying the web thickness over three values, the same was done for the flange thickness. The thicknesses looked at were different depending on if it was the unstiffened or stiffened model that was analysed. The third parameter, distance between transverse stiffeners changed between four different lengths. The same lengths were analysed for both unstiffened and stiffened beam. How the parametric values were chosen is described and stated in Chapter 4.

3.1.2 Force variation

The box beam also experienced different variations of moment and shear force. Three scenarios were investigated. One analysis had an applied shear force corresponding to 100% of the shear capacity and zero bending moment (Case 1). Another analysis had bending moment corresponding to 100% of the moment capacity and zero shear force (Case 2) and a third utilised 80% of the respective capacities, both shear force and moment (Case 3). This was done to illustrate different parts of a fictitious simply supported girder that was analysed in three sections. Figure 3.2 show how this could be interpreted. The part closest to an edge support (Case 1), in the middle of the span (Case 2) and at a mid-support in a continuous two-span beam model (Case 3).

For this comparison, just as for the geometric, the utilisation factor of the effective width method was used as a basis and the utilisation from the reduced stress method was compared against it.

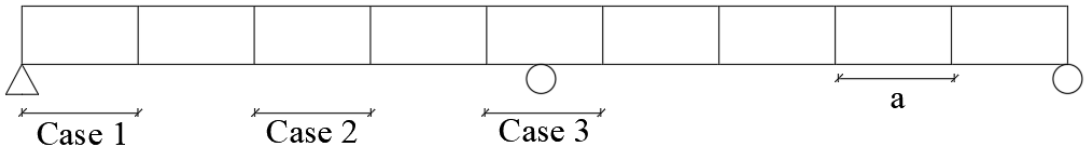

Figure 3.2: *A simply supported girder that show where the three different cases of force configurations can be interpreted. The distance between transverse stiffeners is marked as "a".*

3.2 Execution

The comparisons of the effective width method and reduced stress method were performed by using Eurocode 1993-1-5. For the calculations a Mathcad file for all models were computed. The equations were easily interpreted and visualised through these files. Excel was then used to parametrise the models and calculate the different comparisons that were examined. One row in Excel corresponded to one Mathcad file making the calculations very efficient. The effective width method only needed hand calculated results. However, the reduced stress method needed to use an FE-software in order to receive the results.

The load amplifying factor α_{cr} used in the reduced stress method was calculated using the FE-software ABAQUS. The web and flange panels were separately modelled and analysed since the method required the buckling modes for the web and flange individually. The mode resulting in the most critical case was then used to obtain the results. The FE-computed buckling modes were used in Excel to perform the parametric calculations for the reduced stress method.

A Python script was created to enable the parametric study in ABAQUS with alternating buckling modes associated to different steel panels with the same dimensions and properties as were investigated in the effective width method. The script enabled several different models to be computed simultaneously and the buckling mode for all these cases were easily retrieved at once. See Appendix E for the script of one of the panels.

The software EBPlate has been used to verify some results obtained in ABAQUS. EBPlate is a tool that assesses critical elastic buckling stresses and show buckling modes for plate elements subjected to bending and shear stresses (Centre Technique Industriel de la Construction Metallique (CTICM), n.d.). The software works for both unstiffened and longitudinal and transversely stiffened plates.

3.2.1 Visualisation of the results

To show the impact of the geometric variations, the difference between flange and web slenderness visualises the difference in results between the effective width method and reduced stress method in a good way according to van der Burg (2011, p. 14). Therefore, it was chosen to compare the utilisation difference of the two methods to the slenderness difference of the flange and web. The slenderness difference between the web and flange came from the effective width method since it was the method that was used as a baseline for the comparison of the utilisation.

For the force variations result, each case of flange and web thickness and distance between transverse stiffeners was evaluated with both the reduced stress method and the effective width method. The difference between the two methods were visualised by comparing them case by case for all three force variations, shear, moment and a combination of shear and moment.

4

Beam model

This chapter describes how the model of the box beam that is used in the comparison of the methods is designed. Which dimensions that are chosen and how they are varied. The location of the longitudinal stiffeners and distance between transverse stiffeners. The bending moment and shear force that is applied on the structure is also stated.

4.1 Geometry

The models are divided into one unstiffened model and one stiffened. Figure 4.1 show the two models' cross-sections. The unstiffened model is a box beam that consists of two identical webs and one bottom flange and one top flange. The stiffened model consists of the same structure but has one stiffener added to each web and two stiffeners added to the top flange. The placement of the stiffeners is kept constant throughout the parametric study. In Table 4.1 all the fixed dimensions are stated for both models.

For the stiffened beam the stiffeners are also checked, the stiffeners are designed to be in CSC3 or lower to not buckle locally, Appendix B show the calculations for this. Global buckling can occur and is accounted for by using a reduction factor called ρ_c for the cross-section affected by this, see Section 2.4.2. The placement of the web stiffener is chosen in such a way that the reduction of the effective area is as small as possible. This placement is calculated by iteration to find the optimal placement, for this cross-section the optimal placement is at 288 mm from the top of the web. This corresponds well to what Al-Emrani and Åkesson (2020, p. 89) claims, which is that 20 % down from the top edge is usually a good placement. Therefor the distance of 300 mm is chosen for the beam with height 1500 mm as a simplification. The flange stiffeners are placed at an even distance between each other and the webs.

Table 4.1: *Dimensions that are kept constant throughout the parametrisation.*

	Unstiffened model	**Stiffened model**
Width of flange b_f	1200 mm	1200 mm
Height of web h_w	1500 mm	1500 mm
Thickness of stiffener t_{sl}	-	10 mm
Length of stiffener h_{sl}	-	60 mm
Distance to:		
Web stiffener h_{w1}	-	300 mm
First flange stiffener b_{f1}	-	400 mm
Second flange stiffener b_{f2}	-	800 mm

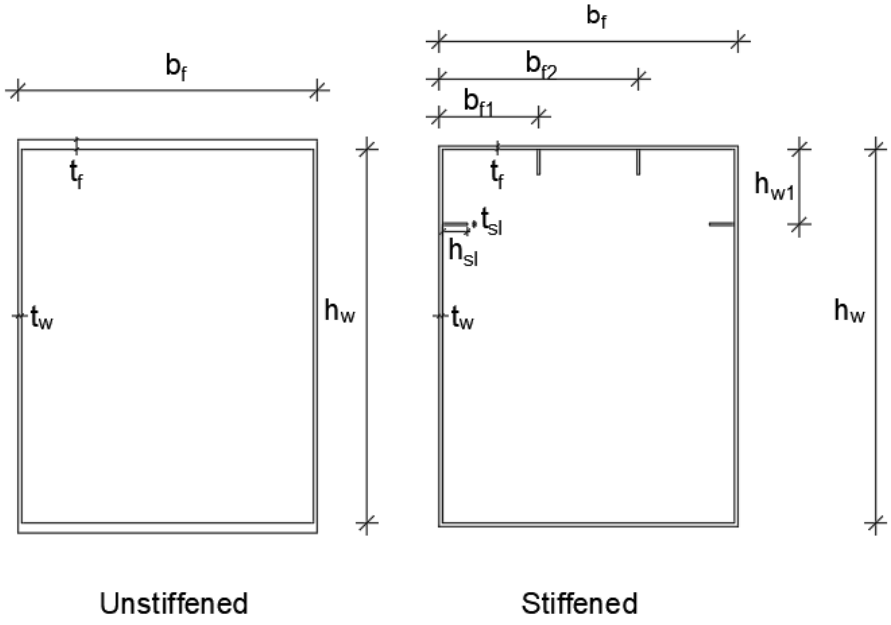

Figure 4.1: *Illustration of cross-sections for the unstiffened and stiffened box beams, thickness and stiffeners are not in scale.*

In the parametrisation of the beam, three parameters are changed. These are the thickness of the flange, the thickness of the web and the distance between the transverse stiffeners. The thicknesses for the two models are based on the cross-section class limits to assign thicknesses that are either on the limit between CSC3 and CSC4 or in CSC4. The cross-section classes for web and flange are calculated according to Appendix B. The thickness is reduced to about 75 % and 50 % of the original thickness for both the unstiffened and the stiffened model. The distance between the transverse stiffeners is chosen to be one, two, three and four times the height of the web. The unstiffened model starts from a much stockier size and the most slender dimension of it corresponds to the most stocky dimensions of the stiffened model. Table 4.2 states the variable dimensions of the beam.

Table 4.2: *Dimensions that change throughout the parametrisation. Thickness of flange and web and distance between transverse stiffeners.*

	Unstiffened model	**Stiffened model**
Thickness of flange t_f	[40, 25, 14] mm	[14, 10, 7] mm
Thickness of web t_w	[14, 11, 8] mm	[8, 6, 4] mm
Distance between transverse stiffeners a	[1.5, 3, 4.5, 6] m	[1.5, 3, 4.5, 6] m

4.2 Forces

Another parameter that is changed is the applied forces. Changing the variations of bending and shear force aids to gather information about how different sections of the beam respond to the two methods that are compared. The different force variations seen in Table 4.3 are supposed to resemble a point of the beam where shear force is dominant, to a point where they both have impact and lastly a point where the moment is dominant.

Table 4.3: *Forces that change throughout the parametrisation. Three different cases are examined. The percentage refers to how much of the capacity is applied.*

	Shear force	**Moment**
Case 1	100 %	0 %
Case 2	0 %	100 %
Case 3	80 %	80 %

5

FE-model

This chapter describes how the FE-model is designed, which element and mesh type and size is used, how boundary conditions and loads are applied and how the model is verified. The verification consists of a convergence study for the mesh, an analysis of the stresses in the plate and a comparison of the stresses and buckling mode to another elastic buckling program called EBPlate.

5.1 Geometry

The FE-model is analysed one panel at a time, meaning that the web and flange plates are evaluated separately. The panel width is the length between two transverse stiffeners. The height of the panel is the height of the web or the width of the flange. For the plates with stiffeners, the stiffener's dimensions are constant. The dimensions used for the FE-model are the same as for the cross-section for which hand calculations are performed, see Tables 4.1 and 4.2.

5.2 Element type and mesh

The panel is created using quadratic 3D shell elements. The elements are assigned a thickness according to Table 4.2. The stiffeners are also modelled with quadratic 3D shell elements.

The mesh used consists of elements with size 45 mm x 45 mm. The same mesh is used for all analyses, both for the unstiffened and stiffened plate and for the web and flange plates, see Figure 5.1 that show the stiffened flange's mesh. A convergence analysis for the mesh size and element type is conducted. The analysis can be seen in Section 5.5.1.

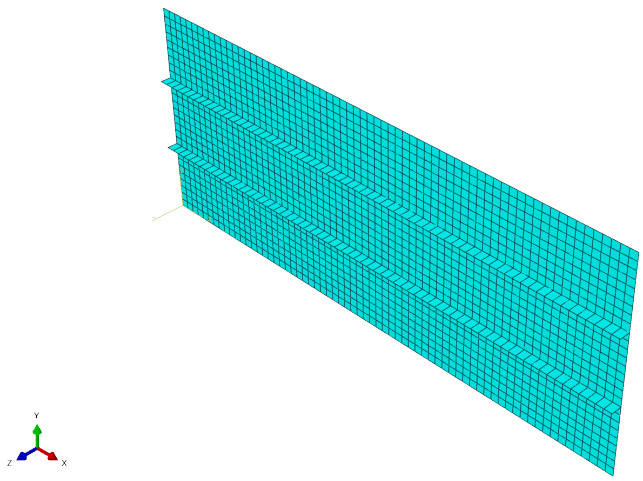

Figure 5.1: *Mesh of flange panel with two stiffeners. Mesh size is 45 x 45 [mm].*

5.3 Boundary conditions

Figures 5.2 and 5.3 show the boundary conditions for the web and flange panels respectively. The panels are fixed around all edges for out-of-plane translation (in z-direction). The bottom left node is fixed against vertical translation in y-direction. The left edge is fixed against longitudinal translation in x-direction. The stiffeners have no boundary condition of their own. Verification for the stress distribution in the panel can be found in Section 5.5.2. The general buckling behaviour of the panel is verified in Section 5.5.3.

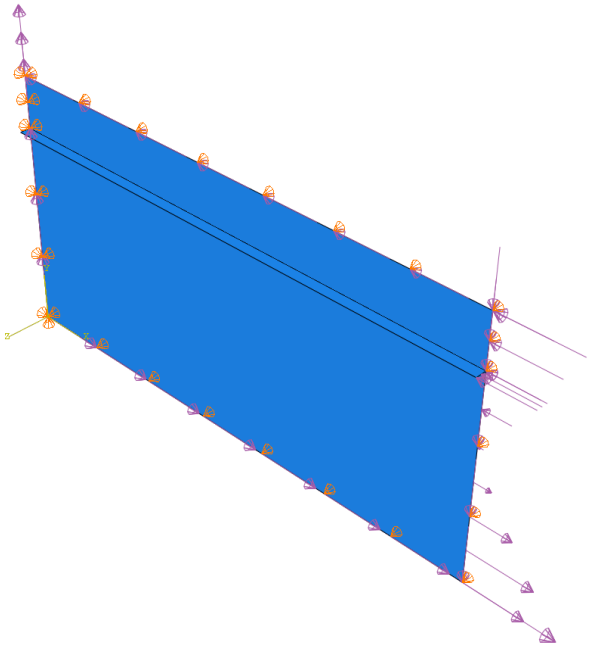

Figure 5.2: *Boundary conditions and loads on the panel in ABAQUS. Here a web panel with one stiffener is shown.*

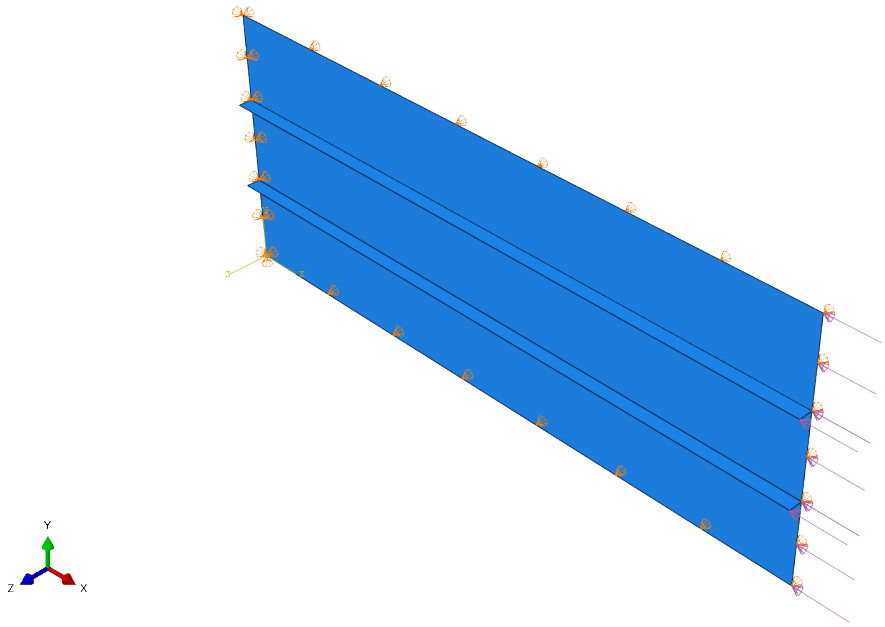

Figure 5.3: *Boundary conditions and loads on the panel in ABAQUS. Here a flange panel with two stiffeners is shown.*

5.4 Loads

The loads that are applied to the panel are modelled as stresses acting on the edges. The size of the stresses is varied for each geometry. There are three sets of load configurations that are applied to the geometries described in Chapter 4. For the web panel both moment and shear force are acting on the structure. Both types are applied as shell edge loads. The moment is acting as stresses with linear distribution and the shear as traction, as can be seen in Figure 5.2. For the stiffened web, the shift in neutral axis due to the stiffener is accounted for in the linearly distributed stresses. For the flange panel, the moment is in uniform compression, and thus uniformly distributed as can be seen in Figure 5.3. No shear stress acts on the flange panel. For the stress distribution and buckling mode to correspond to theory, since the panel is fixed in x-direction on the left edge, the stresses corresponding to the moment is only applied on the right edge for both the web and flange panels.

5.5 Verification of the FE-model

The FE-model needs to be reliable and show accurate results. The first step to verify that it does, is to do a convergence study. With a converged mesh size the other verifications are performed. The stress distribution in the plate confirms if the correct boundary conditions are applied. Further, the model is compared to a commercial elastic buckling program, EBPlate to both compare the buckling mode in size and shape.

The verification is executed for both an unstiffened beam and stiffened beam. The geometry for which the verifications is performed is stated in Table 5.1.

Table 5.1: *The geometry of the web and flange panels that are used in the verification of the FE-model.*

Unstiffened	**Cross-section** Height x Thickness [mm]	**Length of panel** [m]
Web	1500 x 14	3
Flange	1200 x 25	3
Stiffened		
Web	1500 x 8	3
Flange	1200 x 10	3

5.5.1 Convergence analysis of the FE-model

The convergence study is performed as such that the mesh size of the model varies and the result in form of the first buckling mode is plotted in Figure 5.4. The element types, quadratic and linear elements are compared and Figure 5.4 show that for quadratic elements the model can be regarded as converged at the first mesh iteration. For the linear element type, convergence occurs much later, thus quadratic elements are used in the model. The mesh size 45 mm is continued with in the calculations.

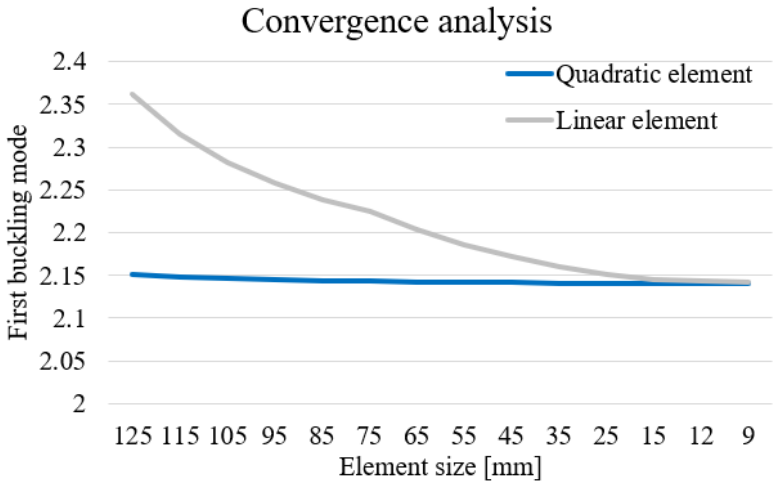

Figure 5.4: *Convergence analysis for mesh size and first buckling mode for linear and quadratic elements.*

5.5.2 Stress distribution in the plate

The stresses at the edges around the whole panel need to show that the boundary conditions give the expected stress distribution in the panel when the loads are applied. The web and flange are both checked since they experience different types

of loads and thus different stress distributions. The stresses are analysed using a path in ABAQUS, showing how the stresses vary along the path. A path is created for each edge to verify the behaviour. Three contour plots are shown in Figures 5.5, 5.6 and 5.7. The web is subjected to solely moment which varies linearly over the left and right edge. The force is applied as stresses σ_{xx} with the same distribution as the load has. In the top edge the panel is compressed and bottom is in tension. For the web subjected to solely shear the whole web is subjected to the same stress. The flange is subjected to uniform compression and thus the whole plate is in compression. Both the unstiffened and the stiffened models' stress distributions are checked and give similar results, hence only the stiffened stress distribution is shown in Figures 5.5, 5.6 and 5.7. All stresses indicate that the plate's boundary conditions are correct.

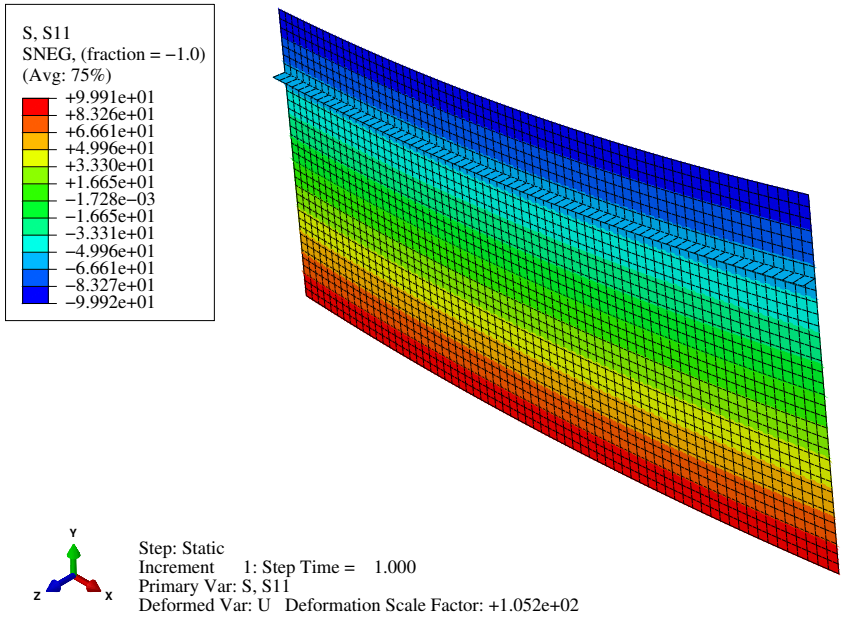

Figure 5.5: *Web panel's stress distribution in σ_{xx} direction for a stiffened web subjected to bending.*

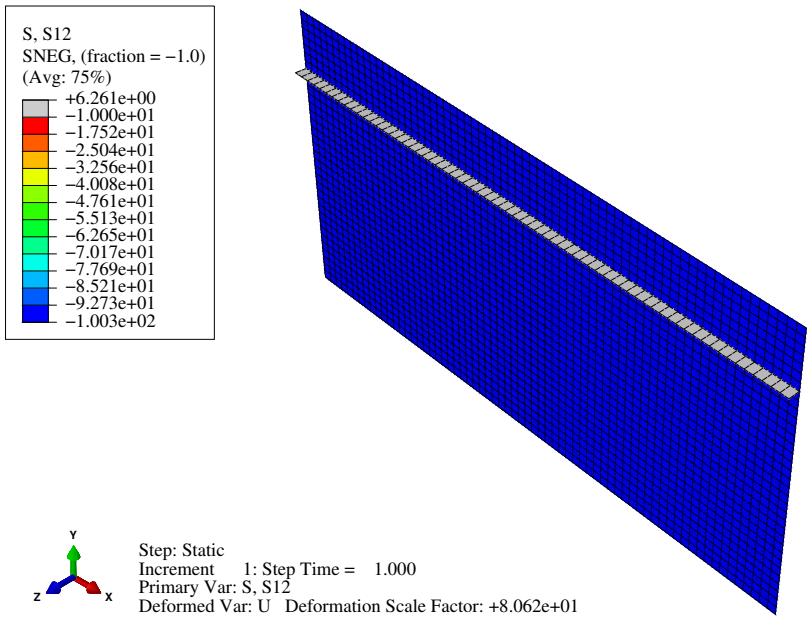

Figure 5.6: *Web panel's stress distribution in σ_{xy} direction for a stiffened web subjected to shear.*

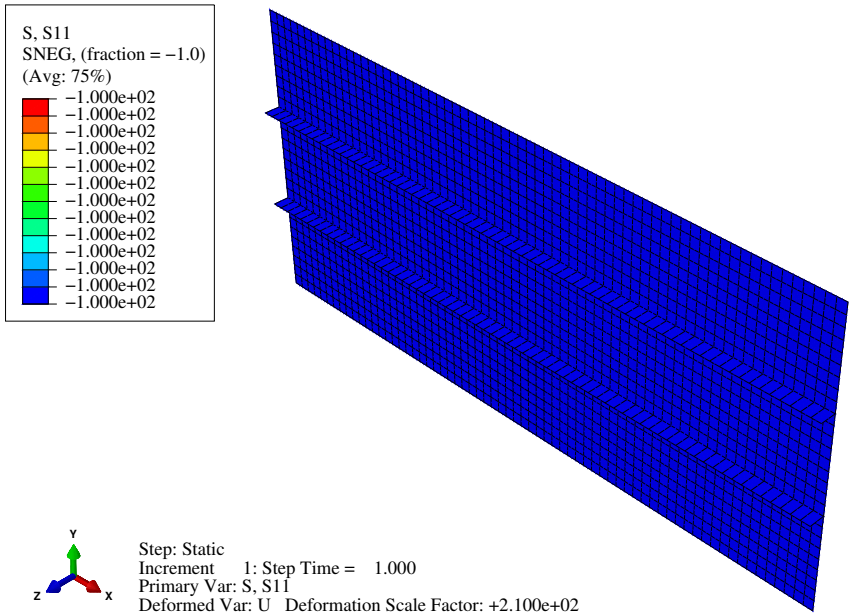

Figure 5.7: *Flange panel's stress distribution in σ_{xx} direction for a stiffened flange subjected to bending.*

5.5.3 Verification of the FE-model against EBPlate

The ABAQUS model that is used in the reduced stress method is verified against the free software EBPlate and hand calculations. The verification is first conducted for

the case of an unstiffened plate and then of a stiffened plate. The verification is made by comparing the stresses of the FE-model created in ABAQUS with analytically solved critical buckling stresses and EBPlate's stresses. Further the buckling mode from ABAQUS is compared to that of EBPlate.

The buckling mode for the stiffened web subjected to both moment and shear stresses is shown in Figure 5.8 and 5.9. As can be seen, the buckling mode looks the same in both softwares meaning that ABAQUS gives results similar to EBPlate and that the model is working correctly.

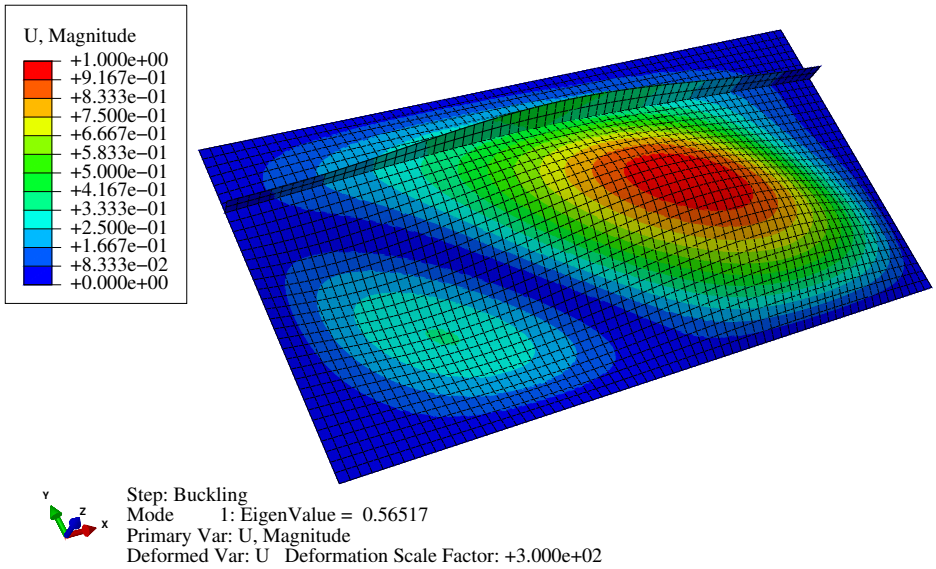

Figure 5.8: *Buckling mode in ABAQUS.*

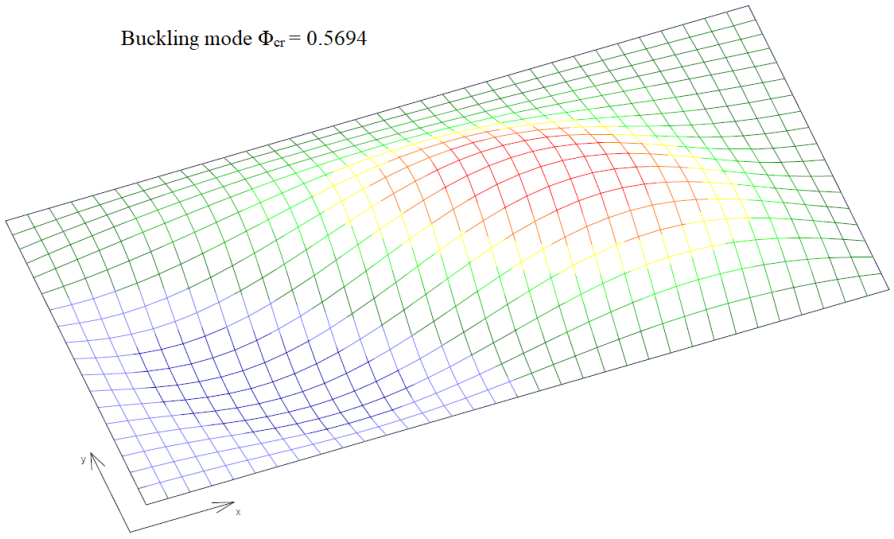

Figure 5.9: *Buckling mode in EBPlate.*

In Table 5.2 the differences of critical stresses calculated with ABAQUS, EBPlate and analytical methods are presented. The difference is calculated according to equation 5.1. For the unstiffened beam the critical stress is calculated and compared to ABAQUS with both an analytical method, i.e. hand calculations, and with EBPlate. All the force variations are also calculated and compared. The difference for the unstiffened beam when comparing ABAQUS with EBPlate show very small and consistent differences between the two methods which further validates the choices of boundary conditions and placement of loads. The consistent difference implies that both computer programs follow the same type of behaviour when the distance "a" is changed, and thus the aspect ratio a/b increases. When the analytically calculated critical stress is compared to ABAQUS the differences are generally quite small, but not as consistent. The results vary depending on the distance "a". The analytical method makes a simplification regarding the buckling coefficients k_σ and k_τ. For a plate that is simply supported and subjected to uniform compression, the buckling coefficient is $k_\sigma = 4$ according to Figure 2.8 that comes from Eurocode 1993-1-5 (2006). However, according to Fujikubo and Yao (2016), this is a simplified value. The buckling coefficient is actually varying depending on the aspect ratio a/b (Fujikubo and Yao, 2016, p. 83). Both EBPlate and ABAQUS use the actual value of the buckling coefficient.

$$Difference = \frac{\sigma_{cr.EBPlate} \quad or \quad \sigma_{cr.Analytical}}{\sigma_{cr.ABAQUS}} \tag{5.1}$$

The difference for the stiffened model is only compared between EBPlate and ABAQUS since the analytical method is very conservative when calculating the critical buckling stress for a stiffened beam. See the results of the comparison in Table 5.2, the difference is calculated according to equation 5.1. The two computer programs generally follow the same behaviour with small differences where most geometries and loading situations are within a margin of 4%, which is considered an acceptable difference. The largest outlier, 5.5% comes from the loading situation of only applying a linearly distributed moment on the web. EBPlate uses beam elements when modelling the stiffener, which could be done in ABAQUS as well but Abaqus and Simulia (2011, p. 6-6) recommends using shell elements if web or flange buckle of the stiffeners is important. In the ABAQUS model shell elements have therefore been used for stiffeners. The beam element could provide some extra capacity due to the beam element having rotational stiffness. The difference 5.5% is accepted and the stiffened model is thus considered validated.

Table 5.2: *Verification of the FE-model compared to EBPlate and analytical critical stress for the geometry 1500 x 8 [mm] for the web and 1200 x 10 [mm] for the flange. The models are subjected to 100 MPa for both moment and shear stresses.*

Type of stress	**Distance "*a*" [m]**	**Critical stress ABAQUS vs EBPlate [%]**	**Critical stress ABAQUS vs analytical [%]**	**Critical stress ABAQUS vs EBPlate [%]**
Model		Unstiffened	Unstiffened	Stiffened
Shear (web)	1.5	0.8	1.0	1.3
	3.0	0.4	-2.8	1.2
	4.5	0.4	-0.6	1.4
	6.0	0.4	-0.3	1.1
Bending (web)	1.5	0.9	-5.4	5.5
	3.0	0.7	0.9	2.5
	4.5	0.6	-0.2	3.2
	6.0	0.6	0.8	3.8
Combined (web)	1.5	0.9	-	2.6
	3.0	0.5	-	1.7
	4.5	0.4	-	1.7
	6.0	0.4	-	1.4
Bending (flange)	1.5	1.8	-3.1	-1.6
	3.0	1.6	-1.7	-1.1
	4.5	1.4	1.0	-2.3
	6.0	1.4	1.4	-1.1

6

Calculation example

This chapter goes through the calculations that are performed for one specific beam section. This example aims to provide a step-by-step execution of the work. First the effective width method is used to calculate the beam's capacity and then the reduced stress method is used to do the same.

The beam section that this calculation example use is a stiffened beam with the same geometry as is verified in the FE-model. The web is 1500 x 8 mm, the flange 1200 x 10 mm and the length of the panels are 3 m, see Table 5.1 for the dimensions. The cross-section with dimensions is shown in Figure 6.1. The load that is used in both Section 6.2 and 6.3 is 80% of the maximum allowed moment and shear force for this cross-section according to the calculations in Section 6.2.

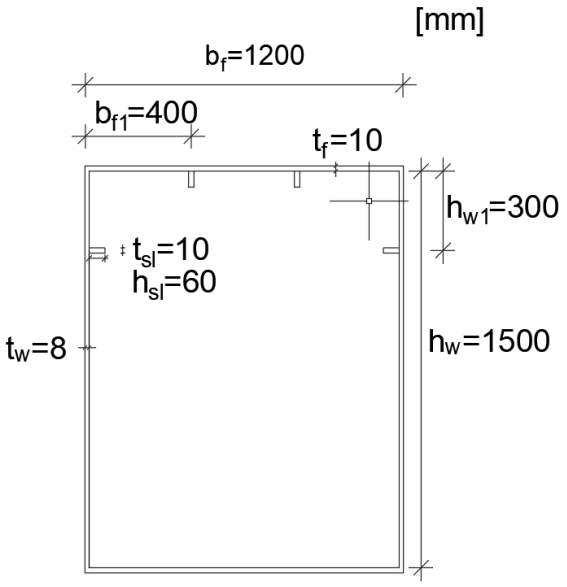

Figure 6.1: *Cross-section of the stiffened beam in the calculation example. The thicknesses are twice the actual size for illustrative purposes.*

6.1 Determine the cross-section class

First the cross-section class for each part or subpanel is determined. The stress that acts on each subpanel is calculated using Navier's formula, see equation 6.1, where d is the lever arm from the centre of gravity of the structure to the centre of the subpanel. If the part is in compression the cross-section class needs to be checked, if in tension the class is 1 and no reduction is needed. The shear stress is calculated in equation 6.2.

$$\sigma = \frac{N_{Ed}}{A_{tot}} + \frac{M_{Ed}}{I_z} \cdot d \tag{6.1}$$

$$\tau_{Ed} = \frac{V_{Ed}}{2 \cdot h_w \cdot t_w} \tag{6.2}$$

The thickness-to-width ratio is the length of the compressed part divided by the thickness of the same part. This ratio is then compared to the limits for cross-section classes stated in Table 5.2 in Eurocode 1993-1-1. The cross-section classes are calculated and stated in Table 6.1. For the flange that is subjected to uniform compression the stress ratio $\psi = 1$ and the buckling factor $k_\sigma = 4$. For the web that is subjected to linearly distributed stress, Figure 2.8 show how stress ratios and buckling factor is calculated and the result is stated in Table 6.1.

Table 6.1: *Cross-section classes, stresses, stress ratios and buckling factors for the stiffened beam.*

Subpanel	**CSC** [-]	**Stress σ top/bottom** [MPa]	**Stress ratio ψ** [-]	**Buckling factor k_σ** [-]
Top flange; outer part	4	-225/-	1	4
Top flange; between stiffeners	4	-225/-	1	4
Bottom flange	1	243/-	1	4
Web: above stiffener	4	-224/-131	0.58	5.02
Web: below stiffener	3	-131/241	-1.84	48.32
		Stress τ		**Buckling factor k_τ**
Flange		-		-
Web		67.25		7.83

6.2 Effective width method

For parts in CSC4 reduction of the area due to buckling of the subpanels are calculated first. Then the effective area due to global buckling of the stiffened section is accounted for.

The reduction of the subpanels consists of calculating the reduction factor ρ and then reducing the area by reducing the widths of the subpanels. Equation 6.3 show the slenderness calculation for the outer part of the top flange, equation 6.4 the reduction factor for the same subpanel and equation 6.5 the effective width of that part. The effective width for the web that has linearly distributed stress is calculated according to Figure 2.8. Table 6.2 then summarises the reduction factors and effective widths of all subpanels and Figure 6.2 illustrates how the effective areas can be interpreted.

$$\bar{\lambda}_p = \frac{\bar{b}/t}{28.4 \cdot \varepsilon \cdot \sqrt{k_\sigma}} = \frac{b_{f1} - t_w - (t_{sl}/2)/t_f}{28.4 \cdot \varepsilon \cdot \sqrt{k_\sigma}} = 0.91 \tag{6.3}$$

$$\rho = \begin{cases} 1 & \text{if } \bar{\lambda}_p \leq 0.5 + \sqrt{0.085 - 0.055\psi} \\ \dfrac{\bar{\lambda}_p - 0.055 \cdot (3+\psi)}{\bar{\lambda}_p^2} \leq 1 & \text{if } \bar{\lambda}_p > 0.5 + \sqrt{0.085 - 0.055\psi} \end{cases} = 0.83 \tag{6.4}$$

$$b_{eff} = \begin{cases} b_{eff1} = 0.5 \cdot \rho \cdot \bar{b} = 168\text{mm} \\ b_{eff2} = 0.5 \cdot \rho \cdot \bar{b} = 168\text{mm} \end{cases} \tag{6.5}$$

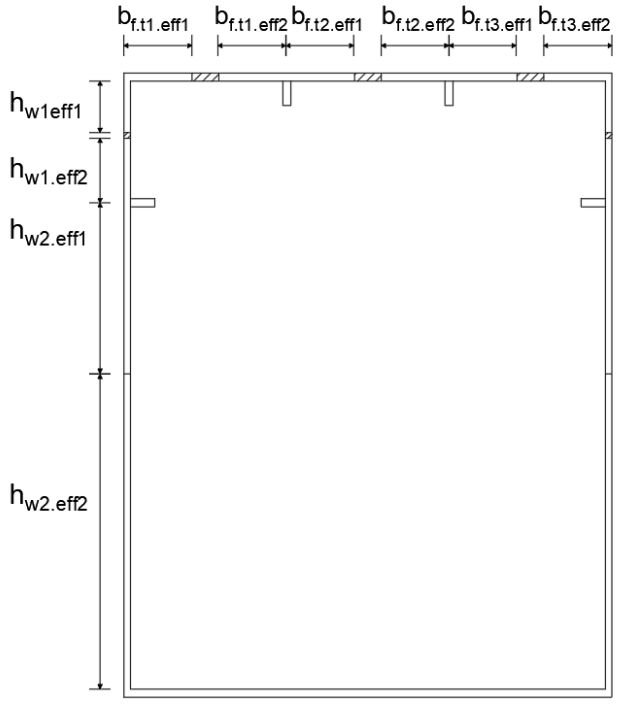

Figure 6.2: *The effective cross-section when the subpanels in CSC4 have been reduced. The thicknesses are twice the actual size for illustrative purposes.*

Table 6.2: *Reduction factor and effective widths of the subpanels.*

Subpanel	**Slenderness** $\bar{\lambda}_p$ [-]	**Reduction factor** ρ [-]	**Effective width** b_{eff} [mm]
Top flange; outer part	0.91	0.83	$b_{f.t1.eff1}$ 168 $b_{f.t1.eff2}$ 168
Top flange; between stiffeners	0.92	0.83	$b_{f.t2.eff1}$= 167 $b_{f.t2.eff1}$= 167
Bottom flange	2.79	1	$b_{f.b.eff1}$= 600 $b_{f.b.eff2}$= 600
Web: above stiffener	0.79	0.95	$h_{w1.eff1}$= 127 $h_{w1.eff2}$= 159
Web: below stiffener	1.02	1	$h_{w.2.eff1}$= 422 $h_{w.2.eff2c}$= 0 $h_{w.2.eff2}$= 778

When the first reduction of the subpanels is done, the global reduction factor ρ_c needs to be calculated. In order to obtain this buckling factor, the effective area of the stiffeners and subpanels that are in the compression zone $A_{c.eff.loc}$ needs to be known. The global buckling behaviour of the panel, web or flange also needs to be obtained. For this both plate and column-like buckling stresses $\sigma_{cr.p}$ and $\sigma_{cr.c}$ of the stiffener with adjacent parts of the subpanel is calculated.

6.2.1 Global buckling reduction of panels

The global reduction factor ρ_c is calculated as a weighted reduction factor for the web and flange sections separately. The weighted factor considers both plate buckling and column-like buckling.

6.2.1.1 Effective area of stiffener

The widths of the subpanels above and below the stiffener in the compression zone are calculated. Since the stress goes from compression to tension in the web somewhere below the stiffener, it is important to only consider the contributing width of the subpanel from the compressed part. The contributing width of the subpanel above the stiffener is calculated in equation 6.6 and for the part below the stiffener in equation 6.7 where b_c is the height of the compression zone. The gross area of the stiffener and adjacent subpanels is $A_{sl.1.w}$ from equation 6.8.

$$b_{inf} = \frac{3 - \psi_{above.stiffener}}{5 - \psi_{above.stiffener}} \left(h_{w.1} - \frac{t_{sl}}{2} \right) = 161 \text{ mm} \tag{6.6}$$

$$b_{sup} = 0.4 \left(b_c - h_{w.1} - \frac{t_{sl}}{2} \right) = 167 \text{ mm} \tag{6.7}$$

$$A_{sl.1.w} = b_{sl.1} \cdot t_w + A_{sl} = (b_{inf} + b_{sup} + t_{sl})t_w + A_{sl} = 3310 \text{ mm}^2 \quad (6.8)$$

The effective width of the contributing parts are calculated in the same way but the instead of the gross heights $h_{w.1}$ and $b_c - h_{w.1}$ it is the effective height of the compression zone of the part above and below the stiffener, $h_{w1.eff1} + h_{w1.eff2}$ and $h_{w2.eff1} + h_{w2.eff2c}$ from Table 6.2 that is used. The effective area of the stiffener and adjacent web panel is

$$A_{sl.1.eff.w} = 3260 \text{ mm}^2$$

Since the web panel only has one stiffener, the effective area of the stiffeners and subpanels that are in the compression zone $A_{c.eff.loc}$ is the same as $A_{sl.1.eff.w}$.

The flange stiffener is calculated similarly, except that the flange is in uniform compression and the contributing parts have a width of half of the subpanels width according to Eurocode 1993-1-5 Section 4.5.1. See equation 6.9 for the gross area of the stiffener and adjacent subpanels $A_{sl.1.f}$ and equation 6.10 for the effective area of the flange stiffener $A_{sl.1.eff.f}$.

$$A_{sl.1.f} = \left(\frac{b_{f.t.1}}{2} + \frac{b_{f.t.2}}{2}\right) t_f + A_{sl} = 4600 \text{ mm}^2 \quad (6.9)$$

$$A_{sl.1.eff.f} = \left(\frac{b_{f.t.eff.1}}{2} + \frac{b_{f.t.eff.2}}{2}\right) t_f + A_{sl} = 3940 \text{ mm}^2 \quad (6.10)$$

The centre of gravity for the contributing web and stiffener $y_{tp.sl.1.w}$ is calculated in equation 6.11. The centre of gravity for the stiffener only $y_{tp.2.sl.1.w}$ is shown in equation 6.12.

$$y_{tp.sl.1.w} = \frac{b_{sl.1} t_w \frac{t_w}{2} + A_{sl}\left(t_w + \frac{h_{sl}}{2}\right)}{A_{sl.1.w}} = 8.7 \text{ mm} \quad (6.11)$$

$$y_{tp.2.sl.1.w} = \frac{A_{sl}\left(t_w + \frac{h_{sl}}{2}\right)}{A_{sl}} = 38 \text{ mm} \quad (6.12)$$

The moment of inertia $I_{sl.1.w}$ for the stiffener and adjacent parts of the panel is calculated in equation 6.13.

$$I_{sl.1.w} = \frac{b_{sl.1}t_w^3}{12} + b_{sl.1}t_w\left(y_{tp.sl.1.w} - \frac{t_w}{2}\right)^2 + \frac{t_{sl}h_{sl}^3}{12} + A_{sl}\left(t_w + \frac{h_{sl}}{2} - y_{tp.sl.1.w}\right)^2$$
$$= 7.7 \cdot 10^5 \text{ mm}^4 \tag{6.13}$$

6.2.1.2 Effective area of stiffener due to shear force

It is only the web that is subjected to shear force, thus only the web panel is regarded in this calculation. The contributing part of the subpanels to the longitudinal stiffener when regarding shear force is calculated according to Eurocode 1993-1-5 section 5.3 and the contribution part of the web is $15\varepsilon t_w$ on each side of the stiffener. The contributing area and centre of gravity is calculated in order to retrieve the moment of inertia of $I_{st} = 6.85 \cdot 10^5 \text{mm}^4$.

6.2.1.3 Reduction of the web panel

The critical plate buckling of the web panel is calculated according to Eurocode 1993-1-5 section A.2.2. The width to the critical buckling point is the distance to the stiffener from above the stiffener b_1, below the stiffener b_2 and total buckling length of the web panel b_w are shown in Table 6.3.

Table 6.3: *Widths of the subpanels to the stiffener i.e the critical buckling point.*

Subpanel	**Width [mm]**
Above stiffener: b_1	300
Below stiffener: b_2	1200
Total buckling length: b_w	1500

The panel length a_c is used as a conditional limit for calculating the critical plate buckling stress in the stiffener $\sigma_{cr.sl.p}$. The critical length a_c is calculated in equation 6.14 and $\sigma_{cr.sl.p}$ is then calculated in equation 6.15. The length of the panel in this example is $a = 3$ m. Further, the stress $\sigma_{cr.sl.p}$ is at the stiffeners level and is interpolated in equation 6.16 to correspond to the stress at the top of the panel $\sigma_{cr.p}$.

$$a_c = 4.33\sqrt[4]{\frac{I_{sl.1} \cdot b_1^2 \cdot b_2^2}{t_w^3 \cdot b_w}} = 2.6 \text{ m} \tag{6.14}$$

$$\sigma_{cr.sl.p} = \begin{cases} \dfrac{1.05 \cdot E}{A_{sl.1}} \cdot \dfrac{\sqrt{I_{sl.1} \cdot t_w^3 \cdot b_w}}{b_1 \cdot b_2} & \text{if } a \geq a_c \quad = 142 \text{ MPa} \\ \dfrac{\pi^2 \cdot E \cdot I_{sl.1}}{A_{sl.1} \cdot a^2} \cdot \dfrac{E \cdot t_w^3 \cdot b_w \cdot a^2}{4 \cdot \pi^2 \cdot (1-\nu^2) \cdot A_{sl.1} \cdot b_1^2 \cdot b_2^2} & \text{if } a < a_c \end{cases} \tag{6.15}$$

$$\sigma_{cr.p} = \sigma_{cr.sl.p} \frac{b_c}{b_c - b_1} = 244 \text{ MPa} \tag{6.16}$$

The slenderness for plate buckling $\bar{\lambda}_p$ is calculated according to Eurocode 1993-1-5 section 4.5.2 in equation 6.17.

$$\bar{\lambda}_p = \sqrt{\frac{\beta_{A.c} \cdot f_y}{\sigma_{cr.p}}} = 1.03 \tag{6.17}$$

with

$$\beta_{A.c} = \frac{A_{c.eff.loc}}{A_{c.w}} = \frac{3260 \text{ mm}^2}{5310 \text{ mm}^2} = 0.61$$

where $A_{c.w}$ is the gross area of the compression zone except the parts of the subpanel closest to the edge of the panel.

The stress ratio of the web is calculated in equation 6.18 where the stresses in the top $\sigma_{w.T}$ and bottom $\sigma_{w.B}$ of the panel is calculated with equation 6.1. The reduction factor ρ_w is then calculated using equation 6.4, resulting in $\rho_w = 0.87$.

$$\psi_w = \frac{max(\sigma_{w.B}, \sigma_{w.T})}{min(\sigma_{w.B}, \sigma_{w.T})} = \frac{max(241, -224) \text{ MPa}}{min(241, -224) \text{ MPa}} = -1.08 \tag{6.18}$$

The column-like buckling of the web panel is calculated according to Eurocode 1993-1-5 section 4.5.3. The elastic critical column-like buckling stress $\sigma_{cr.sl}$ is calculated in equation 6.19, interpolated to the corresponding stress in the edge in equation 6.20.

$$\sigma_{cr.sl.c} = \frac{\pi^2 \cdot E \cdot I_{sl.1}}{A_{sl.1} \cdot a^2} = 54 \text{ MPa} \tag{6.19}$$

$$\sigma_{cr.c} = \sigma_{cr.sl.c} \cdot \frac{b_c}{b_c - h_{w.1}} = 92 \text{ MPa} \tag{6.20}$$

The slenderness for column-like buckling is calculated using equation 6.21.

$$\bar{\lambda}_c = \sqrt{\frac{\beta_{A.c.eff} \cdot f_y}{\sigma_{cr.c}}} = 1.03 \tag{6.21}$$

with

$$\beta_{A.c.eff} = \frac{A_{sl.1.eff.w}}{A_{sl.1.w}} = \frac{3260 \text{ mm}^2}{3310 \text{ mm}^2} = 0.99$$

where $A_{sl.1.w}$ is the gross area of the stiffener and adjacent parts of the subpanels.

The radius of gyration i_w is calculated in equation 6.22. The maximum distance to the combined centre of gravity is e_w in equation 6.23, the parameter α_e from equation 6.24. Using these parameters the parameter ϕ_w is calculated in equation 6.25.

$$i_w = \sqrt{\frac{I_{sl.1.w}}{A_{sl.1.w}}} = 0.02 \text{ m} \tag{6.22}$$

$$e_w = \max\left(y_{tp.sl.1.w} - \frac{t_w}{2}, y_{tp.2.sl.1.w} - y_{tp.sl.1.w}\right) = 29 \text{ mm} \tag{6.23}$$

$$\alpha_e = \alpha_w + \frac{0.09}{i_w/e_w} = 0.66 \tag{6.24}$$

with $\alpha_w = 0.49$ for an open stiffener.

$$\phi_w = 0.5(1 + \alpha_e(\bar{\lambda}_c - 0.2) + \bar{\lambda}_c^2) = 3.4 \tag{6.25}$$

The column-like reduction factor χ_c for the web panel can thus be calculated in equation 6.26.

$$\chi_c = \frac{1}{\phi_w + \sqrt{\phi_w^2 - \bar{\lambda}_c^2}} = 0.17 \tag{6.26}$$

Finally the weighted global reduction factor $\rho_{c.w}$ for the web panel is calculated in equation 6.28. The equation uses the weighting parameter ξ_w that is calculated in equation 6.27.

$$\xi_w = \min(\max(0, \frac{\sigma_{cr.p}}{\sigma_{cr.c}} - 1)1) = 1 \tag{6.27}$$

$$\rho_{c.w} = (\rho_w - \chi_c)\xi_w(2 - \xi_w) + \chi_c = 0.87 \tag{6.28}$$

6.2.1.4 Reduction of the flange panel

The flange panel is reduced due to global buckling in the same manner as the web. The difference is that the top flange consists of two stiffeners and therefore three different buckling situations can occur, see Figure 6.3. The critical plate buckling stress $\sigma_{cr.sl.p}$ is calculated the same as in equation 6.15 where it is the smallest critical stress of the three cases that is used in future calculations. Table 6.4 show the results for the flange critical buckling stress. Since the flange's stiffeners already are located at the top, there is no need to interpolate the stress to the top, $\sigma_{cr.sl.p} = \sigma_{cr.p.f}$.

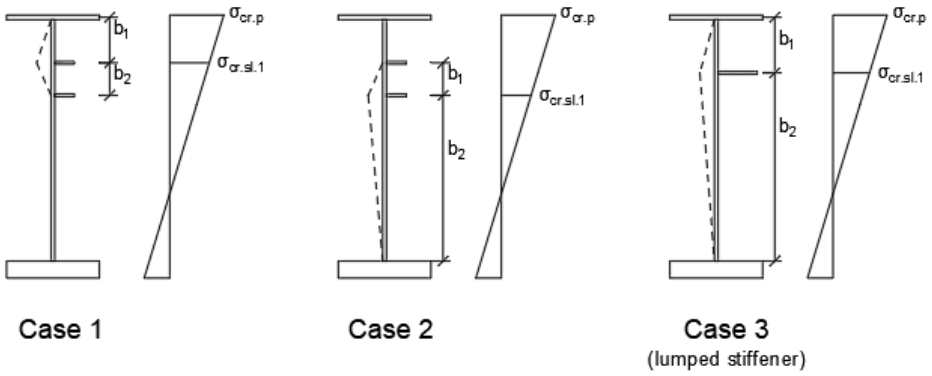

Figure 6.3: *The three cases of how two stiffeners can buckle. Adapted from Eurocode 1993-1-5, 2006, Figure A.3.*

Table 6.4: *Widths to critical buckling points, limit for panel length and critical plate buckling of the stiffener.*

Case	b_1 [mm]	b_2 [mm]	b_f [mm]	a_c [m]	$\sigma_{cr.sl.p}$ [MPa]
1	300	300	600	1.86	481
2	300	300	600	1.86	481
3	450	450	900	2.52	262

The reduction factor for flange buckling ρ_f is calculated following equations 6.11 thru 6.13 and 6.17 thru 6.28 where web dimensions have been replaced with the corresponding flange dimensions. See Table 6.5 for the result.

Table 6.5: *Results for the flange reduction calculations.*

Parameter		**Parameter**	
$y_{tp.sl.1.f}$	-0.43 mm	$\bar{\lambda}_c$	2.9 [-]
$y_{tp.2.sl.1.f}$	30 mm	$\beta_{A.c.eff.f}$	0.86
$I_{sl.1.f}$	$8.5 \cdot 10^5$ mm^4	i_f	0.01 [m]
$\bar{\lambda}_p$	1.94 [-]	$\alpha_{e.f}$	0.69 [-]
$\beta_{A.c.f}$	0.86 [-]	ϕ_f	5.65 [-]
ψ_f	1 [-]	$\chi_{c.f}$	0.1 [-]
ρ_f	0.46	ξ_f	1 [-]
$\sigma_{cr.c.f}$	43 [MPa]	$\rho_{c.f}$	0.46 [-]

6.2.2 Effective cross-section properties

The total effective area of the web and flange panels accounting for reduction of the subpanels and of global buckling is calculated in accordance with Eurocode 1993-1-5 section 4.5.1. The effective area of the top flange is calculated in equation 6.29 and the web's effective area in equation 6.30. The total effective area of the cross-section is then summarised in equation 6.31.

$$A_{f.t.c.eff} = \rho_{c.f} A_{c.eff.loc.f} + (b_{f.t.1.eff1} + b_{f.t.3.eff2}) t_f = 6400 \text{ mm}^2 \tag{6.29}$$

$$A_{w.c.eff} = \rho_{c.w} A_{c.eff.loc.w} + (h_{w1.eff1} + h_{w2.eff2}) t_w = 11300 \text{ mm}^2 \tag{6.30}$$

$$A_{c.eff} = A_{f.t.c.eff} + A_{f.b.eff} + 2A_{w.c.eff} + \rho_{c.f} 2A_{sl} + \rho_{c.w} 2A_{sl} = 42650 \text{ mm}^2 \tag{6.31}$$

With the effective area calculated, some other cross-section properties can be retrieved. The effective centre of gravity $y_{tp.eff} = 0.84$ m, moment of inertia for the members are used to calculate the effective elastic section modulus $W_{el.z.eff} = 0.0175$ m^3.

6.2.3 Capacity calculation

The moment capacity for the effective cross-section is calculated in equation 6.32 and the normal force capacity in equation 6.33. The effective flange moment capacity is calculated in equation 6.34.

$$M_{z.Rd.eff} = \frac{W_{el.z.eff} f_y}{\gamma_{M0}} = 7.36 \text{ MNm} \tag{6.32}$$

$$N_{Rd} = \frac{A_{tot.eff} f_y}{\gamma_{M0}} = 17.9 \text{ MN} \tag{6.33}$$

$$M_{f.Rd.eff} = \frac{f_y(A_{f.t.c.eff}(|-y_{tp.eff}-t_f|) + A_{f.b.eff}(|h_{w.tot}+\frac{t_f}{2}-y_{tp.eff}|))}{\gamma_{M0}} = 5.64 \text{ MNm} \tag{6.34}$$

The shear capacity is calculated in accordance with Eurocode 1993-1-5 sections 5.2, 5.3 and A.3. The shear buckling coefficient can be calculated using equation 6.35 where $k_{\tau.sl}$ is calculated in equation 6.36. The slenderness $\bar{\lambda}_w$ is then calculated in equation 6.37 followed by the shear buckling resistance factor χ_w in equation 6.38 where $\eta = 1.2$.

$$k_\tau = \begin{cases} 5.34 + 4\dfrac{h_{w.tot}}{a} + k_{\tau.sl} & \text{if } \dfrac{h_{w.tot}}{a} \geq 3 \\ \dfrac{6.3 + 0.18\dfrac{I_{st}}{t_w^3 h_w}}{\alpha} + 2.2\sqrt[3]{\dfrac{I_{st}}{t_w^3 h_w}} & \text{if } \dfrac{h_{w.tot}}{a} < 3 \end{cases} = 7.83 \tag{6.35}$$

$$k_{\tau.st} = \max\left(9\left(\frac{h_w}{a}\right)^2 \sqrt[4]{\left(\frac{I_{st}}{t_w^3 h_w}\right)^3}, \frac{2.1}{t_w}\sqrt[3]{\frac{I_{st}}{h_w}}\right) = 2.07 \tag{6.36}$$

$$\bar{\lambda}_w = \frac{h_{w.tot}}{37.4 \cdot t_w \cdot \varepsilon\sqrt{k_\tau}} = 2.39 \tag{6.37}$$

$$\chi_w = \begin{cases} \eta & \text{if } \bar{\lambda}_w < \dfrac{0.83}{\eta} \\ \dfrac{0.83}{\eta} & \text{if } \dfrac{0.83}{\eta} \leq \bar{\lambda}_w < 1.08 \\ \dfrac{0.83}{\eta} & \text{if } \bar{\lambda}_w \geq 1.08 \end{cases} = 0.35 \tag{6.38}$$

The total shear capacity is here considered to be the same as the web's shear capacity since the contribution from the flanges is very small. The web's shear capacity $V_{bw.Rd}$ is calculated in equation 6.39, and the design capacity is calculated in equation 6.40.

$$V_{bw.Rd} = \frac{\chi_w f_y h_w t_w}{\sqrt{3}\gamma_{M1}} = 1009 \text{ kN} \tag{6.39}$$

$$V_{b.Rd} = \begin{cases} 2V_{bw.Rd} & \text{if } \ 2V_{bw.Rd} \leq 2\dfrac{\eta h_{w.tot} t_w f_y}{\sqrt{3}\gamma_{M1}} \\ 2\dfrac{\eta h_{w.tot} t_w f_y}{\sqrt{3}\gamma_{M1}} & \text{otherwise} \end{cases} = 2017 \text{ kN} \tag{6.40}$$

6.2.4 Utilisation

Since no normal force acts on the structure, it is only the moment and shear force that the utilisation is checked for. The controls are performed according to Eurocode 1993-1-5 sections 4.6, 5.5 and 7.1. The utilisation of uniaxial bending η_1 is calculated in equation 6.41, the moment utilisation $\bar{\eta}_1$ in equation 6.42 and the shear force utilisation in equation 6.43. Finally the interaction control between moment and shear force is performed in equation 6.44.

$$\eta_1 = \frac{M_{z.Ed}}{M_{z.Rd.eff}} = 80\% \tag{6.41}$$

$$\bar{\eta}_1 = \frac{M_{z.Ed}}{M_{pl.Rd}} = 70.6\% \tag{6.42}$$

$$\bar{\eta}_3 = \frac{V_{Ed}}{V_{b.Rd}} = 80\% \tag{6.43}$$

$$\bar{\eta}_1 + \left(1 - \frac{M_{f.Rd}}{M_{pl.Rd}}\right)(2\bar{\eta}_3 - 1)^2 \leq 1 \quad \text{for } \ \bar{\eta}_1 \geq \frac{M_{f.Rd}}{M_{pl.Rd}} \ \text{ and } \ \bar{\eta}_3 > 0.5 = 82\% \tag{6.44}$$

The applied moment and shear force is iterated from the utilisation equations to receive the desired utilisation, in this example an 80 % moment utilisation and 80 % shear utilisation. The applied moment M_{Ed} comes from the smallest of η_1 and $\bar{\eta}_1$ see equation 6.45 and the shear force V_{Ed} from $\bar{\eta}_3$ see equation 6.46. These loads are then applied in the reduced stress method to obtain the utilisation when using that method.

$$M_{Ed} = \min(W_{pl}, W_{el.z.eff}) \cdot f_y = 5888 \text{ kNm} \tag{6.45}$$

$$V_{Ed} = V_{b.Rd} = 1614 \text{ kN} \tag{6.46}$$

6.3 Reduced stress method

For a panel in CSC4 the stresses can be reduced in order to calculate the capacity of the section. The stresses are reduced with respect to normal buckling $\rho_{x.w}$ and shear buckling $\chi_{w.w}$. To regard normal buckling the distances b_{inf} and b_{sup} are calculated in the same way as for the effective width method, see equation 6.6 and 6.7. Further, the stresses that are used in this example can be seen in Table 6.1. The normal stresses in transverse direction (z) are not regarded and the variables affected by this are therefor set to appropriate values. The calculations for the reduced stress method is made according to Eurocode 1993-1-5 section 10.

6.3.1 Critical stresses

The critical stress $\sigma_{cr.x}$ is calculated in the same way as in equation 6.15 and $\tau_{cr.w}$ is calculated according to equations 6.47 and 6.48 with k_τ according to Table 6.1.

$$\sigma_{E.w} = \frac{\pi^2 \cdot E \cdot t_w^2}{12 \cdot (1 - \nu^2) \cdot h_w^2} = 5.4 \text{ MPa} \tag{6.47}$$

$$\tau_{cr.w} = k_\tau \cdot \sigma_{E.w} = 42.29 \text{ MPa} \tag{6.48}$$

6.3.2 Minimum load amplifier for characteristic and critical load

The minimum load amplifier is calculated by combining the different loads acting on the panel, see equation 6.49. The minimum load amplifier is also calculated for the critical normal load and the critical shear load see equations 6.50 and 6.51.

$$\alpha_{ult.k} = \sqrt{\frac{1}{\left(\frac{\sigma_{x.Ed}}{f_y/\gamma_{M1}}\right)^2 + \left(\frac{\sigma_{z.Ed}}{f_y/\gamma_{M1}}\right)^2 - \left(\frac{\sigma_{x.Ed}}{f_y/\gamma_{M1}}\right)\left(\frac{\sigma_{x.Ed}}{f_y/\gamma_{M1}}\right) + 3\left(\frac{\tau_{Ed}}{f_y/\gamma_{M1}}\right)^2}} = 1.665 \tag{6.49}$$

$$\alpha_{cr.x.w} = \frac{\sigma_{cr.x.w}}{\max(\sigma_{x.Ed}, 0.001\text{MPa})} = 0.634 \tag{6.50}$$

$$\alpha_{cr.\tau.w} = \frac{\tau_{cr.w}}{\max(\tau_{Ed}, 0.001\text{MPa})} = 0.629 \tag{6.51}$$

The minimum load amplifier for critical load with the total stress field can be calculated according to equation 6.52 or by doing an FE-analysis for the specific plate,

which in this case results in $\alpha_{cr.FE.w} = 0.73767$. The buckling mode from the FE-analysis is used instead of the calculated value since it is regarded as less conservative. See Figure 6.4 for the buckling mode from the FE-analysis.

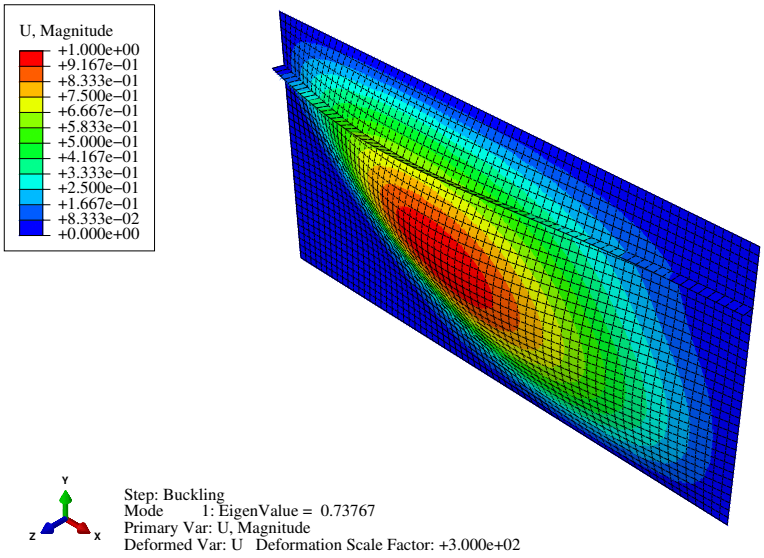

Figure 6.4: *Buckling mode for the web for the calculation example.*

$$\alpha_{cr.h.w} = \frac{1}{\frac{1+\psi_{x.w}}{4\cdot\alpha_{cr.x.w}} + \frac{1+\psi_{z.w}}{4\cdot\alpha_{cr.z.w}}\left(\left(term_1\right)^2 + term_2\right)^{\frac{1}{2}}} = 0.448$$

$$\text{with} \quad term_1 = \frac{1+\psi_{x.w}}{4\cdot\alpha_{cr.x.w}} + \frac{1+\psi_{z.w}}{4\cdot\alpha_{cr.z.w}} \tag{6.52}$$

$$\text{and} \quad term_2 = \frac{1-\psi_{x.w}}{2\cdot\alpha_{cr.x.w}^2} + \frac{1-\psi_{z.w}}{2\cdot\alpha_{cr.z.w}^2} + \frac{1}{2\cdot\alpha_{cr.\tau.w}^2}$$

6.3.3 Reduction factors

When the minimum load amplifiers are obtained the slenderness ratio is calculated according to equation 6.53. The slenderness ratio is later used to calculate the reduction factors ρ_w and $\chi_{c.w}$ in the same way as for the effective width method in equation 6.4 and 6.22 thru 6.26 respectively. With the slenderness and reduction for plate and column-like buckling calculated the reduction factor $\rho_{x.w}$ is calculated in the same manner as equation 6.28. The results can be seen in Table 6.6.

$$\bar{\lambda}_{p.w} = \sqrt{\frac{\alpha_{ult.k}}{\alpha_{cr.FE.w}}} = 1.5 \tag{6.53}$$

Table 6.6: *Parameters to determine the reduction factor $\rho_{x.w}$.*

Parameter	**Value**
Reduction plate buckling: ρ_w	0.619
Radius of gyration: i_w	0.015 [m]
parameter: $a_{e.w}$	0.65 [-]
parameter: ϕ_w	2.1 [-]
Reduction column-like: $\chi_{c.w}$	0.29 [-]
Weighting factor: ξ_w	1 [-]
Reduction factor: $\rho_{x.w}$	0.62 [-]

6.3.4 Utilisation

The reduction factor for shear stress is calculated in the same way as in equation 6.38 resulting in $\chi_{w.w} = 0.55$. Everything that is needed to calculate the utilisation in the web is known and the utilisation calculated according to equations 6.54 and 6.55.

$$U_1 = \frac{\sqrt{\left(\frac{\sigma_{x.Ed}}{f_y/\gamma_{M1}}\right)^2 + \left(\frac{\sigma_{z.Ed}}{f_y/\gamma_{M1}}\right)^2 - \left(\frac{\sigma_{x.Ed}}{f_y/\gamma_{M1}}\right) \cdot \left(\frac{\sigma_{z.Ed}}{f_y/\gamma_{M1}}\right) + 3 \cdot \left(\frac{\tau_{Ed}}{f_y/\gamma_{M1}}\right)^2}}{\min(\rho_{x.w}, \rho_{z.w}, \chi_v)} = 1.09 \tag{6.54}$$

$$\begin{aligned} U_2 = &\left(\frac{\sigma_{x.Ed}}{\rho_{x.w} f_y/\gamma_{M1}}\right)^2 + \left(\frac{\sigma_{z.Ed}}{\rho_{z.w} f_y/\gamma_{M1}}\right)^2 - \left(\frac{\sigma_{x.Ed}}{\rho_{x.w} f_y/\gamma_{M1}}\right) \cdot \left(\frac{\sigma_{z.Ed}}{\rho_{z.w} f_y/\gamma_{M1}}\right) \\ &+3 \cdot \left(\frac{\tau_{Ed}}{\chi_v f_y/\gamma_{M1}}\right)^2 = 0.99 \end{aligned} \tag{6.55}$$

The lowest of the two results from equations 6.54 and 6.55 is used and the utilisation factor is thus 99%.

Then all the same equations are used for the flange element with a few exceptions. The shear force is equal to 0 MPa. The flange also has to consider three different cases of critical buckling around the stiffener in the same way as described in Figure 6.3. The buckling mode calculated from ABAQUS for the flange is $\alpha_{cr.FE.w} = 0.60883$, see Figure 6.5.

By following the same procedure as for the web, the utilisation is calculated for the flange. The first utilisation method U_1 is governing since there is only moment acting on the flange, the utilisation becomes $U_1 = 99.9$ and is thus larger than the utilisation of the web. Therefor it is the flange utilisation that governs this specific

beam and the utilisation when using the reduced stress method is 99.9% for the given load. This is 20 percentage points higher than when using the effective width method.

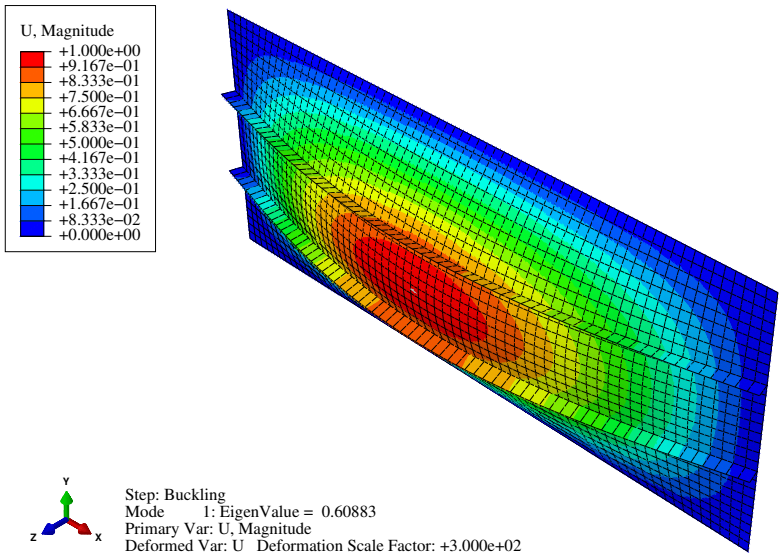

Figure 6.5: *Buckling mode for the flange for calculation example.*

7

Results

In this chapter the results of the comparison between the two methods, the effective width method and reduced stress method are presented. The results consist of comparisons when the geometry is varied and when the applied forces are varied. The effective width method is used as a basis in the results and the differences shown in this chapter are how the reduced stress method perform in comparison to the basis.

The utilisation for the effective width method is the baseline, to which the reduced stress method's utilisation is compared as following:

Reduced stress utilisation [%] - *Effective width utilisation* [%]

When the difference result in a negative value, it means that the reduced stress method has a higher capacity than the effective width method and vice versa. A low utilisation implies that the capacity is not fully utilised and the structure can carry more loads.

7.1 Parametric study results

The parametric study, which is described in the methodology, Chapter 3, consists of three different force variations for moment and shear on 36 different cross-sections. The force variations cases are plotted separately but each plot show every geometric variation that is analysed. First the results from the case of solely applied shear force are presented, then the case of solely moment and finally the case of the combination of shear force and moment on the box beam is presented.

The plots (Figures 7.1, 7.2 and 7.4) show the result in terms of utilisation difference between the reduced stress method and effective width method. Both the 36 geometric variations for the unstiffened beam and the 36 variations for the stiffened beam is plotted in the same graph. This means that the 36 different cases that comes from the geometric parametrisation correspond to the 36 values for each curve in the plot.

7.1.1 Solely shear force

For the case of solely shear force and no moment, it is the shear utilisation that is compared. The shear capacity of the box beam is calculated with the effective width method for all 36 geometric cases for the respective beam, unstiffened or stiffened. The applied shear force corresponds to a utilisation of 100% for each case in the parametrisation when using the effective width method. The shear force is calculated as shown in equation 6.46. This gives the effective width method a 100% utilisation for all 36 cases, seen as $\bar{\eta}_3$ in Table 7.1. The same forces are applied in the reduced stress method. The utilisation is calculated as U_τ since only shear stresses act on the panel there is no need to calculate the utilisation as a combo of shear and normal stresses as in equation 2.50 or 2.51. Further it is only the utilisation of the web panel that is used in the reduced stress method since there are no shear forces acting on the flange panel. The utilisation is stated as U_{max} in Table 7.1. The calculation process for the effective width method and reduced stress method are found in Appendix C and Appendix D respectively.

The comparison of the two methods is performed as the difference in percentage points between the reduced stress utilisation and effective width utilisation, $U_{max} - \bar{\eta}_3$. The difference is shown in Table 7.1 and plotted for the unstiffened and stiffened beam in Figure 7.1. The first three cases have the same thickness of web and the first nine cases have the same distance between transverse stiffeners. The thickness of the flange is the same every third case. The stiffened model results vary depending on both the thickness of the web as well as the distance between transverse stiffeners, whereas the unstiffened model mostly varies in efficiency depending on the distance between transverse stiffeners. The influence of different flange thicknesses does not impact either of the cases.

Table 7.1: *The 36 different cases' utilisation and utilisation differences for the unstiffened and stiffened box beam respectively. The table show the result of the case of applied shear force only.*

Unstiffened
Case: 100% shear, 0% moment

Case	Variable geometry			EW	RS	RS-EW
	a [m]	t_w [mm]	t_f [mm]	$\eta_{3,bar}$ [%]	U_{max} [%]	Difference [%]
1	1,5	14	40	100%	100,5%	0,5%
2	1,5	14	25	100%	100,5%	0,5%
3	1,5	14	14	100%	100,5%	0,5%
4	1,5	11	40	100%	100,4%	0,4%
5	1,5	11	25	100%	100,4%	0,4%
6	1,5	11	14	100%	100,4%	0,4%
7	1,5	8	40	100%	100,3%	0,3%
8	1,5	8	25	100%	100,3%	0,3%
9	1,5	8	14	100%	100,3%	0,3%
10	3,0	14	40	100%	98,6%	-1,4%
11	3,0	14	25	100%	98,6%	-1,4%
12	3,0	14	14	100%	98,6%	-1,4%
13	3,0	11	40	100%	98,5%	-1,5%
14	3,0	11	25	100%	98,5%	-1,5%
15	3,0	11	14	100%	98,5%	-1,5%
16	3,0	8	40	100%	98,5%	-1,5%
17	3,0	8	25	100%	98,5%	-1,5%
18	3,0	8	14	100%	98,5%	-1,5%
19	4,5	14	40	100%	99,7%	-0,3%
20	4,5	14	25	100%	99,7%	-0,3%
21	4,5	14	14	100%	99,7%	-0,3%
22	4,5	11	40	100%	99,6%	-0,4%
23	4,5	11	25	100%	99,6%	-0,4%
24	4,5	11	14	100%	99,6%	-0,4%
25	4,5	8	40	100%	99,6%	-0,4%
26	4,5	8	25	100%	99,6%	-0,4%
27	4,5	8	14	100%	99,6%	-0,4%
28	6,0	14	40	100%	99,9%	-0,1%
29	6,0	14	25	100%	99,9%	-0,1%
30	6,0	14	14	100%	99,9%	-0,1%
31	6,0	11	40	100%	99,8%	-0,2%
32	6,0	11	25	100%	99,8%	-0,2%
33	6,0	11	14	100%	99,8%	-0,2%
34	6,0	8	40	100%	99,8%	-0,2%
35	6,0	8	25	100%	99,8%	-0,2%
36	6,0	8	14	100%	99,8%	-0,2%

Stiffened
Case: 100% shear, 0% moment

Case	Variable geometry			EW	RS	RS-EW
	a [m]	t_w [mm]	t_f [mm]	$\eta_{3,bar}$ [%]	U_{max} [%]	Difference [%]
1	1,5	8	14	100%	97,4%	-2,6%
2	1,5	8	10	100%	97,4%	-2,6%
3	1,5	8	7	100%	97,4%	-2,6%
4	1,5	6	14	100%	99,3%	-0,7%
5	1,5	6	10	100%	99,3%	-0,7%
6	1,5	6	7	100%	99,3%	-0,7%
7	1,5	4	14	100%	103,9%	3,9%
8	1,5	4	10	100%	103,9%	3,9%
9	1,5	4	7	100%	103,9%	3,9%
10	3,0	8	14	100%	98,2%	-1,8%
11	3,0	8	10	100%	98,2%	-1,8%
12	3,0	8	7	100%	98,2%	-1,8%
13	3,0	6	14	100%	99,2%	-0,8%
14	3,0	6	10	100%	99,2%	-0,8%
15	3,0	6	7	100%	99,2%	-0,8%
16	3,0	4	14	100%	101,3%	1,3%
17	3,0	4	10	100%	101,3%	1,3%
18	3,0	4	7	100%	101,3%	1,3%
19	4,5	8	14	100%	101,1%	1,1%
20	4,5	8	10	100%	101,1%	1,1%
21	4,5	8	7	100%	101,1%	1,1%
22	4,5	6	14	100%	100,5%	0,5%
23	4,5	6	10	100%	100,5%	0,5%
24	4,5	6	7	100%	100,5%	0,5%
25	4,5	4	14	100%	101,4%	1,4%
26	4,5	4	10	100%	101,4%	1,4%
27	4,5	4	7	100%	101,4%	1,4%
28	6,0	8	14	100%	102,6%	2,6%
29	6,0	8	10	100%	102,6%	2,6%
30	6,0	8	7	100%	102,6%	2,6%
31	6,0	6	14	100%	102,6%	2,6%
32	6,0	6	10	100%	102,6%	2,6%
33	6,0	6	7	100%	102,6%	2,6%
34	6,0	4	14	100%	102,3%	2,3%
35	6,0	4	10	100%	102,3%	2,3%
36	6,0	4	7	100%	102,3%	2,3%

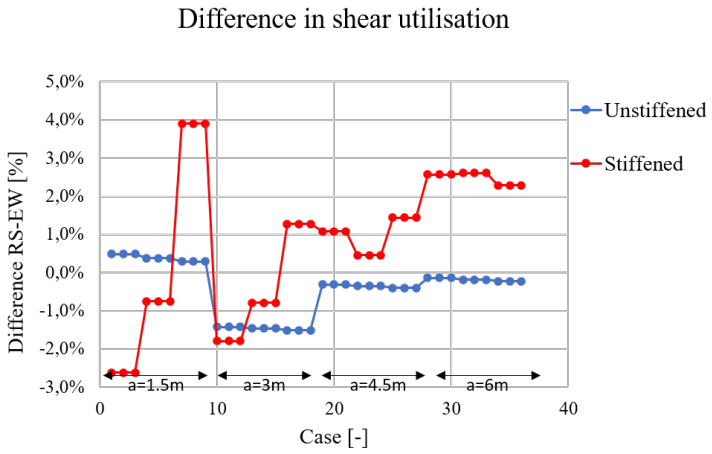

Figure 7.1: *The difference in shear force utilisation of the 36 different geometric cases for the reduced stress method compared to the effective width method. The effective width method is the baseline to which the comparison is performed.*

7.1.2 Solely moment

For the case of solely moment and no shear force on the structure, it is the moment utilisation that is compared. Just as for the shear capacity, the moment capacity is calculated for all 36 different geometric variations with the effective width method as a baseline. The applied moment corresponds to a utilisation of 100% for each case in the parametrisation when using the effective width method. The moment is calculated as shown in equation 6.45. In Table 7.2 it is either η_1 or $\bar{\eta}_1$ that fulfils this criterion of full utilisation. These utilisation factors are calculated with equations 2.23 and 2.43. The same moment is applied in the reduced stress method. Both the web and flange panels are subjected to bending but in the reduced stress method only one panel is used. It is the largest utilisation of either the flange $U_{max.f}$ or the web $U_{max.w}$ that is considered here, as can be seen in Table 7.2. The largest utilisation is stated as U_{max} in Table 7.2. The calculation process for the effective width method and reduced stress method are found in Appendix C and Appendix D respectively.

The comparison of the two methods is performed as the difference in percentage points between the reduced stress utilisation and effective width utilisation, $U_{max} - \eta_1$ or $U_{max} - \bar{\eta}_1$. The difference is shown in Table 7.2 and plotted for the unstiffened and stiffened beam in Figure 7.2.

Table 7.2: *The 36 different cases' utilisation and utilisation differences for the unstiffened and stiffened box beam respectively. The table show the result of the case of applied moment only.*

Unstiffened

Case: 0% shear, 100% moment

Case	Variable geometry			EW		RS			RS-EW
	a [m]	t_w [mm]	t_f [mm]	η_1 [%]	$\eta_{1,bar}$ [%]	$U_{max.f}$ [%]	$U_{max.w}$ [%]	U_{max} [%]	Difference [%]
1	1,5	14	40	94%	100%	88%	88%	88%	-12%
2	1,5	14	25	100%	92%	96%	76%	96%	-4%
3	1,5	14	14	100%	88%	126%	64%	126%	26%
4	1,5	11	40	98%	100%	90%	112%	112%	12%
5	1,5	11	25	100%	84%	91%	89%	91%	-9%
6	1,5	11	14	100%	73%	112%	69%	112%	12%
7	1,5	8	40	100%	99%	92%	153%	153%	53%
8	1,5	8	25	100%	78%	88%	115%	115%	15%
9	1,5	8	14	100%	61%	99%	82%	99%	-1%
10	3,0	14	40	94%	100%	88%	91%	91%	-9%
11	3,0	14	25	100%	92%	97%	78%	97%	-3%
12	3,0	14	14	100%	88%	127%	65%	127%	27%
13	3,0	11	40	98%	100%	90%	115%	115%	15%
14	3,0	11	25	100%	84%	92%	92%	92%	-8%
15	3,0	11	14	100%	73%	112%	71%	112%	12%
16	3,0	8	40	100%	99%	92%	158%	158%	58%
17	3,0	8	25	100%	78%	88%	118%	118%	18%
18	3,0	8	14	100%	61%	100%	85%	100%	-0,4%
19	4,5	14	40	94%	100%	88%	90%	90%	-10%
20	4,5	14	25	100%	92%	98%	78%	98%	-2%
21	4,5	14	14	100%	88%	129%	65%	129%	29%
22	4,5	11	40	98%	100%	90%	115%	115%	15%
23	4,5	11	25	100%	84%	93%	92%	93%	-7%
24	4,5	11	14	100%	73%	114%	71%	114%	14%
25	4,5	8	40	100%	99%	92%	157%	157%	57%
26	4,5	8	25	100%	78%	89%	118%	118%	18%
27	4,5	8	14	100%	61%	101%	84%	101%	1%
28	6,0	14	40	94%	100%	88%	91%	91%	-9%
29	6,0	14	25	100%	92%	98%	78%	98%	-2%
30	6,0	14	14	100%	88%	129%	65%	129%	29%
31	6,0	11	40	98%	100%	90%	115%	115%	15%
32	6,0	11	25	100%	84%	93%	92%	93%	-7%
33	6,0	11	14	100%	73%	114%	71%	114%	14%
34	6,0	8	40	100%	99%	92%	158%	158%	58%
35	6,0	8	25	100%	78%	89%	118%	118%	18%
36	6,0	8	14	100%	61%	101%	85%	101%	1%

Stiffened

Case: 0% shear, 100% moment

Case	Variable geometry			EW		RS			RS-EW
	a [m]	t_w [mm]	t_f [mm]	η_1 [%]	$\eta_{1,bar}$ [%]	$U_{max.f}$ [%]	$U_{max.w}$ [%]	U_{max} [%]	Difference [%]
1	1,5	8	14	100%	76%	125%	107%	125%	25%
2	1,5	8	10	100%	75%	161%	100%	161%	61%
3	1,5	8	7	100%	79%	204%	97%	204%	104%
4	1,5	6	14	100%	69%	119%	127%	127%	27%
5	1,5	6	10	100%	67%	149%	114%	149%	49%
6	1,5	6	7	100%	68%	186%	108%	186%	86%
7	1,5	4	14	100%	64%	114%	201%	201%	101%
8	1,5	4	10	100%	59%	138%	175%	175%	75%
9	1,5	4	7	100%	57%	167%	159%	167%	67%
10	3,0	8	14	100%	90%	105%	86%	105%	5%
11	3,0	8	10	100%	88%	125%	78%	125%	25%
12	3,0	8	7	100%	87%	177%	71%	177%	77%
13	3,0	6	14	100%	79%	96%	99%	99%	-1%
14	3,0	6	10	100%	73%	109%	86%	109%	9%
15	3,0	6	7	100%	67%	145%	74%	145%	45%
16	3,0	4	14	100%	71%	90%	173%	173%	73%
17	3,0	4	10	100%	63%	98%	144%	144%	44%
18	3,0	4	7	100%	53%	121%	112%	121%	21%
19	4,5	8	14	100%	90%	110%	90%	110%	10%
20	4,5	8	10	100%	88%	124%	83%	124%	24%
21	4,5	8	7	100%	90%	140%	78%	140%	40%
22	4,5	6	14	100%	79%	101%	98%	101%	1%
23	4,5	6	10	100%	74%	109%	86%	109%	9%
24	4,5	6	7	100%	71%	117%	76%	117%	17%
25	4,5	4	14	100%	72%	96%	114%	114%	14%
26	4,5	4	10	100%	64%	100%	96%	100%	0%
27	4,5	4	7	100%	58%	102%	81%	102%	2%
28	6,0	8	14	100%	90%	108%	89%	108%	8%
29	6,0	8	10	100%	88%	125%	82%	125%	25%
30	6,0	8	7	100%	90%	151%	77%	151%	51%
31	6,0	6	14	100%	79%	99%	97%	99%	-1%
32	6,0	6	10	100%	74%	110%	85%	110%	10%
33	6,0	6	7	100%	71%	126%	76%	126%	26%
34	6,0	4	14	100%	72%	95%	122%	122%	22%
35	6,0	4	10	100%	64%	101%	103%	103%	3%
36	6,0	4	7	100%	58%	110%	87%	110%	10%

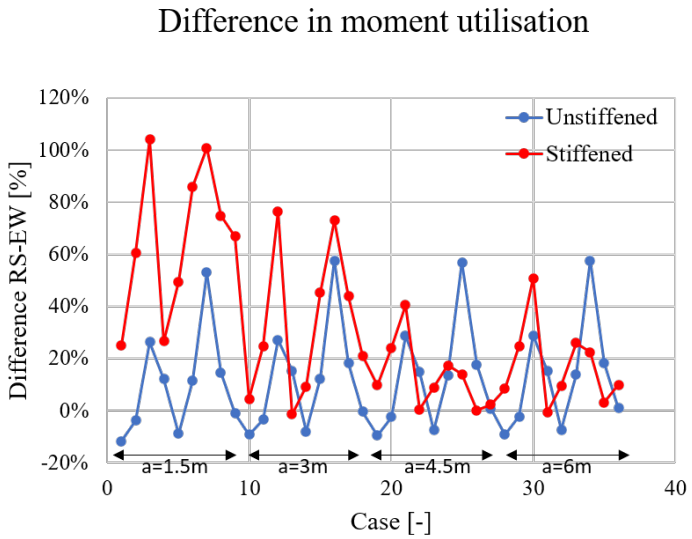

Figure 7.2: *The difference in moment utilisation of the 36 different geometric cases for the reduced stress method compared to the effective width method. The effective width method is the baseline to which the comparison is performed.*

Figure 7.3 show the results of only considering flange moment capacity and excluding the contribution from the web in the effective width method. The same moment as in the original case is applied. The moment utilisation is then calculated as $M_{Ed}/M_{f.Rd}$ instead of $M_{Ed}/(f_y \cdot W_{eff})$ or $M_{Ed}/M_{pl.Rd}$. This is then compared to the flange panel in the reduced stress method. The result is more realistic since in theory it is the flanges that are considered to take the moment. However, the result for the stiffened model for the first distance between transverse stiffeners $a = 1.5$ m stands out. Why the difference between the two methods is so large here is discussed in Chapter 8.1.2.2.

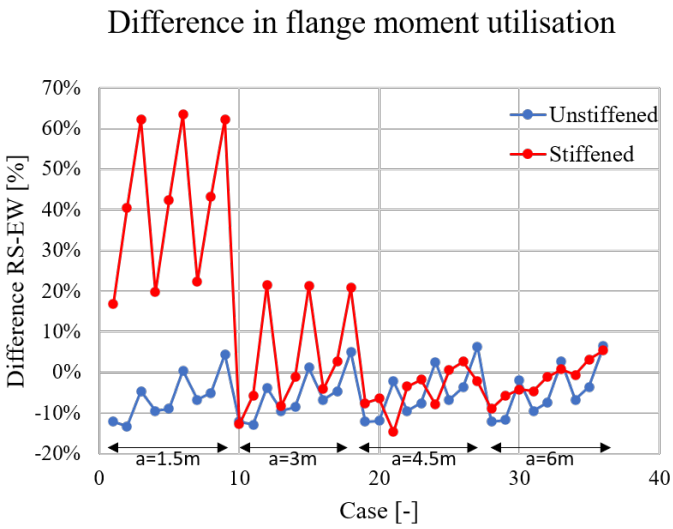

Figure 7.3: *The difference in moment utilisation of the 36 different geometric cases when only assessing the flange capacity for the reduced stress method compared to the effective width method. The effective width method is the baseline to which the comparison is performed.*

7.1.3 Combined moment and shear

The third case consists of both moment and shear forces that both are applied at 80% of the beam's capacity. The utilisation that is compared is the interaction utilisation. Just as the previous cases, the effective width method is used as a baseline, where the moment and shear capacity are calculated. 80% of the moment capacity and 80% of the shear capacity correspond to the magnitude of the forces that are applied to the beam. This means that either η_1 or $\bar{\eta}_1$ and $\bar{\eta}_3$ fulfils the utilisation requirement of 80% which can be seen in Table 7.3 for the unstiffened beam and Table 7.4 for the stiffened beam. The interaction utilisation for the effective width method comes from equation 2.43 but is calculated for all cases and not just those that fulfil the requirements for accounting for interaction, as stated in the same equation. This interaction utilisation is seen in the column *Interaction* in Tables 7.3 and 7.4 and the interaction control in column *Int. control* which show that it is only a few cases that actually have to account for interaction.

The same forces are applied in the reduced stress method. This method accounts for moment and shear simultaneously, as seen in equations 2.50 and 2.51. This means that it is the largest utilisation of either the web $U_{max.web}$ or flange panel $U_{max.flange}$ that is used in the comparison, $U_{max.combo}$ in Tables 7.3 and 7.4. The calculation process for the effective width method and reduced stress method are found in Appendix C and Appendix D respectively.

The comparison of the two methods is performed as the difference in percentage points between the reduced stress utilisation and effective width utilisation, $U_{max.combo} - Interaction$. The difference is shown in Tables 7.3 and 7.4 and plotted

for the unstiffened and stiffened beam in Figure 7.4.

Table 7.3: *The 36 different cases' utilisation and utilisation differences for the unstiffened box beam. The table show the result of the case of the combo of applied moment and shear force.*

Unstiffened
Case: 80% shear, 80% moment

Case	Variable geometry			Effective width					Reduced stress			RS-EW
	a [m]	t_w [mm]	t_f [mm]	η_1 [%]	$\eta_{1.bar}$ [%]	$\eta_{3.bar}$ [%]	Int. Control [%]	Interaction [%]	$U_{max.web}$ [%]	$U_{max.flange}$ [%]	$U_{max.combo}$ [%]	Difference [%]
1	1,5	14	40	75%	80%	80%	0%	80%	115%	70%	115%	35%
2	1,5	14	25	80%	74%	80%	0%	80%	106%	77%	106%	26%
3	1,5	14	14	80%	71%	80%	82%	82%	93%	101%	101%	19%
4	1,5	11	40	78%	80%	80%	0%	80%	133%	72%	133%	53%
5	1,5	11	25	80%	67%	80%	0%	73%	117%	73%	117%	44%
6	1,5	11	14	80%	58%	80%	0%	71%	98%	89%	98%	28%
7	1,5	8	40	80%	80%	80%	0%	79%	166%	74%	166%	87%
8	1,5	8	25	80%	62%	80%	0%	68%	137%	70%	137%	69%
9	1,5	8	14	80%	48%	80%	0%	61%	112%	79%	112%	50%
10	3,0	14	40	75%	80%	80%	0%	80%	117%	70%	117%	37%
11	3,0	14	25	80%	74%	80%	0%	80%	107%	77%	107%	27%
12	3,0	14	14	80%	71%	80%	82%	82%	94%	102%	102%	19%
13	3,0	11	40	78%	80%	80%	0%	80%	135%	72%	135%	55%
14	3,0	11	25	80%	67%	80%	0%	73%	120%	73%	120%	46%
15	3,0	11	14	80%	58%	80%	0%	71%	99%	90%	99%	29%
16	3,0	8	40	80%	80%	80%	0%	79%	169%	74%	169%	89%
17	3,0	8	25	80%	62%	80%	0%	68%	140%	71%	140%	72%
18	3,0	8	14	80%	48%	80%	0%	61%	113%	80%	113%	52%
19	4,5	14	40	75%	80%	80%	0%	80%	117%	70%	117%	37%
20	4,5	14	25	80%	74%	80%	0%	80%	107%	78%	107%	27%
21	4,5	14	14	80%	71%	80%	82%	82%	94%	103%	103%	21%
22	4,5	11	40	78%	80%	80%	0%	80%	135%	72%	135%	55%
23	4,5	11	25	80%	67%	80%	0%	73%	120%	74%	120%	47%
24	4,5	11	14	80%	58%	80%	0%	71%	100%	91%	100%	29%
25	4,5	8	40	80%	80%	80%	0%	79%	168%	74%	168%	89%
26	4,5	8	25	80%	62%	80%	0%	68%	139%	71%	139%	71%
27	4,5	8	14	80%	48%	80%	0%	61%	113%	81%	113%	52%
28	6,0	14	40	75%	80%	80%	0%	80%	117%	70%	117%	37%
29	6,0	14	25	80%	74%	80%	0%	80%	107%	78%	107%	27%
30	6,0	14	14	80%	71%	80%	82%	82%	94%	103%	103%	21%
31	6,0	11	40	78%	80%	80%	0%	80%	135%	72%	135%	55%
32	6,0	11	25	80%	67%	80%	0%	73%	120%	74%	120%	47%
33	6,0	11	14	80%	58%	80%	0%	71%	100%	91%	100%	29%
34	6,0	8	40	80%	80%	80%	0%	79%	168%	74%	168%	88%
35	6,0	8	25	80%	62%	80%	0%	68%	139%	71%	139%	71%
36	6,0	8	14	80%	48%	80%	0%	61%	113%	81%	113%	51%

Table 7.4: *The 36 different cases' utilisation and utilisation differences for the stiffened box beam. The table show the result of the case of the combo of applied moment and shear force.*

Stiffened
Case: 80% shear, 80% moment

Case	Variable geometry			Effective width					Reduced stress			RS-EW
	a [m]	t_w [mm]	t_f [mm]	η_1 [%]	$\eta_{1,bar}$ [%]	$\eta_{3,bar}$ [%]	Int. Control [%]	Interaction [%]	$U_{max,web}$ [%]	$U_{max,flange}$ [%]	$U_{max,combo}$ [%]	Difference [%]
1	1,5	8	14	80%	61%	80%	0%	71%	142%	100%	142%	70%
2	1,5	8	10	80%	60%	80%	0%	74%	138%	129%	138%	64%
3	1,5	8	7	80%	63%	80%	79%	79%	136%	163%	163%	84%
4	1,5	6	14	80%	55%	80%	0%	66%	176%	95%	176%	110%
5	1,5	6	10	80%	53%	80%	0%	67%	170%	120%	170%	103%
6	1,5	6	7	80%	54%	80%	0%	70%	166%	149%	166%	96%
7	1,5	4	14	80%	51%	80%	0%	62%	264%	91%	264%	202%
8	1,5	4	10	80%	47%	80%	0%	61%	248%	111%	248%	188%
9	1,5	4	7	80%	46%	80%	0%	62%	237%	134%	237%	176%
10	3,0	8	14	80%	72%	80%	0%	80%	109%	84%	109%	29%
11	3,0	8	10	80%	71%	80%	82%	82%	101%	100%	101%	19%
12	3,0	8	7	80%	70%	80%	86%	86%	93%	141%	141%	56%
13	3,0	6	14	80%	63%	80%	0%	72%	122%	76%	122%	50%
14	3,0	6	10	80%	59%	80%	0%	71%	108%	87%	108%	37%
15	3,0	6	7	80%	54%	80%	0%	70%	94%	116%	116%	46%
16	3,0	4	14	80%	57%	80%	0%	66%	184%	72%	184%	118%
17	3,0	4	10	80%	50%	80%	0%	63%	165%	79%	165%	103%
18	3,0	4	7	80%	42%	80%	0%	59%	147%	97%	147%	88%
19	4,5	8	14	80%	72%	80%	0%	80%	124%	88%	124%	43%
20	4,5	8	10	80%	71%	80%	82%	82%	117%	99%	117%	35%
21	4,5	8	7	80%	72%	80%	87%	87%	111%	112%	112%	25%
22	4,5	6	14	80%	63%	80%	0%	72%	131%	80%	131%	59%
23	4,5	6	10	80%	59%	80%	0%	71%	121%	87%	121%	50%
24	4,5	6	7	80%	56%	80%	72%	72%	109%	94%	109%	37%
25	4,5	4	14	80%	58%	80%	0%	67%	149%	77%	149%	82%
26	4,5	4	10	80%	51%	80%	0%	64%	135%	80%	135%	72%
27	4,5	4	7	80%	46%	80%	0%	62%	120%	82%	120%	58%
28	6,0	8	14	80%	72%	80%	0%	80%	126%	87%	126%	46%
29	6,0	8	10	80%	71%	80%	82%	82%	121%	100%	121%	39%
30	6,0	8	7	80%	72%	80%	87%	87%	115%	121%	121%	34%
31	6,0	6	14	80%	63%	80%	0%	72%	135%	79%	135%	63%
32	6,0	6	10	80%	59%	80%	0%	71%	126%	88%	126%	55%
33	6,0	6	7	80%	56%	80%	72%	72%	116%	101%	116%	44%
34	6,0	4	14	80%	58%	80%	0%	67%	156%	76%	156%	89%
35	6,0	4	10	80%	51%	80%	0%	64%	141%	81%	141%	77%
36	6,0	4	7	80%	46%	80%	0%	62%	129%	88%	129%	67%

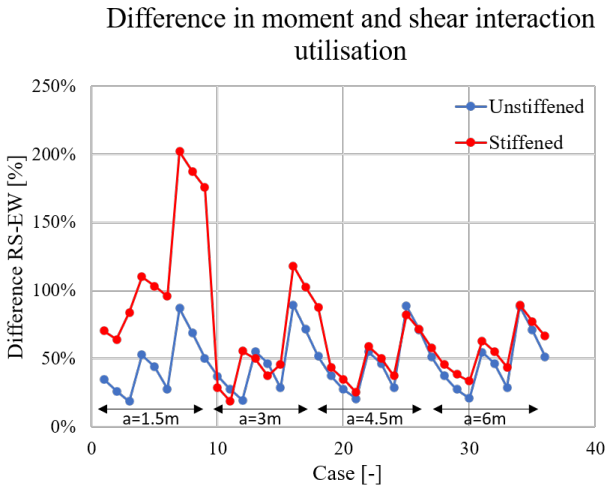

Figure 7.4: *The difference in combined shear and moment utilisation of the 36 different geometric cases for the reduced stress method compared to the effective width method. The effective width method is the baseline to which the comparison is performed.*

In the combined case of the unstiffened beam case 3, 12, 21 and 30 that have a thick web and a thin flange seem to generally result in utilisation closer to the effective width method. However, the difference between the two method is never less than 20 %. The same behaviour can be observed for the stiffened beam except for case 3, 12 and 15 that have very similar dimensions of the flange and web, there is only 1 mm difference. These cases have a distance "a" between the transverse stiffeners that is less than the critical length a_c and thus the critical plate buckling $\sigma_{cr.sl.p}$ is calculated differently, see equation 2.12. The combination of these two effects is probably what causes case 3, 12 and 15 to deviate from the pattern.

7.1.4 3D beam subjected to solely moment

A 3D beam is modelled and subjected to the same moment as the corresponding 2D panels of the web and flange. The applied moment is the same as the moment on the web and flange separately for the same cross-section. The 3D beam is only modelled for one case which is a stiffened beam with a flange that is 14 mm thick and a web that is 6 mm thick and a distance of 4.5 m between the transverse stiffeners. The buckling mode for the 3D beam section is 0.75957 and can be seen in Figure 7.5. The buckling mode of the 3D section is compared to the 2D buckling modes and discussed in Chapter 8.

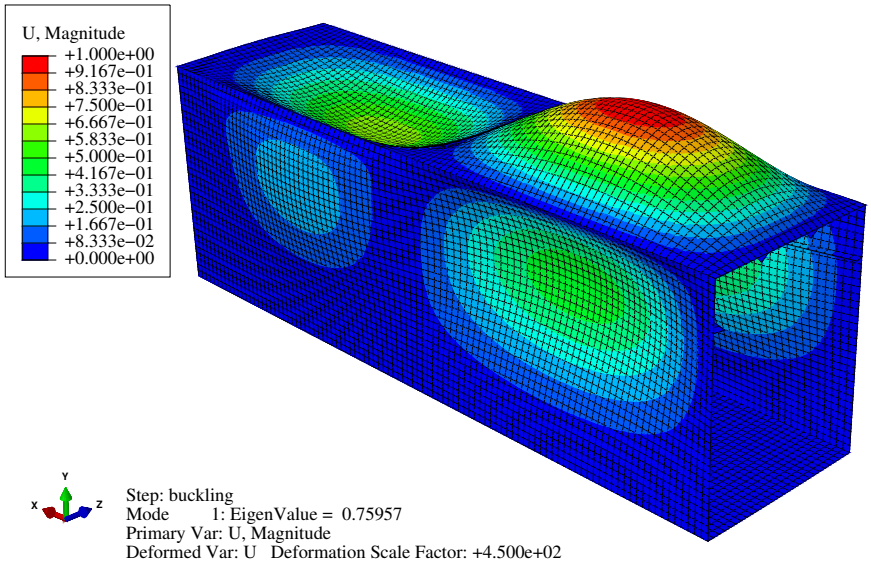

Figure 7.5: *3D modelled beam subjected to solely moment.*

7.2 Geometric variation results

To analyse the impact of the method of choice due to geometric variations, the distance between transverse stiffeners "a", flange thickness t_f and web thickness t_w are all kept constant one at a time when the other parameters are changed. A total of 36 different variations are computed for each box beam, the unstiffened beam and the stiffened beam.

7.2.1 Impact of web and flange thicknesses

It is common to have a section between transverse stiffeners that is three times as long as the height of the beam. Therefore, the distance 4.5 m between transverse stiffeners is chosen as the baseline for the comparison of the thickness' influence on the utilisation. The cases that are compared have only been subjected to moment. This since most literature that describe and compare the two methods look at one type of load at the time. From the parametric results the nine cases of cross-sections with distance $a = 4.5$ m is further analysed.

There exists nine different cases for both the unstiffened and stiffened beams, see Table 7.5 for the thicknesses of the web and flange for each case. The height and width of the box beam is kept constant and the thicknesses varies according to Chapter 4. The slenderness for the flange and web is an indication of the impact of different thicknesses and are stated in Table 7.5.

In order to analyse the impact of flange and web thickness and find correlations between the two, the slenderness of the members are compared. The slenderness $\bar{\lambda}_p$ is calculated using equation 7.1. For the web t_w is used and for the flange t_f. The parameter $\bar{b}$ is the width of the member, for the unstiffened beam it is the total height of the web or width of flange that is used and for the stiffened beam it is the largest height or width of a subpanel to a stiffener that is used. The slenderness difference is calculated in equation 7.2. A small $\Delta\lambda$ correspond to the web and flange both having similar slenderness. The slenderness of the panels and the difference can be found in Table 7.5 and Appendix A for all 36 cases.

$$\bar{\lambda}_p = \frac{\bar{b}/t}{28.4 \cdot \varepsilon \cdot \sqrt{k_\sigma}} \tag{7.1}$$

$$\Delta\lambda = \bar{\lambda}_{p.flange} - \bar{\lambda}_{p.web} \tag{7.2}$$

Table 7.5: *The nine different cases of thickness variations for a beam cross-section and slenderness difference $\Delta\lambda$ between flange and web.*

Case	Unstiffened					Stiffened				
	t_w [mm]	t_f [mm]	$\bar{\lambda}_{p.f}$	$\bar{\lambda}_{p.w}$	$\Delta\lambda$	t_w [mm]	t_f [mm]	$\bar{\lambda}_{p.f}$	$\bar{\lambda}_{p.w}$	$\Delta\lambda$
1	14	40	0.69	1.03	0.34	8	14	0.65	1.03	0.38
2	14	25	1.10	1.03	0.07	8	10	0.91	1.02	0.10
3	14	14	1.97	1.03	0.94	8	7	1.30	1.00	0.30
4	11	40	0.69	1.31	0.62	6	14	0.65	1.36	0.71
5	11	25	1.11	1.31	0.20	6	10	0.92	1.34	0.43
6	11	14	1.98	1.31	0.67	6	7	1.31	1.32	0.01
7	8	40	0.70	1.80	1.11	4	14	0.66	2.02	1.37
8	8	25	1.11	1.80	0.69	4	10	0.92	1.99	1.07
9	8	14	1.99	1.80	0.19	4	7	1.31	1.95	0.63

The difference between the two methods' utilisation compared to the slenderness difference $\Delta\lambda$ is shown in Figure 7.6. For the unstiffened beam the trend line is computed as a linear curve that increase with slenderness differences whereas for the stiffened the linear curve decreases.

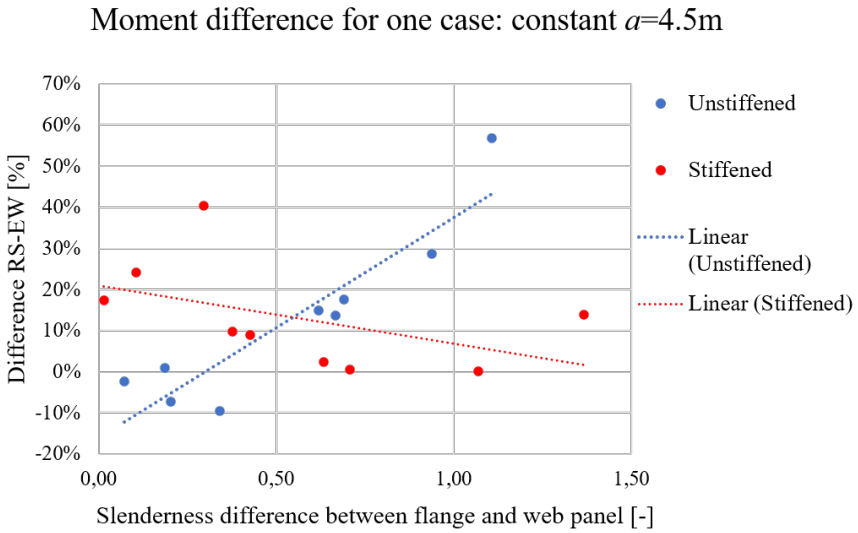

Figure 7.6: *The difference in moment utilisation for nine different geometries of the cross-section for a 4.5 m long beam section. The utilisation is compared to the slenderness difference of the flange and web's slenderness for the unstiffened and stiffened beam respectively.*

7.2.2 Impact of distance between transverse stiffeners

The impact of the distance between transverse stiffeners is analysed in the same way as the thickness of the cross-section. Nine cases of a box beam with varying web and flange thickness as seen in Table 7.5 is compared in terms of slenderness difference. Four different lengths of beam sections, the distance between transverse stiffeners, are compared in the same graph. The utilisation difference between the effective width method and reduced stress method is compared to the slenderness difference of the flange and web for all four cases. For the unstiffened beam, the distance "a" between transverse stiffeners is not accounted for in any of the equations that calculates moment capacity. The distance "a" only affect the shear capacity, see equation 2.32. Due to this since only moment is considered in this comparison, the cases with different distances "a" have almost the same utilisation differences. This can be seen in Figure 7.7 that all 36 cases are located within the same area.

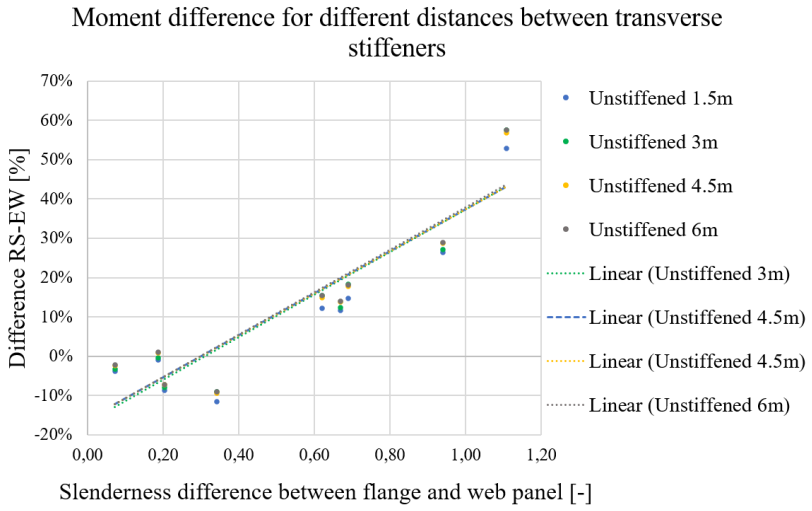

Figure 7.7: *The difference in utilisation for four different unstiffened beam sections. The utilisation is compared to the slenderness difference of the flange and web's slenderness.*

For the longitudinally stiffened beam, the critical stress equation, equation 2.12, is dependent on the distance "a" between transverse stiffeners. The critical stress decides the reduction factor and thus utilisation of the cross-section. Therefore, the utilisation differences vary dependent on which case is analysed, 1.5 m, 3 m, 4.5 m or 6 m between the transverse stiffeners. The 1.5 m and 3 m trends move in one direction and for 4.5 m and 6 m the trend go in the other direction. It is shown clearly in Figure 7.8 that the first case of 1.5 m differs a lot in difference from the other results. There are some outliers marked in the graph, which are discussed in 8.2.2.

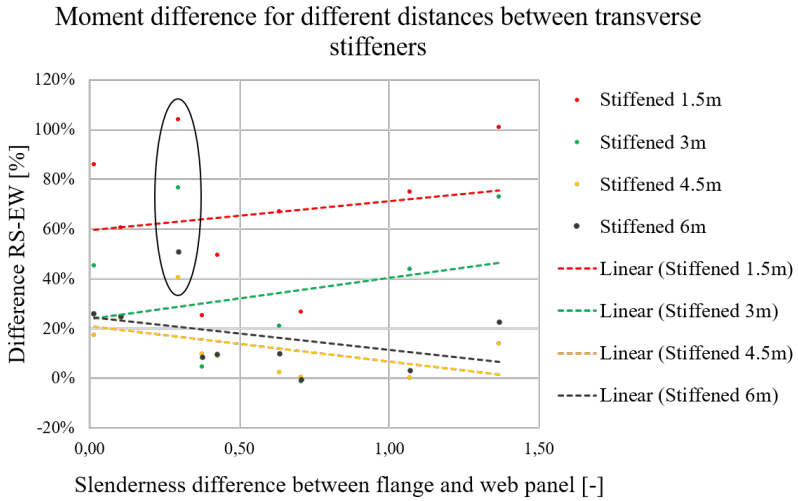

Figure 7.8: *The difference in utilisation for four different stiffened beam sections. The utilisation is compared to the slenderness difference of the flange and web's slenderness.*

8

Discussion

In this chapter the results from the comparison of the effective width method and reduced stress method are discussed. Which method that produce the highest capacity in different scenarios in terms of geometric and force variations is described. Values that appear to differ from the expected behaviour are highlighted and explanations for the deviations are discussed. Further some strange behaviour found in the equations based on Eurocode 1993-1-5 are mentioned.

A low utilisation of the cross-section means that the beam has a higher capacity. When comparing the utilisation differences between the methods, a positive difference means that when using the effective width method it results in a lower utilisation than the reduced stress method. For a negative difference it is the reduced stress method that has a lower utilisation.

What the true capacity is of the beams investigated is not as straightforward as saying that the method resulting in the lowest utilisation always is the best. Hand calculations, which are used in the effective width method, are often simplified. Thus, the FE-calculation should probably yield a more realistic behaviour and result. However, the FE-analysis's result is used in the reduced stress method that is known for being conservative. Since both methods are established in Eurocode 1993-1-5, it is assumed that both methods are sufficiently strong with a utilisation $\leq 100\%$ for any case. The methods are only compared to each other and thus lower utilisation means that the method allows for a higher capacity.

8.1 Parametric study

In this section the parametric study in terms of different loading situations is discussed. Each different loading case's result is discussed in terms of interpretation of the utilisation and if there are any strange results. First the solely shear force case is discussed followed by the solely moment case and finally the case of the combination of the shear and moment.

8.1.1 Solely shear

In the loading situation when only shear force is applied the difference when comparing the two methods are quite small for both the unstiffened and stiffened beam, see Figure 7.1. This suggests that both methods are calculating the shear force acting on the web in a similar manner. However, for the unstiffened beam there are some differences in the results between different distances of transverse stiffeners. It seems like the effective width method results in slightly higher capacity when the distance between transverse stiffeners are 1.5 m and slightly lower capacity for the other distances. The reduced stress method provides a slightly larger capacity for beams with aspect ratio two or higher (distance $a = 3$ m).

When looking at the stiffened beam the more slender webs seem to yield higher utilisation in the reduced stress method compared to the effective width method, the utilisation difference is above zero. See Table 7.1 where it is the three last cases per distance "a" that correspond to the most slender webs. The pattern changes when the aspect ratio becomes three or higher (distance $a = 4.5$ m).

Generally, both the effective width method and the reduced stress method work very well on structures subjected to shear stresses. The utilisation difference for an unstiffened beam has a maximum value of 1.5 percentage points and for stiffened 4 percentage points. For stiffened beams the effective width method yields a less conservative result and allows for a bit more shear capacity.

8.1.2 Solely moment

For the results from the case where solely moment is acting on the structure, there are some large variations in the utilisation difference of the two methods. A clear impact on the results is the thickness of the member as well as the distance between transverse stiffeners.

8.1.2.1 Influence from the thickness of the web

The effective width method considers redistribution of stresses, meaning that one part can buckle while the rest of the structure continues to be loaded. Since the reduced stress method do not allow for this but can only be loaded to the first buckle, the effective width method is assumed to yield a higher capacity when a whole cross-section is considered. van der Burg (2011, p. 14) states that the effective width method result in a higher plate buckling capacity for most cases when subjected to bending moment only. The thicknesses of the flange and web is of great interest and the most clear cases when the effective width method yield a higher capacity is when the difference in slenderness between the web and flange is large (van der Burg, 2011). Seen in Figure 7.2, the cases that have a utilisation difference greater than zero are also the cases that have a large difference in slenderness between the plate parts. This is in line with van der Burg's (2011, p. 14) claims that the effective width method yield a higher capacity for these cases.

In Figure 7.2, there is one cross-section that stands out for every distance "a" for

the unstiffened beam. It is the seventh case for the four different lengths of panels. With a very thin web and a large flange the reduced stress method gives a 60% difference in utilisation. Seen in Table A.1 in Appendix A, it is this case that has the largest difference in slenderness by far. This case is described by Beg (2012, p. 305) to be known to give a very conservative result with the reduced stress method. Since the effective width method allows for buckling before reaching its capacity, and redistribution of stresses between flange and web occur, the applied moment can be very high. When the same moment then is applied in the reduced stress method to a very slender web panel the critical load is regarded to be much lower at the first buckle, and thus the capacity of the beam is very low.

8.1.2.2 Comparison of the capacity of the whole cross-section versus flange

In the effective width method redistribution of stresses is allowed and the capacity for moment is calculated by using the effective cross-section. This leads to extra moment capacity when the web is relatively thick compared to the flange. However, when executing the reduced stress method one steel panel is examined which does not allow for stress redistribution and the capacity of the members are calculated on their own. Sinur et al. (2013) notes that the reduced stress method results in a higher utilisation when the web is contributing a lot to the total capacity. This raises the question of how the reduced stress method performs when compared to a similar situation in the effective width method where no redistribution is allowed and only the capacity of the flange is of interest. This is investigated and Figure 7.3 show the results if only considering flange moment capacity and excluding the contribution from the web in the effective width method. When only comparing the flange moment, the difference between the two methods decreases compared to when the whole cross-section is used in the analysis, compare Figure 7.2 and 7.3. For the unstiffened beam the difference between the two methods decrease for all cases. The largest change occurs for the cases that have a very thin web and thick flange, case 7, 16, 25 and 34. The utilisation difference change from around 60% to -8% making the reduced stress method less conservative. This large change in which method yields the lowest utilisation is due to the fact that the thin web is not governing the design of the moment capacity any more since only the flange capacity is considered in Figure 7.3.

The overall behaviour for the unstiffened beam when only considering the flange moment instead of whole cross-section's capacity is changed, compare Figure 7.2 to Figure 7.3. The reduced stress method results in higher capacities for almost all cases when only regarding the flange moment, except when the flange is thin and especially case 6 and 9 for each distance "a" in which the effective width method still result in a lower utilisation. For the stiffened beam the cases' values in Figure 7.2 compared to Figure 7.3 differs with around 25-30%. For cases 10-36 the flange moment utilisation difference varies around +/- 15% but for the first nine cases, where the distance between transverse stiffeners is 1.5 m the results stand out in utilisation difference between 25-55%.

For the stiffened beam, the result of which method yields the highest capacity when only the flange is considered varies. Beg (2012, p. 313) also analyses a longitudinally stiffened and compressed beam and arrives at the same conclusion, that the reduced stress method can perform with both higher and lower utilisation compared to the effective width method.

The values that stand out the most when comparing flange moment utilisation for the effective width method and the reduced stress method are the cases where column-like buckling is the main contributor to global buckling reduction. This happens when the plate is short and the flange is thin, see the first nine cases of the stiffened beam in Figure 7.3. This means that column-like buckling has a larger influence on the reduced stress method than it has on effective width method. When the effective width method accounts for global column buckling in the flanges it only reduces the top flange parts adjacent to stiffeners including the stiffeners and not the edge parts or the bottom flange. However, in the reduced stress method the total stress is reduced due to the global column buckling in the flanges. In the reduced stress method there is only one reduction, the worst case between global and local buckling. Therefore, when global buckling reduction is relatively high it has a worsening effect on the capacity compared to the effective width method that reduces the cross-section both due to global and local buckling. In the effective width method the edge parts are not reduced due to global buckling, but these edge part is a rather large part of the total flange, up to 1/3 of the total top flange area which is why large differences between the methods are observed.

8.1.2.3 Influence of the distance between transverse stiffeners

For the unstiffened beam there are practically no influence from the distance between transverse stiffeners. However, for the stiffened beam quite big differences in utilisation can be seen in Figure 7.3 that mainly originates from the equation for calculating global plate buckling in the stiffeners $\sigma_{cr.sl.p}$, see equation 2.12. The constant a_c gives a condition for how $\sigma_{cr.sl.p}$ should be calculated. This factor a_c lies between 1.5 m and 3 m for most of the nine cases of varying thickness, thus depending on if the distance "a" is smaller or larger than a_c, different equations to calculate the critical stress $\sigma_{cr.sl}$ are used. Since the only difference between case 1-9 and 10-18 is the distance "a", the only difference between the utilisation can be due to which equation is used to calculate the critical stress at the stiffener. The factor a_c is larger than 3 m for the cases with the thinnest flange, therefore the first time the distance between transverse stiffeners is exceeding a_c is in case 21. In this case the behaviour of the utilisation difference changes and becomes less conservative for the reduced stress method, see every third case from 21 until 36 compared to every third case from 1 to 20 in Figure 7.3.

8.1.3 Combined moment and shear

When examining the results from the combined loading situation in Figure 7.4 it seems clear that the reduced stress method yields a lower capacity than the effective width method for all cases. The lack of redistribution between the plates result in

a lower capacity of the structure since the web and flange is individually analysed in the reduced stress method.

Compared to the effective width method the reduced stress method appears to be very conservative when assessing combinations of high moment with high shear. This is because stress redistribution is not allowed in the reduced stress method. Even for the geometries that the reduced stress method seems to yield low utilisation for there is a difference in utilisation of 20%. However, the result might be different if less slender webs were analysed. All webs that are considered in this parametrisation are quite slender. If a thicker web was analysed the effects discussed in Section 8.1.2.2 would apply, the web would not govern the moment capacity and the utilisation differences between the two methods would decrease. For a cross-section where the flange is much larger than the web the two methods might be comparable in terms of combined moment and shear force. However, this is something that needs to be investigated further.

There are mentions in *Commentary and Worked Examples To En 1993-1-5 " Plated Structural Elements "* (Johansson et al., 2007) of ways to improve the reduced stress method with some tolerance for redistribution that makes the results less conservative. However, such improvements have not been implemented in this thesis, instead the guidelines from Eurocode 1993-1-5 (2006) is governing.

8.2 Geometric variations

In this section the results are used to find and discuss if there is a correlation between geometry and which method that yields the highest capacity. It is the thickness of flange and web in terms of slenderness of the members that is discussed. Further, the influence of the distance between transverse stiffeners is also discussed.

8.2.1 Impact of web and flange thickness

The results are discussed in terms of slenderness, since all parameters except the thicknesses of the flange and web are kept constant. The slenderness is in turn a measurement of how the thicknesses impact the utilisation.

In Figure 7.6, for the unstiffened beam the reduced stress method yields a slightly higher capacity for low differences in slenderness for the flange and web than the effective width method does. For higher slenderness differences the effective width method results in higher capacity of the cross-section. The correlation between the slenderness difference of the web and flange panels and the utilisation difference for the unstiffened beam appears to be linear with a constant increase for higher slenderness differences. However, for the stiffened beam the behaviour seems to yield the opposite results. The lowest capacity for the reduced stress method is reached for low slenderness differences, but for larger differences the trend seems to suggest a less conservative result.

8.2.2 Impact of distance between transverse stiffeners

Figure 7.8 describes how the utilisation difference for a stiffened beam varies depending on what distance between transverse stiffeners is used. For the cases of 1.5 m and 3 m the trend seem to increase with higher slenderness difference. For all cases but especially clear for the two mentioned, when the difference in slenderness is above one the difference between the reduced stress method and effective width method is large. A reason for this is that a large moment is applied since the flange is thick but the web is thin and in the reduced stress method the web is governing the whole beam section's capacity resulting in a lower capacity and thus higher utilisation. Further, for the distance "a" = 1.5 m and 3 m, in the equation used to calculate the plate stress the conditional statement of the parameter a_c is used. For theses two cases $a < a_c$ whereas in the other two cases where "a" = 4.5 m and 6 m the opposite applies. If the cases with slenderness difference larger than one is removed, the trend decreases for all four cases and look like the trends of the cases where "a" = 4.5 m and 6 m. For the case where the distance is 1.5 m it can clearly be seen that the reduced stress method is more conservative for all slenderness differences that have been observed in this thesis. When observing the other three distances, 3 m, 4.5 m and 6 m, they share a similar behaviour of it being conservative to use the reduced stress method when the slenderness difference is small, but it is almost no difference between the methods for higher slenderness ratio for case 4.5 m and 6 m.

In Figure 7.8 for a stiffened beam, a few outliers have been highlighted where they deviate from the general trend. What differentiate these from the rest of the data points are that the flange is thinner than the web, which is highly uncommon. If these points are disregarded, the trend still stands that for low slenderness differences the effective width method results in lower utilisation and for higher slenderness differences the two methods yield very similar results. However, since the result of the stiffened section is dependent on so many different factors it is difficult to draw any real conclusions of one method being more conservative for some specific geometries, especially when the distance between transverse stiffeners is less than a_c.

8.3 Difference between a stiffened or unstiffened box beam

For the unstiffened beam the reduced stress method generally yields a higher capacity compared to the effective width method than the stiffened beam does. When subjected to solely shear or solely moment the unstiffened beam even yields a higher capacity when using the reduced stress method for some geometric variations, not just relative to the stiffened case. The shear utilisation benefits from the reduced stress method in all cases except the first nine, see Figure 7.1. For beams subjected to moment a thin flange seems to produce the largest difference in utilisation, with a less conservative result for the effective width method for both unstiffened and stiffened beams, when looking at the flange moment utilisation, see Figure 7.3. However, the unstiffened beam suffers from the same shortcomings as the stiffened

in the combined load combinations but does not have the same varying difference in utilisation with different distances between transverse stiffeners. The stiffened beam appears to get similar differences as the unstiffened beam when the distance between transverse stiffeners increases. At 4.5 m and longer, the unstiffened and stiffened beam have utilisation differences of the same magnitude which can be seen in Figure 7.4.

A difference between the unstiffened and stiffened beam is which method that gives the lowest utilisation. Figure 7.6 show that the larger the difference in slenderness between flange and web becomes, the lower the effective width method utilisation is in comparison to the reduced stress method for unstiffened beams. However, for the stiffened beam the behaviour is the opposite. For larger slenderness differences both methods seem to be usable, the reduced stress method might even be less conservative in some cases.

8.4 3D box beam

In the reduced stress method, the web and flange panels are analysed separately and the FE-analysis on the buckling modes are performed for the web panel and flange panel respectively. However, to show if there are any differences in the answer when regarding the web and flange separately, a 3D model is created in order to investigate if more capacity could be found by modelling the whole cross-section at once and performing a buckling analysis.

The result showed the buckling mode to be equal to 0.75957 for the 3D modelled beam. That buckling mode can be compared to the smallest buckling mode of the individual plates which was equal to 0.76933 which corresponds to the flange panel in the 2D analysis. The difference is only about 1% and no large differences can be seen between using a 2D or 3D analysis. This supports the reduced stress method's approach of calculating one panel at a time. No additional capacity was found by modelling the whole cross-section in 3D for this specific case.

8.5 Odd behaviours that occurs in Eurocode 1993-1-5

During the calculations and computations of the results some strange behaviours have been noted. In some of the equations from Eurocode 1993-1-5 that hold conditional statements, the change of equation when the conditions are changed do not have a homogeneous interpolation or shift. The equations that this occurs in is equation 2.20 and 2.40, the interpolation between plate and column-like buckling and the shear buckling factor k_τ respectively.

Further there are differences in the FE-analysis compared to hand calculations where the aspect ratio a/b plays a big part in the result variations. This is noted in Table 5.2 where the difference between hand calculations and FE-analysis is influenced by

the aspect ratio.

8.5.1 Interaction between column-like buckling and plate buckling

For stiffened beams, plate and column-like interaction is checked in order to receive the reduction factor for the cross-section when the buckling behaviour is in between plate or column-like buckling. When calculations are made between the different cases of geometries some strange behaviour in the interaction formula appears that is investigated further. The purpose of the interaction is to take account for the type of buckling behaviour that is most dominant in the current cross-section. The interaction between column-like and plate buckling is done according to equation 2.20 with the condition stated in equation 2.21. If the plate is short, it is generally column-like buckling that governs and if the plate is longer, it is plate buckling that is governing. The individual critical buckling stress for each respective type is described in equations 2.18 and 2.12. They are both dependent on the distance between transverse stiffeners up until the distance a_c, after that distance it is only the column-like buckling that is dependent on the increase of the distance "a". In Figure 8.1 the buckling behaviour for one case is visualised. It is the reduction factor for plate buckling ρ, column-like buckling χ_c and interaction ρ_c that is plotted against the distance between transverse stiffeners. The same behaviour occurs for all cross-sections.

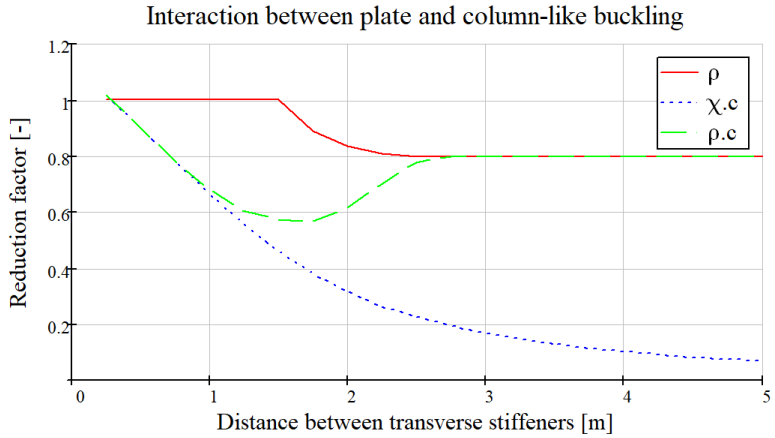

Figure 8.1: *Interaction between plate and column-like buckling over different lengths between transverse stiffeners of a beam panel.*

The interpolated reduction curve follows the column-like buckling curve until the critical plate buckling is the same as critical column-like buckling. Thereafter it diverges as the ratio between the plate and column-like stresses increases, see equation 2.21. Instead of smoothly shift to the plate buckling curve, the interpolation equation makes the curve follow a parabolic shape, increasing the reduction factor until it behaves like the plate buckling curve. The column-like buckling factor χ_c is very

conservative and the reduction ρ_c is on the safe side when following the column-like buckling curve (Beg, 2012, p. 310). To receive a smoother interpolation between column-like and plate buckling, the deviation from column-like buckling could begin almost immediately and the reduction factor ρ_c would be less conservative.

The reduction peaks for a point where the column-like buckling is dominant and the reduction factor ρ_c is at its smallest value. The reduction factor then increases, corresponding to less reduction when the distance between transverse stiffeners increases. For some distances "a" the reduction decrease when the distance between transverse stiffeners gets longer which is illogical. However, this is how the interpolation equation works according to Eurocode 1993-1-5 (2006) and there are no guidelines that describes that any modification are needed.

An observation is made that the peak in the interpolated reduction factor occurs at a distance between transverse stiffeners of 1.5 m. In Figure 7.3 it is at this distance that there is a striking difference between the two methods. This phenomenon is something that could be further investigated to see if there is a correlation.

8.5.2 Non-homogeneous shift in shear buckling factor

The critical shear capacity is dependent on the shear buckling coefficient k_τ. For a longitudinally stiffened beam with one or two stiffeners equation 2.40 states that when the aspect ratio of the panel is less than 3 one equation should be used to obtain the shear buckling coefficient and another equation when the aspect ratio is equal to or larger than 3. However, in the calculations made it was noticed that the two conditional equations did not converge at any point. When the change in equation is made, there is a shift in the shear buckling coefficient behaviour, which can be seen in Figure 8.2. The jump in k_τ indicates that the aspect ratio 3 is wrong and that the change of which equation is used should come for much smaller aspect ratios. However, this is what Eurocode 1993-1-5 use but as a structural designer it is good to be aware of this jump.

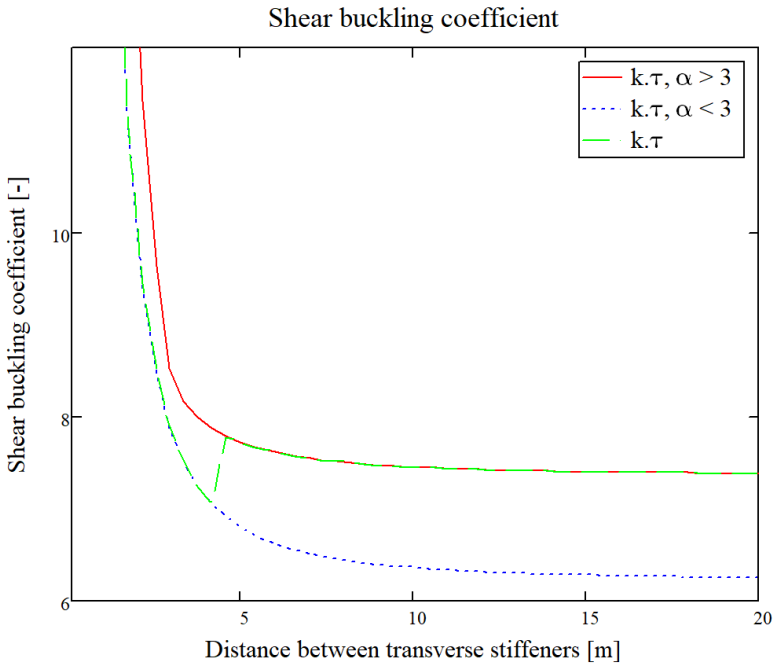

Figure 8.2: *Shear buckling coefficient for a stiffened panel with one or two stiffeners. The aspect ratio α states which equation should be used.*

8.5.3 Aspect ratio impact on FE-calculations

The difference between the critical stress in ABAQUS vs EBplate and the difference between ABAQUS vs analytical calculations show some differences in the verification of the model, Chapter 5.5. The differences can be seen in Table 5.2 which shows that there are some simplifications made in Eurocode when deciding the buckling coefficient k_σ. For a plate that is simply supported around all edges and subjected to uniform compression the buckling coefficient is 4.0 according to Eurocode 1993-1-5 (2006) for an internal member. But in FE-analysis the actual value of k_σ is calculated with half sinus waves, according to Fujikubo and Yao (2016, p. 82). The values of the normal buckling coefficient used in the FE-analysis can be seen in Figure 8.3 where m is the number of half sinus wave or buckling modes. The aspect ratios α that are investigated in Section 5.5.3 are between $\alpha = 1$ and $\alpha = 2$. This is where observations are made that there is a large divergence between the simplified, analytical value of Eurocode and the actual values used in EBPlate and ABAQUS. In Table 5.2 a large difference of -3.1% can be seen for a flange subjected to uniform compression at the distance "a"= 1.5 m. The distance gives "a"= 1.5 m an aspect ratio of 1.25, k_σ is large at this aspect ratio in the FE-analysis, see Figure 8.3. For the web in compression, at 1.5 m between transverse stiffeners (aspect ratio 1) a difference of -5.4% is seen in the same table. There are differences in k_σ for the linearly distributed compression too. The difference between FE-analysis and analytical calculation is the explanation for the large value. However, they are not discussed in detail here.

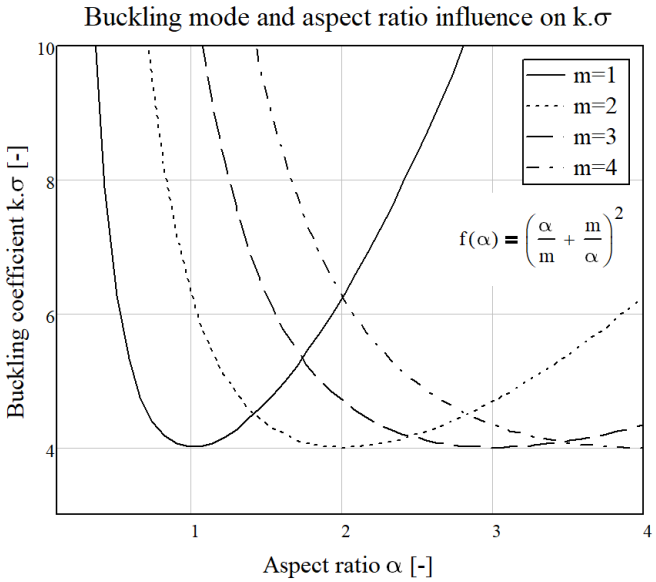

Figure 8.3: *Actual buckling coefficient used in FE-analysis depending on the aspect ratio for a simply supported on four edges plate subjected to uniform compression.*

The increased capacity that can be obtained from FE-analysis by having an aspect ratio α between one and two is something the designer should keep in mind. It might be unwise to expect the extra capacity obtained by FE-analysis compared to the analytical value used in Eurocode when calculating the capacity. However, this use of different buckling coefficients used in analytical and FE software can explain differences in the results when compared to one another.

9

Conclusion

From the parametric study performed in this thesis, the two studied methods yield different results and that the differences vary dependent on the geometry at hand as well as the loading conditions. The method that results in the lowest utilisation of the cross-section is the least conservative method. The conclusions regarding impact of longitudinal stiffeners, applied load type, geometry in terms of difference in slenderness, FE-obtained buckling coefficient and interaction between column-like and plate buckling are presented in the list below:

- **Impact of longitudinal stiffeners:** When comparing the reduced stress method with the effective width method there are generally less difference for the unstiffened beams compared to the longitudinally stiffened beams. There is less variance between different cross-section and distances between transverse stiffeners. For a stiffened beam there are a lot more factors that determines which method yields the most conservative result.

- **Impact of applied load on a stiffened beam:** The different load variations of moment and shear force affect how much difference in utilisation there is between the two methods. For the stiffened beam the smallest difference occurs when the beam is subjected to solely shear. When the case of solely moment is considered the effective width method gives lower utilisation factors for most of the geometries. If only the flange capacity is considered, there are more variations to which method yields the highest capacity, see Figure 7.3. For the stiffened beam the effective width method generally yields higher capacities for all load combinations. Further, the load case of combined moment and shear force results in the effective width method giving a higher capacity for all geometries that were considered.

- **Impact of applied load on an unstiffened beam:** The unstiffened beam has a very small difference in utilisation between the two methods when considering solely shear. The difference between the two methods when the beam is subjected to solely moment yields slightly higher capacity when using the reduced stress method for about half of the cases. However, when the effective width method results in lower utilisation, the difference in utilisation is very large, up to 58%. Considering only the flange moment utilisation the reduced stress method yields a higher capacity for a majority of the considered ge-

ometries. When the unstiffened beam is subjected to both moment and shear force the effective width method results in lower utilisation and thus higher capacity for all geometries.

- **Impact of geometry:** The geometry plays a big part when comparing the two methods. The reduced stress method is less conservative to use for geometries where the web has minimum influence on the moment capacity. The choice of method depends more on the slenderness difference between the flange panel and web panel than it does on the individual geometries. For a high slenderness difference, i.e. the slenderness of the individual members (web and flange) differs a lot, for an unstiffened beam the effective width method results in lower utilisation. However, for a stiffened beam it is difficult to draw any conclusions on how the difference in slenderness impact the utilisation of the studied geometries since the results depend on many different factors.

- **Impact of FE-obtained buckling coefficient:** The designer should keep in mind that a longer distance between transverse stiffeners may yield a higher capacity if using an FE-software that calculates the actual normal buckling coefficient. This behaviour is most significant when the aspect ratio between width and height of the panel is between one and two. It could be dangerous to rely on the extra capacity to achieve the required capacity.

- **Impact of interaction between column-like and plate buckling:** The designer should be aware of the interaction between column-like and plate buckling when performing the calculations for buckling capacity. The highest reduction is achieved when there is an interaction between column-like and plate buckling. The reduction decreases as the distance between transverse stiffeners increase and plate buckling being governing for the panel, see Figure 8.1.

9.1 Future studies

The reduced stress method lacks the possibility to redistribute loads. There are recommendations for implementation on how to account for redistribution of stresses (Johansson et al., 2007). Investigation on this and if it would have any impact on which method to choose can be further studied.

There has been quite little work done on comparison between the effective width method and reduced stress method on panels with one or two stiffeners. The work of this type of structural members can be continued on for other types of loads such as patch loading, normal forces and combinations of loads.

In Eurocode 1993-1-5 there are a few irregularities discussed in this thesis, but further work on the interaction formula, equation 2.20 between column-like and panel buckling as well as the two equations used in determining the shear buckling coefficient k_τ should be studied.

Further investigation on if there is a correlation between the strange interaction factor ρ_c in Figure 8.1 and the large difference in utilisation at 1.5 m between transverse stiffeners in Figure 7.3.

Bibliography

Abaqus, A., & Simulia. (2011). *ABAQUS 6.11: Getting started with ABAQUS* (Keyword Ed). Dassault Systèmes.

Al-Emrani, M., & Åkesson, B. (2020). *Steel Structures*. Department of Architecture; Civil Engineering, Chalmers University of Technology.

Al-Emrani, M., Engström, B., Johansson, M., & Johansson, P. (2013). *Bärande konstruktioner Del 1*. Department of Civil; Environmental Engineering, Chalmers University of Technology.

Basler, K., Yen, B.-T., Muller, J. A., & Trülimann, B. (1960). Web buckling tests on welded plate girders. Part 4: tests on plate girders subjected to combined bending and shear. WRC Bulletin, 64, (September 1960), Reprint No. 165 (60-5). *Fritz Laboratory Reports*, (Paper 67). https://core.ac.uk/download/pdf/228622348.pdf

Beg, D. (2012). Design of plated structures according to EN 1993-1-5 with the emphasis on longitudinal compression. *Stahlbau*, *81*(4), 304–314. https://doi.org/10.1002/stab.201201561

Beg, D., Kuhlmann, U., Davaine, L., & Braun, B. (2010). *Design of a Plated Structures* (1st). ECCS – European Convention for Constructional Steelwork.

Boverkets Författningssamling. (2011). *Boverkets föreskrifter och allmänna råd om tillämpning av europeiska konstruktionsstandarder (eurokoder)* (tech. rep.). https://rinfo.boverket.se/EKS/PDF/BFS2011-10-EKS8.pdf

Centre Technique Industriel de la Construction Metallique (CTICM). (n.d.). EBPlate. https://www.cesdb.com/ebplate.html

Eurocode 1993-1-1. (2005). *Eurocode 3 - Design of steel structures - Part 1-1: General rules and rules for buildings*. European Committee for Standardisation (CEN).

Eurocode 1993-1-5. (2006). *Eurocode 3 - Design of steel structures - Part 1-5: Plated structural elements*. European Committee for Standardisation (CEN).

Fujikubo, M., & Yao, T. (2016). Chapter 4 - Buckling/Plastic Collapse Behavior and Strength of Rectangular Plate Subjected to Uni-Axial Thrust. *Buckling and ultimate strength of ship and ship-like floating structures* (pp. 82–84). Elsevier Science & Technology. https://doi.org/https://doi.org/10.1016/B978-0-12-803849-9.00004-6

Hendy, C., & Iles, D. (2015). *Guidance notes on best practice in steel bridge construction* (6th). SCI. https://www.steelconstruction.info/images/1/10/SCI_P185.pdf

Höglund, T. (1997). Shear buckling resistance of steel and aluminium plate girders. *Thin-Walled Structures*, *29*(1-4), 13–30. https://doi.org/10.1016/s0263-8231(97)00012-8

Johansson, B., Maquoi, R., Sedlacek, G., Müller, C., & Beg, D. (2007). *Commentary and Worked Examples To En 1993-1-5 " Plated Structural Elements "* (First edit, Vol. 3). JRC-ECCS. https://publications.jrc.ec.europa.eu/repository/handle/JRC38239

Johansson, B., & Veljkovic, M. (2009). Review of plate buckling rules in EN 1993-1-5. *Steel Construction*, *2*(4), 228–234. https://doi.org/10.1002/stco.200910031

Kuhlmann, U., Schmidt-Rasche, C., Jörg, F., Pourostad, V., Spiegler, J., & Euler, M. (2021). Update on the revision of Eurocode 3. *Steel Construction*, *14*(1), 2–13. https://doi.org/https://doi.org/10.1002/stco.202000048

Scandella, C., Neuenschwander, M., Mosalam, K. M., Knobloch, M., & Fontana, M. (2020). Structural Behaviour of Steel-Plate Girders in Shear: Experimental Study and Review of Current Design Principles. *Journal of Structural Engineering*, *146*(11). https://doi.org/https://doi.org/10.1061/(ASCE)ST.1943-541X.0002804

Simon-Talero, J. M., & Caballero, A. (2010). Plate Buckling According to Eurocode 3. Comparison of the Effective Width Method and the Reduced Stress Method. *SDSS'Rio 2010 Stability and Ductility of Steel Structures*, 1051–1060.

Sinur, F., Brecelj, M., & Beg, D. (2013). Longitudinally Stiffened Girders Subjected to Bending Moment. *Jármai K., Farkas J. (eds) Design, Fabrication and Economy of Metal Structures*, 235–240. https://doi.org/https://doi.org/10.1007/978-3-642-36691-8{_}36

van der Burg, M. (2011). *Plate buckling in design codes: The difference between NEN 6771 and NEN-EN 1993-1-5* (Doctoral dissertation). Delft University of Technology.

A

Slenderness difference between web and flange

This Appendix contains a table, Table A.1, that describes the difference between the flange's and web's slenderness for the different geometric cases for both the unstiffened and stiffened beam. The slenderness is obtained by the effective width method calculations.

Table A.1: *The difference in slenderness of the 36 different geometric cases for the effective width method.*

Unstiffened beam

Case	Variable geometry			Slenderness		
	a	tw	tf	λ.ft	λ.w1	Difference λ.ft-λ.w1
	[m]	[mm]	[mm]	[-]	[-]	[-]
1	1,5	14	40	0,69	1,03	0,34
2	1,5	14	25	1,10	1,03	0,07
3	1,5	14	14	1,97	1,03	0,94
4	1,5	11	40	0,69	1,31	0,62
5	1,5	11	25	1,11	1,31	0,20
6	1,5	11	14	1,98	1,31	0,67
7	1,5	8	40	0,70	1,80	1,11
8	1,5	8	25	1,11	1,80	0,69
9	1,5	8	14	1,99	1,80	0,19
10	3,0	14	40	0,69	1,03	0,34
11	3,0	14	25	1,10	1,03	0,07
12	3,0	14	14	1,97	1,03	0,94
13	3,0	11	40	0,69	1,31	0,62
14	3,0	11	25	1,11	1,31	0,20
15	3,0	11	14	1,98	1,31	0,67
16	3,0	8	40	0,70	1,80	1,11
17	3,0	8	25	1,11	1,80	0,69
18	3,0	8	14	1,99	1,80	0,19
19	4,5	14	40	0,69	1,03	0,34
20	4,5	14	25	1,10	1,03	0,07
21	4,5	14	14	1,97	1,03	0,94
22	4,5	11	40	0,69	1,31	0,62
23	4,5	11	25	1,11	1,31	0,20
24	4,5	11	14	1,98	1,31	0,67
25	4,5	8	40	0,70	1,80	1,11
26	4,5	8	25	1,11	1,80	0,69
27	4,5	8	14	1,99	1,80	0,19
28	6,0	14	40	0,69	1,03	0,34
29	6,0	14	25	1,10	1,03	0,07
30	6,0	14	14	1,97	1,03	0,94
31	6,0	11	40	0,69	1,31	0,62
32	6,0	11	25	1,11	1,31	0,20
33	6,0	11	14	1,98	1,31	0,67
34	6,0	8	40	0,70	1,80	1,11
35	6,0	8	25	1,11	1,80	0,69
36	6,0	8	14	1,99	1,80	0,19

Stiffened beam

Case	Variable geometry			Slenderness		
	a	tw	tf	λ.ft	λ.w1	Difference λ.ft-λ.w1
	[m]	[mm]	[mm]	[-]	[-]	[-]
1	1,5	8	14	0,65	1,03	0,38
2	1,5	8	10	0,91	1,02	0,10
3	1,5	8	7	1,30	1,00	0,30
4	1,5	6	14	0,65	1,36	0,71
5	1,5	6	10	0,92	1,34	0,43
6	1,5	6	7	1,31	1,32	0,01
7	1,5	4	14	0,66	2,02	1,37
8	1,5	4	10	0,92	1,99	1,07
9	1,5	4	7	1,31	1,95	0,63
10	3,0	8	14	0,65	1,03	0,38
11	3,0	8	10	0,91	1,02	0,10
12	3,0	8	7	1,30	1,00	0,30
13	3,0	6	14	0,65	1,36	0,71
14	3,0	6	10	0,92	1,34	0,43
15	3,0	6	7	1,31	1,32	0,01
16	3,0	4	14	0,66	2,02	1,37
17	3,0	4	10	0,92	1,99	1,07
18	3,0	4	7	1,31	1,95	0,63
19	4,5	8	14	0,65	1,03	0,38
20	4,5	8	10	0,91	1,02	0,10
21	4,5	8	7	1,30	1,00	0,30
22	4,5	6	14	0,65	1,36	0,71
23	4,5	6	10	0,92	1,34	0,43
24	4,5	6	7	1,31	1,32	0,01
25	4,5	4	14	0,66	2,02	1,37
26	4,5	4	10	0,92	1,99	1,07
27	4,5	4	7	1,31	1,95	0,63
28	6,0	8	14	0,65	1,03	0,38
29	6,0	8	10	0,91	1,02	0,10
30	6,0	8	7	1,30	1,00	0,30
31	6,0	6	14	0,65	1,36	0,71
32	6,0	6	10	0,92	1,34	0,43
33	6,0	6	7	1,31	1,32	0,01
34	6,0	4	14	0,66	2,02	1,37
35	6,0	4	10	0,92	1,99	1,07
36	6,0	4	7	1,31	1,95	0,63

B

Mathcad sheet for input data and cross-section class

This Appendix contains the input parameters such as geometry and material parameters that is used in Appendix C and D for the Mathcad calculations. In this appendix the cross-section classes are calculated.

Johan Ahlstrand
Ellen Johansson

INPUT

Material

Yielding limit $f_{yk} := 420MPa$

Modulus of elasticity $E_s := 210GPa$

Particalfactor $\gamma_{M0} := 1.0$

Particalfactor $\gamma_{M1} := 1.0$

Particalfactor $\gamma_{M2} := 1.1$

Dimensioning yielding limit $f_{yd} := \frac{f_{yk}}{\gamma_{M0}} = 420 \cdot MPa$

Poisson's ratio $v := 0.3$

Factor for classification of cross-section $\varepsilon_{class} := \sqrt{\frac{235MPa}{420MPa}} = 0.748$

Geometry cross-section

Distance between transverse stiffeners $a_w := 1.5m$

Web height $h_w := 1200mm$

Web above stiffener $h_{w.1} := 300mm$

Web below stiffener $h_{w.2} := h_w - h_{w.1} = 900 \cdot mm$

Web thickness $t_w := 8mm$

Width flange $b_{f.t} := 1200mm$

Width of flange until first stiffener $b_{f.t.1} := 400mm$

Width of flange after second stiffener $b_{f.t.3} := b_{f.t.1}$

Width of flange between stiffeners $b_{f.t.2} := b_{f.t} - b_{f.t.1} - b_{f.t.3} = 400 \cdot mm$

Width of lower flange $b_{f.b} := b_{f.t} = 1.2\,m$

Thickness of flanges $t_f := 14mm$

Johan Ahlstrand
Ellen Johansson

Cross-section of longitudinal stiffeners

Height of web stiffener $h_{sl.w} := 60mm$

Height of flange stiffener $h_{sl.f} := 60mm$

Thickness web stiffener $t_{sl.w} := 10mm$

Thickness flange stiffener $t_{sl.f} := 10mm$

Web above stiffener

Slenderness of upper part of web $\beta_{w.1} := \frac{h_{w.1}}{t_w} = 37.5$

Stress ratio $\psi_1 := 0.6$

Ratio for compression zone $\alpha_1 := \min\left[\frac{1}{(1-\psi_1)}, 1\right] = 1$

Limits for cross-section classes

$$Class_{1.w1} := \text{if}\left(\alpha_1 > 0.5, \frac{396}{13\cdot\alpha_1 - 1}, \frac{36}{\alpha_1}\right)\cdot\varepsilon_{class} = 24.7$$

$$Class_{2.w1} := \text{if}\left(\alpha_1 > 0.5, \frac{456}{13\cdot\alpha_1 - 1}, \frac{41.5}{\alpha_1}\right)\cdot\varepsilon_{class} = 28.4$$

$$Class_{3.w1} := \text{if}\left[\psi_1 > -1, \frac{42}{0.67 + 0.33\cdot\psi_1}, 62\cdot(1-\psi_1)\cdot\sqrt{-\psi_1}\right]\cdot\varepsilon_{class} = 36.19$$

Control of classification of upper web

$$Class_{w.1} := \begin{cases} 1 & \text{if } \beta_{w.1} \le Class_{1.w1} \\ 2 & \text{if } Class_{1.w1} < \beta_{w.1} \le Class_{2.w1} \\ 3 & \text{if } Class_{2.w1} < \beta_{w.1} \le Class_{3.w1} \\ 4 & \text{otherwise} \end{cases} = 4$$

Johan Ahlstrand
Ellen Johansson

Web below stiffener

Web slenderness

$$\beta_{w.2} := \frac{h_{w.2}}{t_w} = 112.5$$

Stress ratio

$$\psi_2 := -1.77$$

Ratio for compression zone

$$\alpha_2 := \begin{cases} 1 & \text{if } \psi_2 = 1 \\ \min\left[\frac{1}{(1-\psi_2)}, 1\right] & \text{otherwise} \end{cases} = 0.36$$

Limits for cross-section classes

$$Class_{1.w2} := \text{if}\left(\alpha_2 > 0.5, \frac{396}{13\cdot\alpha_2 - 1}, \frac{36}{\alpha_2}\right)\cdot\varepsilon_{class} = 74.6$$

$$Class_{2.w2} := \text{if}\left(\alpha_2 > 0.5, \frac{456}{13\cdot\alpha_2 - 1}, \frac{41.5}{\alpha_2}\right)\cdot\varepsilon_{class} = 86$$

$$Class_{3.w2} := \text{if}\left[\psi_2 > -1, \frac{42}{0.67 + 0.33\cdot\psi_2}, 62\cdot(1-\psi_2)\cdot\sqrt{-\psi_2}\right]\cdot\varepsilon_{class} = 170.9$$

Control of classification of lower web

$$Class_{w.2} := \begin{cases} 1 & \text{if } \beta_{w.2} \le Class_{1.w2} \\ 2 & \text{if } Class_{1.w2} < \beta_{w.2} \le Class_{2.w2} \\ 3 & \text{if } Class_{2.w2} < \beta_{w.2} \le Class_{3.w2} \\ 4 & \text{otherwise} \end{cases} = 3$$

Johan Ahlstrand
Ellen Johansson

Top flange

Flange slenderness

$$\beta_{f.t.1} := \frac{b_{f.t.1} - t_w - \frac{t_{sl.f}}{2}}{t_f} = 27.643$$

Limits for cross-section classes

$$Class_{1.ft} := 33 \cdot \varepsilon_{class} = 24.7$$

$$Class_{2.ft} := 38 \cdot \varepsilon_{class} = 28.4$$

$$Class_{3.ft} := 42 \cdot \varepsilon_{class} = 31.4$$

Control of classification of flange

$$Class_{f.t.1} := \begin{cases} 1 & \text{if } \beta_{f.t.1} \le Class_{1.ft} \\ 2 & \text{if } Class_{1.ft} < \beta_{f.t.1} \le Class_{2.ft} \\ 3 & \text{if } Class_{2.ft} < \beta_{f.t.1} \le Class_{3.ft} \\ 4 & \text{otherwise} \end{cases} = 2$$

Same width and loading situation gives the same class for all parts of the flange

$$Class_{f.t.2} := Class_{f.t.1}$$

$$Class_{f.t.3} := Class_{f.t.1}$$

Stiffener

Stiffener slenderness

$$\beta_{sl} := \frac{h_{sl.f}}{t_{sl.f}} = 6$$

Area of stiffener

$$A_{stiffener} := h_{sl.f} \cdot t_{sl.f} = 6 \times 10^{-4}\ m^2$$

Slenderness limit

$$Class_{1.sl} := 9 \cdot \varepsilon_{class} = 6.7$$

$$Class_{2.sl} := 10 \cdot \varepsilon_{class} = 7.5$$

$$Class_{3.sl} := 14 \cdot \varepsilon_{class} = 10.5$$

Control of stiffeners CSC

$$Class_{sl} := \begin{cases} 1 & \text{if } \beta_{sl} \le Class_{1.sl} \\ 2 & \text{if } Class_{1.sl} < \beta_{sl} \le Class_{2.sl} \\ 3 & \text{if } Class_{2.sl} < \beta_{sl} \le Class_{3.sl} \\ 4 & \text{otherwise} \end{cases} = 1$$

$$CSC\_web := \begin{cases} \text{"Change stiffener dimensions"} & \text{if } Class_{sl} = 4 \\ \text{"OK"} & \text{otherwise} \end{cases} = \text{"OK"}$$

Web without stiffeners

Thickness web

$$t_w := 14mm$$

Slenderness of upper part of web

$$\beta_w := \frac{h_w}{t_w} = 85.714$$

Stress ratio

$$\psi_1 := -1$$

Ratio for compression zone

$$\alpha_1 := \min\left[\frac{1}{\left(1 - \psi_1\right)}, 1\right] = 0.5$$

Limits for cross-section classes

$$Class_{1.w1} := \text{if}\left(\alpha_1 > 0.5, \frac{396}{13\cdot\alpha_1 - 1}, \frac{36}{\alpha_1}\right)\cdot\varepsilon_{class} = 53.9$$

$$Class_{2.w1} := \text{if}\left(\alpha_1 > 0.5, \frac{456}{13\cdot\alpha_1 - 1}, \frac{41.5}{\alpha_1}\right)\cdot\varepsilon_{class} = 62.1$$

$$Class_{3.w1} := \text{if}\left[\psi_1 > -1, \frac{42}{0.67 + 0.33\cdot\psi_1}, 62\cdot\left(1 - \psi_1\right)\cdot\sqrt{-\psi_1}\right]\cdot\varepsilon_{class} = 92.8$$

Control of classification of lower web

$$Class_w := \begin{cases} 1 & \text{if } \beta_w \le Class_{1.w1} \\ 2 & \text{if } Class_{1.w1} < \beta_w \le Class_{2.w1} \\ 3 & \text{if } Class_{2.w1} < \beta_w \le Class_{3.w1} \\ 4 & \text{otherwise} \end{cases} = 3$$

Top flange without stiffener

$t_f := 40mm$

Flange slenderness

$$\beta_{f.t} := \frac{b_{f.t} - 2t_w}{t_f} = 29.3$$

Limits for cross-section classes för avankhet

$$Class_{1.ft} := 33 \cdot \varepsilon_{class} = 24.7$$

$$Class_{2.ft} := 38 \cdot \varepsilon_{class} = 28.4$$

$$Class_{3.ft} := 42 \cdot \varepsilon_{class} = 31.4$$

Control of classification of flange

$$Class_{f.t} := \begin{cases} 1 & \text{if } \beta_{f.t} \le Class_{1.ft} \\ 2 & \text{if } Class_{1.ft} < \beta_{f.t} \le Class_{2.ft} \\ 3 & \text{if } Class_{2.ft} < \beta_{f.t} \le Class_{3.ft} \\ 4 & \text{otherwise} \end{cases} = 3$$

C

Mathcad sheet for effective width method

This Appendix contains the Mathcad calculations for the effective width method for one example of the beam with the cross-section dimension $t_f = 14mm$, $t_w = 8mm$ and $a = 1.5m$. In the loading situation of 80% moment capacity and 80% shear capacity. The input and cross-section sections are not visible, since they are calculated in Appendix B. To perform calculations for an unstiffened beam this sheet could be used by excluding Sections 5 to 8 and parts of Section 9 in this appendix regarding the reduction factor ρ_c. It does require some small additional changes, but the overall procedure is the same.

Johan Ahlstrand
Ellen Johansson

EFFECTIVE WIDTH METHOD: STIFFENERS

1. Input

2. Gross cross-section properties

2 GROSS CROSS SECTION PROPERTIES

Reductionfactor for flange width for shear deformation calculated according to EN1993-1-5 Section 3.2.1

Part of construction
1: Beam
2: End support
3: cantilever

$type := 1$

Width of half the flange

$$b_0 := \frac{b_{f.t.tot} - t_w}{2} = 0.6\,m$$

Area stiffener

$$A_{sl.f} := h_{av.f} \cdot t_{av.f} = 600 \cdot mm^2$$

Factor

$$\alpha_0 := \sqrt{1 + \frac{A_{sl.f}}{b_0 \cdot t_{f.t}}} = 1.05$$

Reduction faktor β

$$\beta(type, \kappa) := \left| \begin{array}{l} \beta_1 \leftarrow \left| \begin{array}{ll} 1 & \text{if } \kappa < 0.02 \\ \frac{1}{1 + 6.4 \cdot \kappa^2} & \text{if } 0.02 \le \kappa < 0.7 \\ \frac{1}{1 + 5.9 \cdot \kappa} & \text{if } 0.7 \le \kappa \end{array} \right. \\ \beta_2 \leftarrow \left| \begin{array}{ll} 1 & \text{if } \kappa < 0.02 \\ \frac{1}{1 + 6 \cdot \left(\kappa - \frac{1}{2500 \cdot \kappa} \right) + 1.6 \cdot \kappa^2} & \text{if } 0.02 \le \kappa < 0.7 \\ \frac{1}{1 + 8.6 \cdot \kappa} & \text{if } 0.7 \le \kappa \end{array} \right. \\ \beta \leftarrow \beta_1 \text{ if } M_{z.Ed} > 0\,kN \cdot m \\ \beta \leftarrow \beta_2 \text{ if } M_{z.Ed} \le 0\,kN \cdot m \\ \beta \leftarrow \min\left[\left(0.55 + \frac{0.025}{\kappa} \right) \cdot \beta_1, \beta_1 \right] \text{ if } type = 2 \\ \beta \leftarrow \beta_2 \text{ if } type = 3 \\ \beta \end{array} \right.$$

Effective length according to EN1993-1-5 Figure 3.1.

Span length between supports

$$L_1 := 9\,m$$

Adjacent span length

$$L_2 := 9\,m$$

Span type

1: End

2: Mid

$Span := 2$

Effective length

$$L_e := \begin{cases} 0.85 \cdot L_1 & \text{if } Span = 1 \\ 0.7 \cdot L_2 & \text{if } Span = 2 \\ 0.25 \cdot (L_1 + L_2) & \text{if } M_{z.Ed} \le 0\,kN \cdot m \end{cases} \quad \text{if } M_{z.Ed} > 0\,kN \cdot m = 6.3\,m$$

Factor for calculation of effective width, top

$$\kappa_t := \frac{\alpha_0 \cdot 0.5 (b_{f.t.tot} - t_w)}{L_e} = 0.099$$

Factor for calculation of effective width, bottom

$$\kappa_b := \frac{0.5 (b_{f.b} - t_w)}{L_e} = 0.095$$

Reduction factor, top

$$\beta_t := \begin{cases} \beta(type, \kappa_t) & \text{if } b_0 < \frac{L_e}{50} \\ 1 & \text{otherwise} \end{cases} = 1$$

Reduction factor, bottom

$$\beta_b := \begin{cases} \beta(type, \kappa_b) & \text{if } b_0 < \frac{L_e}{50} \\ 1 & \text{otherwise} \end{cases} = 1$$

Area top flange

$$A_{f.t} := t_{f.t} \cdot b_{f.t.tot} \cdot \beta_t = 0.012\,m^2$$

Area bottom flange

$$A_{f.b} := t_{f.b} \cdot b_{f.b} \cdot \beta_b = 0.012\,m^2$$

Area web

$$A_w := t_w \cdot h_{w.tot} = 0.012\,m^2$$

Total area lweb stiffener

$$A_{av.w} := n_{av.w} \cdot (h_{av.w} \cdot t_{av.w}) = 6 \times 10^{-4}\,m^2$$

Total area flange stiffener

$$A_{av.f} := n_{av.f} \cdot (h_{av.f} \cdot t_{av.f}) = 1.2 \times 10^{-3}\,m^2$$

Cross section area

$$A_{tot} := A_{f.t} + A_{f.b} + 2A_w + A_{av.f} + 2A_{av.w} = 0.0504\,m^2$$

Center of gravity (for gross cs)

$$y_{tp\_start} := \frac{-A_{f.t} \cdot \frac{t_{f.t}}{2} + 2A_w \cdot \left(\frac{h_{w.tot}}{2}\right) + 2A_{av.w} \cdot (h_{w.1}) \cdots}{+ A_{av.f} \cdot \left(\frac{h_{av.f}}{2}\right) + A_{f.b} \cdot \left(h_{w.tot} + \frac{t_{f.b}}{2}\right)} = 0.722\,m$$

Moment of inertia of web stiffener

$$I_{av.w} := 2n_{av.w}\frac{h_{av.w}\cdot t_{av.w}^{3}}{12} + 2h_{av.w}\cdot t_{av.w}\cdot\left(y_{tp\_start} - h_{w.1}\right)^{2} = 0.0002\,m^{4}$$

Moment of inertia of flange stiffener

$$I_{av.f} := n_{av.f}\frac{h_{av.f}\cdot t_{av.f}^{3}}{12} + n_{av.f}\,h_{av.f}\cdot t_{av.f}\cdot\left(y_{tp\_start} - \frac{h_{av.f}}{2}\right)^{2} = 0.0006\,m^{4}$$

Moment of inertia

$$\begin{aligned} I_z := {} & 2\left[\frac{t_w\cdot h_{w.tot}^{3}}{12} + t_w\cdot h_{w.tot}\cdot\left(y_{tp\_start} - \frac{h_{w.tot}}{2}\right)^{2}\right] \ldots \\ & + \frac{b_{f.t.tot}\cdot t_{f.t}^{3}}{12} + b_{f.t.tot}\cdot t_{f.t}\cdot\left(y_{tp\_start} + \frac{t_{f.t}}{2}\right)^{2} \ldots \\ & + \frac{b_{f.b}\cdot t_{f.b}^{3}}{12} + b_{f.b}\cdot t_{f.b}\cdot\left(h_{w.tot} + \frac{t_{f.b}}{2} - y_{tp\_start}\right)^{2} \ldots \\ & + I_{av.f} + I_{av.w} \end{aligned} = 0.019\,m^{4}$$

Elastic section modulus

$$W_{el.z} := \min\left(\frac{I_z}{y_{tp\_start} + t_{f.t}}, \frac{I_z}{h_{w.tot} + t_{f.b} - y_{tp\_start}}\right) = 0.024\cdot m^{3}$$

Plastic section modulus

$$\begin{aligned} W_{pl} := {} & A_{f.t}\cdot\left(y_{tp\_start} + \frac{t_{f.t}}{2}\right) + A_{f.b}\cdot\left(h_{w.tot} + \frac{t_{f.b}}{2} - y_{tp\_start}\right) \ldots \\ & + 2A_w\cdot\left(\frac{h_{w.tot}}{2} - y_{tp\_start}\right) + A_{av.w}\cdot\left(y_{tp\_start} - h_{w.1}\right) \ldots \\ & + A_{av.f}\cdot\left(y_{tp\_start} - \frac{h_{av.f}}{2}\right) \end{aligned} = 1.99 \times 10^{7}\cdot mm^{3}$$

Dimensioning plastic moment capacity

$$M_{pl.Rd} := \frac{W_{pl}\cdot f_{yd}}{\gamma_{M0}} = 8.35 \times 10^{3}\cdot kNm$$

Center of gravity

$$y_{tp} := y_{tp\_start}$$

2. Gross cross-section properties

3. Cross-section class

4. Reduction buckling

4 REDUCTION BUCKLING

Reduction for parts in cross-section class 4 made according to EN1993-1-5 Section 4.4.

4.1 Top outer flange

Stress ratio

$$\psi_{f.t.1} := 1$$

Buckling factor

$$k_{\sigma.ft} := 4$$

Slenderness

$$\lambda_{f.t.edge} := \frac{\beta_{f.t.1}}{28.4 \cdot \varepsilon_{class} \cdot \sqrt{k_{\sigma.ft}}} = 0.91$$

Reduction factor

$$\rho_{f.t.1} := \text{if}\left(\text{class}_{f.t.1} = 4,\ \begin{vmatrix} 1 & \text{if } \lambda_{f.t.edge} \le 0.5 + \sqrt{0.085 - 0.055\psi_{f.t.1}} \\ \dfrac{\lambda_{f.t.edge} - 0.055\max\left(3 + \psi_{f.t.1}, 0\right)}{\lambda_{f.t.edge}^{\,2}} & \text{otherwise} \end{vmatrix},\ 1\right) = 0.83$$

Effective width edge

$$b_{f.t.1.eff.1} := \left(0.5 \cdot b_{f.t.1} - t_w\right)\beta_t \cdot \rho_{f.t.1} + t_w = 167.88 \cdot \text{mm}$$

Effective width mid

$$b_{f.t.1.eff.2} := \left(0.5 \cdot b_{f.t.1} - \frac{t_{av.f}}{2}\right)\beta_t \cdot \rho_{f.t.1} + \frac{t_{av.f}}{2} = 167.38 \cdot \text{mm}$$

Total effective width outer top flange

$$b_{f.t.1.eff} := b_{f.t.1.eff.1} + b_{f.t.1.eff.2} = 0.34\,\text{m}$$

4.2 Top flange between stiffener

Stress ratio

$$\psi_{f.t.2} := 1$$

Buckling factor

$$k_{\sigma.ft} = 4$$

Slenderness

$$\lambda_{f.t.mid} := \frac{\beta_{f.t.2}}{28.4 \cdot \varepsilon_{class} \cdot \sqrt{k_{\sigma.ft}}} = 0.92$$

Reduction factor

$$\rho_{f.t.2} := \text{if}\left(\text{class}_{f.t.2} = 4,\ \begin{vmatrix} 1 & \text{if } \lambda_{f.t.mid} \le 0.5 + \sqrt{0.085 - 0.055\psi_{f.t.2}} \\ \dfrac{\lambda_{f.t.mid} - 0.055\max\left(3 + \psi_{f.t.2}, 0\right)}{\lambda_{f.t.mid}^{\,2}} & \text{otherwise} \end{vmatrix},\ 1\right) = 0.83$$

Effective width mid

$$b_{f.t.2.eff.1} := 0.5\beta_{f.t.2}\cdot t_{f.t}\cdot\rho_{f.t.2} + \frac{t_{av.f}}{2} = 166.52\cdot mm$$

$$b_{f.t.2.eff.2} := 0.5\beta_{f.t.2}\cdot t_{f.t}\cdot\rho_{f.t.2} + \frac{t_{av.f}}{2} = 166.52\cdot mm$$

Total effective mid

$$b_{f.t.2.eff} := b_{f.t.2.eff.1} + b_{f.t.2.eff.2} = 0.33\,m$$

4.3 Bottom flange

Stress ratio

$$\psi_{fb} := 1$$

Buckling factor

$$k_{\sigma.fb} := 4$$

Slenderness

$$\lambda_{f.b} := \frac{\beta_{f.b}}{28.4\cdot\varepsilon_{class}\cdot\sqrt{k_{\sigma.fb}}} = 2.79$$

Reduction factor

$$\rho_{f.b} := \text{if}\left(\text{class}_{fb} = 4,\ \begin{cases} 1 & \text{if } \lambda_{f.b} \le 0.5 + \sqrt{0.085 - 0.055\psi_{fb}} \\ \dfrac{\lambda_{f.b} - 0.055\max\left(3 + \psi_{fb}, 0\right)}{\lambda_{f.b}^{\,2}} & \text{otherwise} \end{cases},\ 1\right) = 1$$

Effective width left side

$$b_{f.b.eff.1} := 0.5\beta_{f.b}\cdot t_{f.b}\cdot\rho_{f.b} + t_w = 600\cdot mm$$

Effective width right side

$$b_{f.b.eff.2} := 0.5\beta_{f.b}\cdot t_{f.b}\cdot\rho_{f.b} + t_w = 600\cdot mm$$

Total effective width

$$b_{f.b.eff} := b_{f.b.eff.1} + b_{f.b.eff.2} = 1.2\,m$$

4.4 Top part of web

Ratio

$$\psi_1 = 0.58$$

Function for buckling factor

$$k_{\sigma.w}(\psi) := \begin{cases} \dfrac{8.2}{(1.05 + \psi)} & \text{if } 1 \ge \psi > 0 \\ 7.81 - 6.29\cdot\psi + 9.78\cdot\psi^2 & \text{if } 0 \ge \psi > -1 \\ 5.98\cdot(1 - \psi)^2 & \text{if } -1 \ge \psi > -3 \\ \left[5.98\cdot(1 - -3)^2\right] & \text{otherwise} \end{cases}$$

Buckling factor

$$k_{\sigma.w1} := k_{\sigma.w}\left(\psi_1\right) = 5.02$$

Slenderness

$$\lambda_{w.1} := \frac{\beta_{w.1}}{28.4\cdot\varepsilon_{class}\cdot\sqrt{k_{\sigma.w1}}} = 0.79$$

Reduction factor

$$\rho_{w.1} := \text{if}\left(\text{class}_{w.1} = 4,\ \begin{cases} 1 & \text{if } \lambda_{w.1} \le 0.5 + \sqrt{0.085 - 0.055\psi_1} \\ \dfrac{\lambda_{w.1} - 0.055\cdot\max\left(3 + \psi_1, 0\right)}{\lambda_{w.1}^{\,2}} & \text{otherwise} \end{cases},\ 1\right) = 0.95$$

Height of the web closest to the top

$$h_{w1.1} := \text{if}\left[\text{class}_{w.1} = 4,\ \left|\begin{array}{ll} \dfrac{2\cdot\left(\left(h_{w.1} - \dfrac{t_{av.w}}{2}\right)\right)}{5 - \psi_1} & \text{if } \text{sign}\left(\sigma_{w.1.T}\right) = -1 \wedge \text{sign}\left(\sigma_{w.1.B}\right) = -1, h_{w.1} \\ 0.4\cdot\dfrac{\left(h_{w.1} - \dfrac{t_{av.w}}{2}\right)}{1 - \psi_1} & \text{if } \text{sign}\left(\sigma_{w.1.T}\right) = -1 \wedge \text{sign}\left(\sigma_{w.1.B}\right) = 1 \\ 0 & \text{otherwise} \end{array}\right.\right] = 0.13\cdot\text{m}$$

Height of the web closest to the stiffener

$$h_{w1.2} := \text{if}\left[\text{class}_{w.1} = 4,\ \left|\begin{array}{ll} \left(h_{w.1} - \dfrac{t_{av.w}}{2}\right) - h_{w1.1} & \text{if } \text{sign}\left(\sigma_{w.1.T}\right) = -1 \wedge \text{sign}\left(\sigma_{w.1.B}\right) = -1, 0 \\ 0.6\cdot\dfrac{\left(h_{w.1} - \dfrac{t_{av.w}}{2}\right)}{1 - \psi_1} & \text{if } \text{sign}\left(\sigma_{w.1.T}\right) = -1 \wedge \text{sign}\left(\sigma_{w.1.B}\right) = 1 \\ 0 & \text{otherwise} \end{array}\right.\right]$$

$$h_{w1.2} = 0.161\,\text{m}$$

Effective height according to Tabel 4.1 EN1993-1-5

$$h_{w1.eff1} := \rho_{w.1}\cdot h_{w1.1} = 0.127\,\text{m}$$

Effective height above stiffener, including stiffener

$$h_{w1.eff2} := h_{w1.2}\cdot\rho_{w.1} + \frac{t_{av.w}}{2} = 0.159\,\text{m}$$

Height of excluded part

$$h_{w1.exkl} := \text{if}\left(\text{class}_{w.1} = 4, h_{w.1} - h_{w1.eff1} - h_{w1.eff2}, 0\right) = 0.014\cdot\text{m}$$

Total effective height

$$h_{w1.eff} := h_{w1.eff1} + h_{w1.eff2} = 0.29\,\text{m}$$

4.5 Bottom part of web

Stress ratio

$$\psi_2 = -1.84$$

Buckling factor

$$k_{\sigma.w2} := k_{\sigma.w}\left(\psi_2\right) = 48.32$$

Width

$$b_{bar.w.2} := h_{w.tot} - h_{w.1} - \frac{t_{av.w}}{2} = 1.2\,\text{m}$$

Slenderness

$$\lambda_{w.2} := \frac{\beta_{w.2}}{28.4\cdot\varepsilon_{class}\cdot\sqrt{k_{\sigma.w2}}} = 1.02$$

Reduction factor

$$\rho_{w.2} := \text{if}\left(\text{class}_{w.2} = 4,\ \left|\begin{array}{ll} 1 & \text{if } \lambda_{w.2} \le 0.5 + \sqrt{0.085 - 0.055\psi_2} \\ \dfrac{\lambda_{w.2} - 0.055\cdot\max\left(3 + \psi_2, 0\right)}{\lambda_{w.2}^{\,2}} & \text{otherwise} \end{array}\right.,\ 1\right) = 1$$

Height closest to stiffener

$$h_{w2.1} := \text{if}\left(\text{class}_{w.2} = 4,\ \left|\begin{array}{ll} \dfrac{2}{5 - \psi_2} b_{bar.w.2} & \text{if } \text{sign}\left(\sigma_{w.2.T}\right) = -1 \wedge \text{sign}\left(\sigma_{w.2.B}\right) = -1 \\ 0.4\cdot\dfrac{b_{bar.w.2}}{1 - \psi_2} & \text{if } \text{sign}\left(\sigma_{w.2.T}\right) = -1 \wedge \text{sign}\left(\sigma_{w.2.B}\right) = 1 \\ 0 & \text{otherwise} \end{array}\right.,\ b_c - h_{w.1}\right) = 0.42\cdot\text{m}$$

Height closest to tensile zone

$$h_{w2.2} := \text{if}\left(\text{class}_{w.2} = 4,\ \left|\begin{array}{ll} b_{bar.w.2} - h_{w2.1} & \text{if } \text{sign}\left(\sigma_{w.2.T}\right) = -1 \wedge \text{sign}\left(\sigma_{w.2.B}\right) = -1 \\ 0.6\cdot\dfrac{b_{bar.w.2}}{1 - \psi_2} & \text{if } \text{sign}\left(\sigma_{w.2.T}\right) = -1 \wedge \text{sign}\left(\sigma_{w.2.B}\right) = 1 \\ 0 & \text{otherwise} \end{array}\right.,\ 0\right) = 0\cdot\text{m}$$

Effective height below stiffener including stiffener

$$h_{w2.eff1} := h_{w2.1}\cdot\rho_{w.2} = 0.422\,\text{m}$$

Effective height in compression zone

$$h_{w2.eff2.c} := h_{w2.2}\cdot\rho_{w.2} = 0\,\text{m}$$

Height in tension zone

$$h_{w.2.t} := h_{w.tot} - b_c = 0.778\,\text{m}$$

Effective part closest to bottom flange

$$h_{w2.eff2} := \text{if}\left(\text{class}_{w.2} = 4, h_{w2.eff2.c} + h_{w.2.t}, h_{w.2.t}\right) = 0.78\cdot\text{m}$$

Height excluded part

$$h_{w2.exkl} := \text{if}\left(\text{class}_{w.2} = 4, b_c - h_{w.1} - h_{w2.eff1} - h_{w2.eff2.c}, 0\right) = 0\cdot\text{m}$$

Total effective height

$$h_{w2.eff} := h_{w2.eff1} + h_{w2.eff2} = 1.2\,\text{m}$$

Total effective height in compression zone

$$h_{w2.eff.c} := h_{w2.eff1} + h_{w2.eff2.c} = 0.42\,\text{m}$$

4.6 Summarisation

Calculations according to EN1993-1-5 Section 3.3 and 4.4

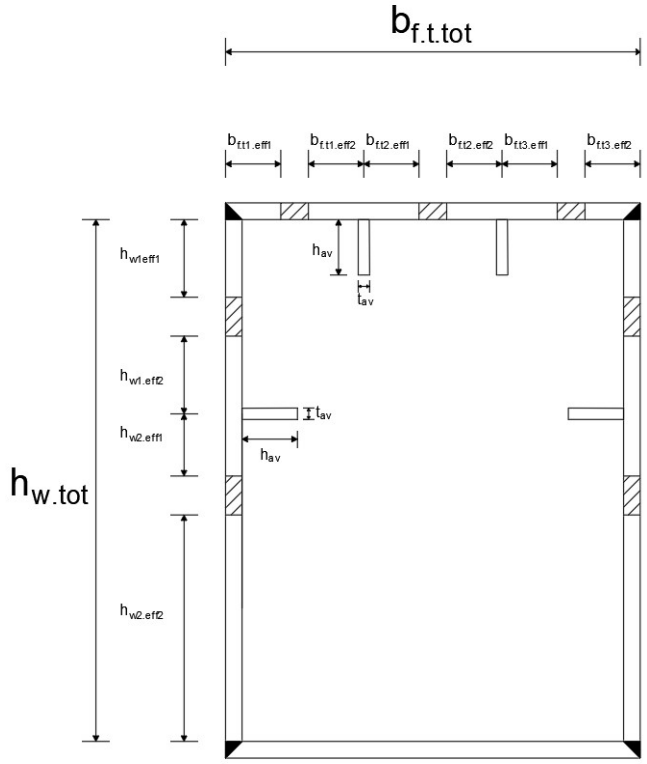

$b_{f.t.1.eff.1} = 0.17\,m$

$b_{f.t.1.eff.2} = 0.17\,m$

$b_{f.t.2.eff.1} = 0.17\,m$

$b_{f.t.2.eff.2} = 0.17\,m$

$b_{f.t.3.eff.1} := b_{f.t.1.eff.2} = 0.17\,m$

$b_{f.t.3.eff.2} := b_{f.t.1.eff.1} = 0.17\,m$

$b_{f.b.eff} = 1.2\,m$

$h_{w1.eff1} = 0.13\,m$

$h_{w1.eff2} = 0.16\,m$

$h_{w2.eff1} = 0.4221\,m$

$h_{w2.eff2} = 0.7779\,m$

$h_{w.2.t} = 0.78\,m$

Gross area web inc. stiffener excluding edges in compression zone

$$A_{c.w} := \left(b_c - h_{w1.1} - h_{w2.2}\right)\cdot t_w + A_{av.w} = 5.31 \times 10^{-3}\,m^2$$

Effective area top flange including stiffener. exduding edges.

$$A_{c.eff.loc.f} := \begin{pmatrix} b_{f.t.1.eff.2} + b_{f.t.2.eff.1} + b_{f.t.2.eff.2} \cdots \\ + b_{f.t.3.eff.1} \end{pmatrix}\cdot t_{f.t} + A_{av.f} = 7.88 \times 10^{-3}\,m^2$$

Gross area top flange including stiffener. exduding edges.

$$A_{c.f} := \left(\frac{b_{f.t.1}}{2} + b_{f.t.2} + \frac{b_{f.t.3}}{2}\right)\cdot t_{f.t} + A_{av.f} = 9.2 \times 10^{-3}\,m^2$$

4. Reduction buckling

5. Cross-section properties web stiffener

5 CROSS SECTION PROPERTIES WEB STIFFENER

5.1 Longitudinal single stiffener

Moment of inertia is needed even for the single web stiffener with the highest compression stress. Contributing width in the web according to Figure A.1 in EN1993-1-5.

Contributing web width to single web stiffener

$$\psi_{1.sl} := \text{if}\left(\text{sign}\left(M_{z.Ed}\right) = 1, \psi_1, \psi_2\right) = 0.58$$

$$\psi_{2.sl} := \text{if}\left(\text{sign}\left(M_{z.Ed}\right) = 1, \psi_2, \psi_1\right) = -1.84$$

$$b_{1.inf} := \frac{3 - \psi_{1.sl}}{5 - \psi_{1.sl}} \cdot \left(h_{w.1} - \frac{t_{av.w}}{2}\right) = 0.161\,\text{m}$$

$$b_{2.sup} := 0.4 \cdot \left(b_c - h_{w.1} - \frac{t_{av.w}}{2}\right) = 0.167\,\text{m}$$

Contributing part of the web

$$b_{sl.1} := t_{av.w} + b_{1.inf} + b_{2.sup} = 0.338\,\text{m}$$

Area of contr. web and stiffener

$$A_{sl.1.w} := b_{sl.1} \cdot t_w + \frac{A_{av.w}}{n_{av.w}} = 3.31 \times 10^3 \cdot \text{mm}^2$$

Effective contr. width of web

$$b_{1.inf.eff} := \frac{3 - \psi_{1.sl}}{5 - \psi_{1.sl}} \cdot \left(h_{w1.eff} - \frac{t_{av.w}}{2}\right) = 0.154\,\text{m}$$

$$b_{2.sup.eff} := 0.4 \cdot \left(h_{w2.eff.c} - \frac{t_{av.w}}{2}\right) = 0.167\,\text{m}$$

Total effective contr. part of the web to the stiffener

$$b_{sl.1.eff} := t_{av.w} + b_{1.inf.eff} + b_{2.sup.eff} = 0.33\,\text{m}$$

Effective area of web and stiffener

$$A_{sl.1.eff.w} := \left(b_{1.inf.eff} + b_{2.sup.eff} + t_{av.w}\right) \cdot t_w + \frac{A_{av.w}}{n_{av.w}} = 3.24 \times 10^3 \cdot \text{mm}^2$$

Effective area web incl. stiffeners

$$A_{c.eff.loc.w} := A_{sl.1.eff.w} = 3.24 \times 10^{-3}\,\text{m}^2$$

Center of gravity for web and sitffener

$$y_{tp.sl.1.w} := \frac{b_{sl.1}\cdot t_w\cdot\frac{t_w}{2} + h_{av.w}\cdot t_{av.w}\cdot\left(\frac{h_{av.w}}{2}\right)}{A_{sl.1.w}} = 8.72\cdot mm$$

Moment of inertia for stiffener

$$I_{sl.1.w} := \frac{b_{sl.1}\cdot t_w^{3}}{12} + b_{sl.1}\cdot t_w\cdot\left(y_{tp.sl.1.w} - \frac{t_w}{2}\right)^2 \ldots + \frac{t_{av.w}\cdot h_{av.w}^{3}}{12} + t_{av.w}\cdot h_{av.w}\cdot\left(t_w + \frac{h_{av.w}}{2} - y_{tp.sl.1.w}\right)^2 = 7.691\times 10^{5}\cdot mm^4$$

Distance to center of gravity of stiffener only

$$y_{tp.2.sl.1.w} := \frac{n_{av.w}\cdot h_{av.w}\cdot t_{av.w}\cdot\left(t_w + \frac{h_{av.w}}{2}\right)}{n_{av.w}\cdot h_{av.w}\cdot t_{av.w}} = 38\cdot mm$$

Distance to combined center of gravity from web's or stiffener's ytp

$$e_w := \max\left(y_{tp.sl.1.w} - \frac{t_w}{2}, y_{tp.2.sl.1.w} - y_{tp.sl.1.w}\right) = 29.28\cdot mm$$

5.2 Longitudinal stiffener (shear force)

At control of shear moment of inertia is calculated with contributing part according to Figure 5.3 (b) in EN 1993-1-5.

Contributing part of web

$$b_{st.w} := t_{av.w} + 2\cdot 15\cdot\varepsilon_{class}\cdot t_w = 0.19\,m$$

Area of contr. web and stiffener

$$A_{st.i.w} := b_{st.w}\cdot t_w + h_{av.w}\cdot t_{av.w} = 2116\cdot mm^2$$

Center of gravity

$$y_{tp.st.w} := \frac{b_{st.w}\cdot t_w\cdot\frac{t_w}{2} + h_{av.w}\cdot t_{av.w}\cdot\left(t_w + \frac{h_{av.w}}{2}\right)}{A_{st.i.w}} = 13.64\cdot mm$$

Moment of inertia for the stiffener

$$I_{st.i.w} := \frac{b_{st.w}\cdot t_w^{3}}{12} + b_{st.w}\cdot t_w\cdot\left(y_{tp.st.w} - \frac{t_w}{2}\right)^2 \ldots + \frac{t_{av.w}\cdot h_{av.w}^{3}}{12} + t_{av.w}\cdot h_{av.w}\cdot\left(t_w + \frac{h_{av.w}}{2} - y_{tp.st.w}\right)^2 = 6.85\times 10^{-7}\,m^4$$

Moment of inertia for all stiffeners in web

$$I_{st.w} := n_{av.w}\cdot I_{st.i.w} = 6.85\times 10^{5}\cdot mm^4$$

5. Cross-section properties web stiffener

6. Reduction of web stiffeners

6 REDUCTION OF WEB STIFFENER

6.1 Effective area

Gross area and effective are for web is defined by Figure A.1 in EN1993.1.5.

Gross area

$$A_{c.w} = 5.31 \times 10^{3} \cdot mm^{2}$$

Effective area

$$A_{c.eff.loc.w} = 3.24 \times 10^{3} \cdot mm^{2}$$

Effective area ratio

$$\beta_{A.c} := \frac{A_{c.eff.loc.w}}{A_{c.w}} = 0.61$$

6.2 Critical plate buckling

Calculation according to EN1993-1-5 Section A.2.2

Width from top edge of web to critical buckling point

$$b_1 := h_{w.1} = 0.3 \cdot m$$

Width from bottom edge of web to critical buckling point

$$b_2 := h_{w.2} = 1.2 \cdot m$$

Total buckling length

$$b_w := b_1 + b_2 = 1.5\,m$$

Limit for panel width

$$a_c := 4.33 \cdot \sqrt[4]{\frac{I_{sl.1.w} \cdot {b_1}^2 {b_2}^2}{{t_w}^3 \cdot b_w}} = 2.599\,m$$

Critical stress in stiffener

$$\sigma_{cr.sl.p} := \begin{cases} \frac{1.05 \cdot E_s}{A_{sl.1.w}} \cdot \frac{\sqrt{I_{sl.1.w} \cdot {t_w}^3 \cdot b_w}}{b_1 \cdot b_2} & \text{if } a_w \geq a_c \\ \frac{\pi^2 \cdot E_s \cdot I_{sl.1.w}}{A_{sl.1.w} \cdot {a_w}^2} + \frac{E_s \cdot {t_w}^3 \cdot b_w \cdot {a_w}^2}{4 \cdot \pi^2 \cdot \left(1 - v^2\right) \cdot A_{sl.1.w} \cdot {b_1}^2 \cdot {b_2}^2} & \text{if } a_w < a_c \end{cases} = 142.4 \cdot MPa$$

Critical stress in the panel

$$\sigma_{cr.p} := \sigma_{cr.sl.p} \cdot \frac{b_c}{b_c - b_1} = 243.59 \cdot MPa$$

Slenderness for plate buckling

$$\lambda_p := \sqrt{\frac{\beta_{A.c} \cdot f_{yd}}{\sigma_{cr.p}}} = 1.03$$

Stress ratio

$$\psi_{liv} := \frac{\max\left(\sigma_{w.B}, \sigma_{w.T}\right)}{\min\left(\sigma_{w.B}, \sigma_{w.T}\right)} = -1.08$$

Reduction factor due to plate buckling

$$\rho_w := \begin{cases} 1 & \text{if } \lambda_p \le 0.5 + \sqrt{0.085 - 0.055\psi_{liv}} \\ \min\left(\frac{\lambda_p - 0.055\cdot\max(3 + \psi_{liv}, 0)}{\lambda_p^{\,2}}, 1\right) & \text{otherwise} \end{cases} = 0.87$$

6.3 Column-like buckling

Calculations according to 1993-1-5 Section 4.5.3 and EN1993-1-1 Section 6.3.1.2. Allowable stresses for column-like buckling according to EN1993-1-5 Section 4.5.3 (3) Note.

Critical normal stress

$$\sigma_{cr.c} := \frac{\pi^2\cdot E_s\cdot I_{sl.1.w}}{A_{sl.1.w}\cdot a_w^{\,2}}\cdot\frac{b_c}{b_c - h_{w.1}} = 92\cdot\text{MPa}$$

Ratio for effective area for single stiffener

$$\beta_{A.c.eff} := \frac{A_{sl.1.eff.w}}{A_{sl.1.w}} = 0.98$$

Slenderness for column-like plate buckling

$$\lambda_{.c} := \sqrt{\frac{\beta_{A.c.eff}\cdot f_{yd}}{\sigma_{cr.c}}} = 2.12$$

Parameter for open cross section (stiffener)

$$\alpha_w := 0.49$$

Radius of gyration for stiffener

$$i_w := \sqrt{\frac{I_{sl.1.w}}{A_{sl.1.w}}} = 0.02\,\text{m}$$

Max distance to combined center of gravity

$$e_w = 29.28\cdot\text{mm}$$

Parameter

$$\alpha_e := \alpha_w + \frac{0.09}{\frac{i_w}{e_w}} = 0.66$$

Parameter

$$\phi_w := 0.5\cdot\left[1 + \alpha_e\cdot(\lambda_{.c} - 0.2) + \lambda_{.c}^{\,2}\right] = 3.38$$

Reduction factor for column-like buckling

$$\chi_c := \frac{1}{\phi_w + \sqrt{\phi_w^{\,2} - \lambda_{.c}^{\,2}}} = 0.17$$

6.4 Interpolation: plate and column-like buckling

Calculations according to 1993-1-5 Section 4.5.4.

Parameter for weighting

$$\xi_w := \min\left(\max\left(0, \frac{\sigma_{cr.p}}{\sigma_{cr.c}} - 1\right), 1\right) = 1$$

Weighted reduction factor for web stiffeners

$$\rho_{c.w} := (\rho_w - \chi_c)\cdot\xi_w\cdot(2 - \xi_w) + \chi_c = 0.87$$

6. Reduction of web stiffeners

7 CROSS SECTION PROP. FLANGE STIFFENER

7.1 Longitudinal single stiffener

Cross-section properties for flange stiffeners are calculated for normal stresses since the flange is not subjected to shear.

Moment of inertia is needed for the stiffener subjected to the highest compression stress.
Contributing width according o Figure 4.4

Area of contr. flange and stiffener

$$A_{sl.1.f} := \left(\frac{b_{f.t.1}}{2} + \frac{b_{f.t.2}}{2}\right) t_{f.t} + \frac{A_{av.f}}{n_{av.f}} = 4.6 \times 10^{3} \cdot mm^{2}$$

Effective area of flange and stiffener

$$A_{sl.1.eff.f} := \left(b_{f.t.1.eff.2} + b_{f.t.2.eff.1}\right) t_{f.t} + \frac{A_{av.f}}{n_{av.f}} = 3.94 \times 10^{3} \cdot mm^{2}$$

Center of gravity for flange and sitffener

$$y_{tp.sl.1.f} := \frac{\left(\frac{b_{f.t.1}}{2} + \frac{b_{f.t.2}}{2}\right) t_{f.t} \cdot \left(\frac{-t_{f.t}}{2}\right) + h_{av.f} \cdot t_{av.f} \cdot \left(\frac{h_{av.f}}{2}\right)}{A_{sl.1.f}} = -0.43 \cdot mm$$

Moment of inertia for stiffener

$$I_{sl.1.f} := \frac{t_{f.t}^{3} \cdot \left(\frac{b_{f.t.1}}{2} + \frac{b_{f.t.2}}{2}\right)}{12} \ldots + t_{f.t} \cdot \left(\frac{b_{f.t.1}}{2} + \frac{b_{f.t.2}}{2}\right) \cdot \left(-\frac{t_{f.t}}{2} - y_{tp.sl.1.f}\right)^{2} \ldots + \frac{h_{av.f}^{3} \cdot t_{av.f}}{12} + t_{av.f} \cdot h_{av.f} \cdot \left(\frac{h_{av.f}}{2} - y_{tp.sl.1.f}\right)^{2} = 8.52464 \times 10^{5} \cdot mm^{4}$$

Distance to center of gravity of stiffener only

$$y_{tp.2.sl.1.f} := \frac{h_{av.f} \cdot t_{av.f} \cdot \left(\frac{h_{av.f}}{2}\right)}{h_{av.f} \cdot t_{av.f}} = 30 \cdot mm$$

Distance to combined center of gravity from flange's or stiffener's ytp

$$e_{f} := \max\left(\left|y_{tp.sl.1.f} + \frac{t_{f.t}}{2}\right|, \left|y_{tp.2.sl.1.f} - y_{tp.sl.1.f}\right|\right) = 30.43 \cdot mm$$

8. Reduction of flange stiffeners

8 REDUCTION OF FLANGE STIFFENER

Calculations according to EN1993-1-5 Section 4.5.3

8.1 Effektiv area

According to Figure 4.4 in EN-1993-1-5

Gross area for single stiffener

$$A_{sl.1.f} = 4.6 \times 10^{-3}\ m^2$$

Effective area for single stiffener

$$A_{sl.1.eff.f} = 3.94 \times 10^{-3}\ m^2$$

Effective area ratio

$$\beta_{A.c.f} := \frac{A_{sl.1.eff.f}}{A_{sl.1.f}} = 0.86$$

8.2 Critical plate buckling

Calculations according to EN1993-1-5 Section A.2.2 Since the flange has two stiffeners the three different cases are calculated.

Width from left edge of flange to critical buckling point

$$b_{1.f} := \begin{pmatrix} b_{f.t.1} \\ b_{f.t.2} \\ \frac{b_{f.t.tot}}{2} \end{pmatrix} = \begin{pmatrix} 0.4 \\ 0.4 \\ 0.6 \end{pmatrix} \cdot m$$

Width from right edge of flange to critical buckling point

$$b_{2.f} := \begin{pmatrix} b_{f.t.2} \\ b_{f.t.3} \\ \frac{b_{f.t.tot}}{2} \end{pmatrix} = \begin{pmatrix} 0.4 \\ 0.4 \\ 0.6 \end{pmatrix} \cdot m$$

Total buckling length

$$b_{flange} := b_{1.f} + b_{2.f} = \begin{pmatrix} 0.8 \\ 0.8 \\ 1.2 \end{pmatrix} m$$

Moment of inertia

$$I_{sl.1.fp} := \begin{pmatrix} I_{sl.1.f} \\ I_{sl.1.f} \\ 2 \cdot I_{sl.1.f} \end{pmatrix} = \begin{pmatrix} 8.52 \times 10^{-7} \\ 8.52 \times 10^{-7} \\ 1.7 \times 10^{-6} \end{pmatrix} m^4$$

Area

$$A_{sl.1.fp} := \begin{pmatrix} A_{sl.1.f} \\ A_{sl.1.f} \\ 2 \cdot A_{sl.1.f} \end{pmatrix} = \begin{pmatrix} 4.6 \times 10^{-3} \\ 4.6 \times 10^{-3} \\ 9.2 \times 10^{-3} \end{pmatrix} m^2$$

Limit for panel width

$$a_{c.f} := \left| \begin{array}{l} \text{for } i \in 0..2 \\ t_i \leftarrow 4.33 \cdot \sqrt[4]{\dfrac{I_{sl.1.fp_i} \cdot \left(b_{1.f_i}\right)^2 \left(b_{2.f_i}\right)^2}{t_{f.t}^{\,3} \cdot b_{flange_i}}} \\ t \end{array} \right. = \begin{pmatrix} 1.76 \\ 1.76 \\ 2.84 \end{pmatrix} \text{m}$$

Critical stress in stiffener

$$\sigma_{cr.sl.p.f} := \left| \begin{array}{l} \text{for } i \in 0..2 \\ t_i \leftarrow \left| \begin{array}{ll} \dfrac{1.05 \cdot E_s}{A_{sl.1.fp_i}} \cdot \dfrac{\sqrt{I_{sl.1.fp_i} \cdot t_{f.t}^{\,3} \cdot b_{flange_i}}}{b_{1.f_i} \cdot b_{2.f_i}} & \text{if } a_w \geq a_{c.f_i} \\ \dfrac{\pi^2 \cdot E_s \cdot I_{sl.1.fp_i}}{A_{sl.1.fp_i} \cdot a_w^{\,2}} + \dfrac{E_s \cdot t_{f.t}^{\,3} \cdot b_{flange_i} \cdot a_w^{\,2}}{4 \cdot \pi^2 \cdot \left(1 - v^2\right) \cdot A_{sl.1.fp_i} \cdot \left(b_{1.f_i}\right)^2 \cdot \left(b_{2.f_i}\right)^2} & \text{if } a_w < a_{c.f_i} \end{array} \right. \\ t \end{array} \right.$$

$$\sigma_{cr.sl.p.f} = \begin{pmatrix} 247.41 \\ 247.41 \\ 95.23 \end{pmatrix} \cdot \text{MPa}$$

Stress in plate

$$\sigma_{cr.p.f} := \min\left(\sigma_{cr.sl.p.f}\right) = 95.23 \cdot \text{MPa}$$

Slenderness for column-like plate buckling

$$\lambda_{p.f} := \sqrt{\frac{\beta_{A.c.f} \cdot f_{yd}}{\sigma_{cr.p.f}}} = 1.94$$

Stress ratio

$$\psi_f := \frac{\sigma_{f.t}}{\sigma_{f.t}} = 1$$

Reduction factor due to column-like plate buckling

$$\rho_f := \left| \begin{array}{ll} 1 & \text{if } \lambda_{p.f} \leq 0.5 + \sqrt{0.085 - 0.055\psi_f} \\ \min\left(\dfrac{\lambda_{p.f} - 0.055 \cdot \max\left(3 + \psi_f, 0\right)}{\lambda_{p.f}^{\,2}}, 1\right) & \text{otherwise} \end{array} \right. = 0.46$$

8.3 Column-like buckling

Calculations according to 1993-1-5 Section 4.5.3 and EN1993-1-1 Section 6.3.1.2.

Critical normal stress

$$\sigma_{cr.c.f} := \frac{\pi^2 \cdot E_s \cdot I_{sl.1.f}}{A_{sl.1.f} \cdot a_w^2} = 43 \cdot MPa$$

Slenderness for column-like plate buckling

$$\lambda_{c.f} := \sqrt{\frac{\beta_{A.c.f} \cdot f_{yd}}{\sigma_{cr.c.f}}} = 2.9$$

Parameter for open cross section (stiffener)

$$\alpha_f := 0.49$$

Radius of gyration for stiffener

$$i_f := \sqrt{\frac{I_{sl.1.f}}{A_{sl.1.f}}} = 0.01\,m$$

Parameter

$$\alpha_{e.f} := \alpha_f + \frac{0.09}{\frac{i_f}{e_f}} = 0.69$$

Parameter

$$\phi_f := 0.5 \cdot \left[1 + \alpha_{e.f} \cdot \left(\lambda_{c.f} - 0.2\right) + \lambda_{c.f}^2\right] = 5.65$$

Reduction factor for column-like buckling

$$\chi_{c.f} := \frac{1}{\phi_f + \sqrt{\phi_f^2 - \lambda_{c.f}^2}} = 0.1$$

8.4 Interpolation: plate and column-like buckling

Calculations according to 1993-1-5 Section 4.5.4.

Parameter for weighting

$$\xi_f := \min\left(\max\left(0, \frac{\sigma_{cr.p.f}}{\sigma_{cr.c.f}} - 1\right), 1\right) = 1$$

Weighted reduction factor for flange stiffeners

$$\rho_{c.f} := \left(\rho_f - \chi_{c.f}\right) \cdot \xi_f \cdot \left(2 - \xi_f\right) + \chi_{c.f} = 0.46$$

8. Reduction of flange stiffeners

9. Effective cross-section properties

9 EFFECTIVE CROSS SECTION PROPERTIES

9.1 Whole cross-section

Reduction of flanges with regard to shear lag according to Section 3.3 and effective areas according to Section 4.5 in EN1993-1-5

Redution factor top edge $\beta_t = 1$

Redution factor bottom edge $\beta_b = 1$

Excluding parts of the web with regar to local buckling which is considered with reduction of $A_{c.eff.loc}$

Reduction factor stiffeners in compression in web $\rho_{c.w} = 0.87$

Reduction factor stiffeners in compression in flange $\rho_{c.f} = 0.46$

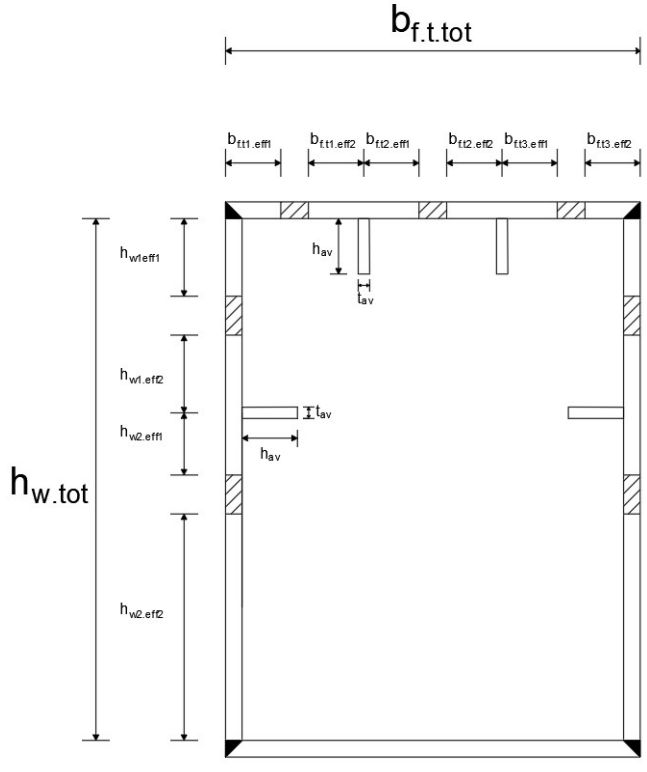

$b_{f.t.1.eff.1} = 0.17\,m$

$b_{f.t.1.eff.2} = 0.17\,m$

$b_{f.t.2.eff.1} = 0.17\,m$

$b_{f.t.2.eff.2} = 0.17\,m$

$b_{f.t.3.eff.1} = 0.17\,m$

$b_{f.t.3.eff.2} = 0.17\,m$

$b_{f.b.eff} = 1.2\,m$

$h_{w1.eff1} = 0.13\,m$

$h_{w1.eff2} = 0.16\,m$

$h_{w2.eff1} = 0.42\,m$

$h_{w2.eff2} = 0.78\,m$

$h_{w.2.t} = 0.78\,m$

Effective area top flange

$$A_{f.t.c.eff} := \rho_{c.f}\cdot\left(b_{f.t.1.eff.2} + b_{f.t.2.eff.1} + b_{f.t.2.eff.2} + b_{f.t.3.eff.1}\right)\cdot t_{f.t} + \left(b_{f.t.1.eff.1} + b_{f.t.3.eff.2}\right)\cdot t_{f.t} \ldots = 6.4\times 10^{3}\cdot mm^{2}$$

Factor

$$\alpha_{0.ult} := \sqrt{\frac{A_{f.t.c.eff}\cdot 0.5}{b_0\cdot t_{f.t}}} = 0.73$$

Factor

$$\kappa_{ult} := \alpha_{0.ult}\cdot\frac{b_0}{L_e} = 0.07$$

Shear lag factor in top

$$\beta_{ult} := \begin{cases} \beta\left(type, \kappa_{ult}\right) & \text{if } b_0 < \frac{L_e}{50} \\ 1 & \text{otherwise} \end{cases} = 1$$

Effective area bottom flange

$$A_{f.b.c.eff} := b_{f.b.eff}\cdot t_{f.t} = 0.012\,m^{2}$$

Factor

$$\alpha_{0.ult.b} := \sqrt{\frac{A_{f.b.c.eff}\cdot 0.5}{b_0\cdot t_{f.t}}} = 1$$

Factor

$$\kappa_{ult.b} := \alpha_{0.ult.b}\cdot\frac{b_0}{L_e} = 0.09$$

Shear lag factor in top

$$\beta_{ult.b} := \begin{cases} \beta\left(type, \kappa_{ult.b}\right) & \text{if } b_0 < \frac{L_e}{50} \wedge sign\left(\sigma_{f.b}\right) = -1 \\ 1 & \text{otherwise} \end{cases} = 1$$

Effective area top flange incl. shear lag

$$A_{f.t.eff} := \beta_{ult}\cdot A_{f.t.c.eff} = 6.405\times 10^{-3}\,m^{2}$$

Effective area bottom flange incl. shear lag

$$A_{f.b.eff} := \beta_{ult.b}\cdot A_{f.b.c.eff} = 0.012\,m^{2}$$

Effective area web

$$A_{w.eff} := \rho_{c.w}\cdot\left(h_{w1.eff2} + h_{w2.eff1}\right)\cdot t_w + \left(h_{w1.eff1} + h_{w2.eff2}\right)\cdot t_w = 1.13\times 10^{4}\cdot mm^{2}$$

Effective area web stiffener

$$A_{av.eff.w} := \rho_{c.w}\cdot\left(h_{av.w}\cdot t_{av.w}\right) = 5.243\times 10^{-4}\,m^{2}$$

Effective area flange stiffener

$$A_{av.eff.f} := \rho_{c.f}\cdot n_{av.f}\cdot\left(h_{av.f}\cdot t_{av.f}\right) = 5.476\times 10^{-4}\,m^{2}$$

Total effective area

$$A_{tot.eff} := A_{f.t.eff} + A_{f.b.eff} + 2A_{w.eff} + 2A_{av.eff.w} + A_{av.eff.f} = 4.26003\times 10^{4}\cdot mm^{2}$$

Effective center of gravity

$$y_{tp.eff} := \frac{\begin{aligned} &-A_{f.t.eff}\cdot\left(\frac{t_{f.t}}{2}\right) + 2A_{av.eff.w}\cdot h_{w.1} + A_{av.eff.f}\cdot\left(\frac{h_{av.f}}{2}\cdot\rho_{c.f}\right) \dots \\ &+ 2h_{w1.eff1}\cdot t_w\cdot\left(\frac{h_{w1.eff1}}{2}\right) + 2h_{w2.eff2}\cdot t_w\cdot\left(h_{w.tot} - \frac{h_{w2.eff2}}{2}\right) \dots \\ &+ 2\rho_{c.w}\cdot\left[\begin{aligned} &h_{w1.eff2}\cdot t_w\cdot\left(h_{w.1} - \frac{h_{w1.eff2}}{2}\right) \dots \\ &+ h_{w2.eff1}\cdot t_w\cdot\left(h_{w.1} + \frac{h_{w2.eff1}}{2}\right) \end{aligned}\right] \dots \\ &+ A_{f.b.eff}\cdot\left(h_{w.tot} + \frac{t_{f.b}}{2}\right) \end{aligned}}{A_{tot.eff}} = 0.841\,\text{m}$$

Moment of inertia for web stiffener

$$I_{av.eff.w} := 2\cdot\rho_{c.w}\left[\frac{h_{av.w}\cdot t_{av.w}^{3}}{12} + h_{av.w}\cdot t_{av.w}\cdot\left[\left(y_{tp.eff} - h_{w.1}\right)^2\right]\right] = 0.00031\,\text{m}^4$$

Moment of inertia for flange stiffener

$$I_{av.eff.f} := \rho_{c.f}\cdot n_{av.f}\cdot\left[\begin{aligned} &\frac{h_{av.f}\cdot t_{av.f}^{3}}{12} \dots \\ &+ h_{av.w}\cdot t_{av.w}\cdot\left[\left(y_{tp.eff} - \frac{h_{av.f}\cdot\rho_{c.f}}{2}\right)^2\right] \end{aligned}\right] = 3.745\cdot10^{-4}\,\text{m}^4$$

Effective moment of inertia flanges

$$I_{f.eff} := \begin{aligned} &\frac{\left(\frac{A_{f.t.eff}}{t_{f.t}}\right)\cdot t_{f.t}^{3}}{12} + A_{f.t.eff}\cdot\left(y_{tp.eff} + \frac{t_{f.t}}{2}\right)^2 \dots \\ &+ \frac{\left(\frac{A_{f.b.eff}}{t_{f.b}}\right)\cdot t_{f.b}^{3}}{12} + A_{f.b.eff}\cdot\left(h_{w.tot} + \frac{t_{f.b}}{2} - y_{tp.eff}\right)^2 \end{aligned} = 9.87653\times10^{-3}\,\text{m}^4$$

Effective moment of inertia web

$$I_{w.eff} := \frac{2t_w \cdot h_{w1.eff1}^{3}}{12} + 2h_{w1.eff1} \cdot t_w \cdot \left(y_{tp.eff} - \frac{h_{w1.eff1}}{2} \right)^2 \ldots = 4.354 \times 10^{-3}\,\mathrm{m}^4$$
$$+ 2\rho_{c.w} \cdot \left[\frac{t_w \cdot h_{w1.eff2}^{3}}{12} + h_{w1.eff2} \cdot t_w \cdot \left[y_{tp.eff} - \left(h_{w.1} - \frac{h_{w1.eff2}}{2} \right) \right]^2 \right] \ldots$$
$$+ 2\rho_{c.w} \cdot \left[\frac{t_w \cdot h_{w2.eff1}^{3}}{12} + h_{w2.eff1} \cdot t_w \cdot \left[y_{tp.eff} - \left(h_{w.1} + \frac{h_{w2.eff1}}{2} \right) \right]^2 \right] \ldots$$
$$+ \frac{2t_w \cdot h_{w2.eff2}^{3}}{12} + 2h_{w2.eff2} \cdot t_w \cdot \left[y_{tp.eff} - \left(h_{w.tot} - \frac{h_{w2.eff2}}{2} \right) \right]^2$$

Effective moment of inertia around stiff axis

$$I_{z.eff} := I_{f.eff} + I_{w.eff} + I_{av.eff.w} + I_{av.eff.f} = 0.01491\,\mathrm{m}^4$$

Effective elastic section modulus

$$W_{el.z.eff} := \min\left(\frac{I_{z.eff}}{y_{tp.eff} + t_{f.t}}, \frac{I_{z.eff}}{h_{w.tot} + t_{f.b} - y_{tp.eff}} \right) = 0.01753 \cdot \mathrm{m}^3$$

9. Effective cross-section properties

10. Capacities

10 CAPACITIES

10.1 Moment and normal force

Elastic moment capacity for gross cross section

$$M_{z.Rd} := \frac{W_{el.z} \cdot f_{yd}}{\gamma_{M0}} = 10.13 \cdot MN \cdot m$$

Elastic moment capacity for effective cross section

$$M_{z.Rd.ef} := \frac{W_{el.z.eff} \cdot f_{yd}}{\gamma_{M0}} = 7.36 \cdot MN \cdot m$$

Normal force capacity

$$N_{Rd} := \frac{A_{tot.eff} \cdot f_{yd}}{\gamma_{M0}} = 17.89 \cdot MN$$

10.2 Shear force

Calculations according to EN1993-1-5 Section 5.2, 5.3, 5.4 and A.3.

Moment of inertia for longitudinal web stiffener

$$I_{st} := I_{st.w} = 6.85 \times 10^{-7}\ m^4$$

Addition to longitudinal stiffeners

$$k_{\tau sl} := \max\left[9 \cdot \left(\frac{h_{w.tot}}{a_w}\right)^2 \cdot \sqrt[4]{\left(\frac{I_{st}}{t_w^3 \cdot h_{w.tot}}\right)^3}, \frac{2.1}{t_w} \cdot \sqrt[3]{\frac{I_{st}}{h_{w.tot}}}\right] = 2.07$$

Slenderness parameter

$$k_\tau := \begin{cases} 5.34 + 4 \cdot \left(\frac{h_{w.tot}}{a_w}\right)^2 + k_{\tau sl} & \text{if } \frac{a_w}{h_{w.tot}} \geq 3 \\ 4.1 + \frac{6.3 + 0.18 \cdot \frac{I_{st}}{t_w^3 \cdot h_{w.tot}}}{\left(\frac{a_w}{h_{w.tot}}\right)^2} + 2.2 \sqrt[3]{\frac{I_{st}}{t_w^3 \cdot h_{w.tot}}} & \text{if } \frac{a_w}{h_{w.tot}} < 3 \end{cases} = 7.83$$

Slenderness

$$\lambda_w := \frac{h_{w.tot}}{37.4 \cdot t_w \cdot \varepsilon_{class} \cdot \sqrt{k_\tau}} = 2.39$$

Reduction factor for shear is calculated according to EN1993-1-5 Section 5.2, 5.3 and 5.4.

Material parameter

$\eta := 1.2$

Stiff or not

Stiff := "NO"

Shear buckling resistance factor

$$\chi_w := \begin{cases} \eta & \text{if } \lambda_w < \frac{0.83}{\eta} \\ \frac{0.83}{\lambda_w} & \text{if } \frac{0.83}{\eta} \le \lambda_w < 1.08 \\ \text{if}\left(\text{Stiff} = \text{"YES"}, \frac{1.37}{0.7 + \lambda_w}, \frac{0.83}{\lambda_w}\right) & \text{if } \lambda_w \ge 1.08 \end{cases} = 0.35$$

Shear capacity

$$V_{b.Rd} = V_{bw.Rd} + V_{bf.Rd} \le \frac{\eta \cdot h_{w.tot} \cdot t_w \cdot f_{yd}}{\sqrt{3} \cdot \gamma_{M1}}$$

Design shear resistance web

$$V_{bw.Rd} := \frac{\chi_w \cdot h_{w.tot} \cdot t_w \cdot f_{yd}}{\sqrt{3} \cdot \gamma_{M1}} = 1009 \cdot \text{kN}$$

Included width of flange adjacent to the web

$$b_f := \min\left(b_{f.b}, 2 \cdot 15 \cdot \varepsilon_{class} \cdot t_{f.b}\right) = 0.22 \text{ m}$$

Distance between plastic points

$$c := a_w \cdot \left(0.25 + \frac{1.6 \cdot b_f \cdot t_{f.b}^2 \cdot f_{yd}}{t_w \cdot h_{w.tot}^2 \cdot f_{yd}}\right) = 0.76 \text{ m}$$

Characteristic moment in flanges

$$M_{f.k} := f_{yk}\left[A_{f.t.eff} \cdot \left(\left|-y_{tp.eff} - t_{f.t}\right|\right) + A_{f.b.eff} \cdot \left(\left|h_{w.tot} + \frac{t_{f.b}}{2} - y_{tp.eff}\right|\right)\right] = 5.64 \times 10^3 \cdot \text{kNm}$$

Design moment in flanges

$$M_{f.Rd} := \frac{M_{f.k}}{\gamma_{M0}} \cdot \left[1 - \frac{N_{Ed}}{\left(\frac{A_{f.t.eff} + A_{f.b.eff}}{\gamma_{M0}}\right) \cdot f_{yd}}\right] = 5.6365 \cdot \text{MN} \cdot \text{m}$$

The shear capacity from the flanges are assumed to not have an impact since they are generally really small

Design shear resistance

$$V_{b.Rd} := \begin{cases} 2V_{bw.Rd} & \text{if } 2V_{bw.Rd} \le 2\frac{\eta \cdot h_{w.tot} \cdot t_w \cdot f_{yd}}{\sqrt{3} \cdot \gamma_{M1}} \\ 2\frac{\eta \cdot h_{w.tot} \cdot t_w \cdot f_{yd}}{\sqrt{3} \cdot \gamma_{M1}} & \text{otherwise} \end{cases} = 2.0171 \times 10^3 \cdot \text{kN}$$

Control according to EN1993-1-5 Section 5.1 (2)

$$\text{Controll}_{VbRd} := \begin{cases} \text{"Shear buckling can occur"} & \text{if } \frac{h_{w.tot}}{t_w} > \frac{31}{\eta} \cdot \varepsilon_{class} \cdot \sqrt{k_\tau} \\ \text{"Shear buckling can't occur"} & \text{otherwise} \end{cases}$$

$\text{Controll}_{VbRd} = \text{"Shear buckling can occur"}$

10. Capacities

11. Verification

11 VERIFICATION

11.1 Whole cross-section

Calculations according to EN1993-1-5 Section 4.6, 5.5 and 7.1

Eccentricity due to normal force in CSC4

$e_N := y_{tp} - y_{tp.eff} = -118.54 \cdot mm$

$e_N \cdot N_{Ed} = 0 \cdot kN \cdot m$

Utilisation of uniaxial bending

$$\eta_1 := \frac{N_{Ed}}{\frac{A_{tot.eff} \cdot f_{yd}}{\gamma_{M0}}} + \frac{\left(M_{z.Ed} + e_N \cdot N_{Ed}\right)}{\left(\frac{f_{yd} \cdot W_{el.z.eff}}{\gamma_{M0}}\right)} = 79.98 \cdot \%$$

Control according to EN1993-1-5 Section 4.6:

$\eta_{1.check} := \text{if}\left(\eta_1 \le 1, \text{"OK"}, \text{"NOT OK"}\right) = \text{"OK"}$

Utilisation of moment

$$\eta_{1.bar} := \frac{M_{z.Ed}}{M_{pl.Rd}} = 70.55 \cdot \%$$

Moment capacity according to EN1993-1-5 Section 7.1:

$\eta_{1.bar.check} := \text{if}\left(\eta_{1.bar} \le 1, \text{"OK"}, \text{"NOT OK"}\right) = \text{"OK"}$

Utilisation of shear force

$$\eta_{3.bar} := \frac{V_{Ed}}{V_{b.Rd}} = 80.02 \cdot \%$$

Tvärkraftskapacitet enligt EN1993-1-5 avsnitt 5.5:

$\eta_3 := \text{if}\left(\eta_{3.bar} \le 1, \text{"OK"}, \text{"NOT OK"}\right) = \text{"OK"}$

Interaction control

$$\text{interaction} := \begin{cases} \eta_{1.bar} + \left(1 - \frac{M_{f.Rd}}{M_{pl.Rd}}\right) \cdot \left(2 \cdot \eta_{3.bar} - 1\right)^2 & \text{if } \eta_{3.bar} > 0.5 \wedge \eta_{1.bar} \ge \frac{M_{f.Rd}}{M_{pl.Rd}} \\ 0 & \text{otherwise} \end{cases} = 0.82$$

$\text{check}_{interaction} := \text{if}\left(\text{interaction} \le 1, \text{"OK"}, \text{"Redo design"}\right) = \text{"OK"}$

11. Verification

D

Mathcad sheet for reduced stress method

This Appendix contains the Mathcad calculations for the reduced stress method for one example of the beam with the cross-section dimension $t_f = 14mm$, $t_w = 8mm$ and $a = 1.5m$. In the loading situation of 80% moment capacity and 80% shear capacity. The input and cross-section sections are not visible, since they are calculated in Appendix B. To perform calculations for an unstiffened beam this sheet could be used by excluding Sections 3 and 6 in this appendix. It does require some small additional changes, but the overall procedure is the same.

Johan Ahlstrand
Ellen Johansson

REDUCED STRESS METHOD: STIFFENERS

1. Input

2. Gross cross-section properties

3. Cross-section properties web stiffener

3 CROSS SECTION PROPERTIES WEB STIFFENER

3.1 Normal buckling

Contributing width according to EN 1993-1-5 Section A.2.

Stress ratio field 1

$$\psi_{w.1} := \frac{\sigma_{w.av}}{\sigma_{w.T}} = 0.59$$

Stress ratio field 2

$$\psi_{w.2} := \frac{\sigma_{w.B}}{\sigma_{w.av}} = -1.81$$

Compression zone

$$b_c := \begin{cases} -\frac{h_w - 0}{\left(\sigma_{w.B} - \sigma_{w.T}\right)} \cdot \sigma_{w.B} + h_w & \text{if } \operatorname{sign}\left(\sigma_{w.T}\right) \neq \operatorname{sign}\left(\sigma_{w.B}\right) \\ h_w & \text{otherwise} \end{cases} = 0.7266 \cdot m$$

Contributing width of web above stiffener

$$b_{1.inf} := \frac{3 - \psi_{w.1}}{5 - \psi_{w.1}} \cdot \left(h_{w.1} - \frac{t_{sl.w}}{2} \right) = 0.161\,m$$

Contributing width of web below stiffener

$$b_{2.sup} := 0.4 \cdot \left(b_c - h_{w.1} - \frac{t_{sl.w}}{2} \right) = 0.1686\,m$$

Total contributing part of the web to the stiffener

$$b_{tot.sl.1} := t_{sl.w} + b_{1.inf} + b_{2.sup} = 0.34\,m$$

Area of contr. web and stiffener

$$A_{sl.1.w} := b_{tot.sl.1} \cdot t_w + t_{sl.w} \cdot h_{sl.w} = 3.32 \times 10^3 \cdot mm^2$$

Area of stiffener

$$A_{sl.2.w} := t_{sl.w} \cdot h_{sl.w} = 600 \cdot mm^2$$

Combined center of gravity

$$x_{tp.sl.1} := \frac{t_{sl.w} \cdot h_{sl.w} \cdot \left(\frac{h_{sl.w}}{2} + t_w \right) + b_{tot.sl.1} \cdot \frac{t_w^2}{2}}{A_{sl.1.w}} = 10.15 \cdot mm$$

Center of gravity of stiffener

$$x_{tp.sl.2} := \frac{t_{sl.w} \cdot h_{sl.w} \cdot \left(\frac{h_{sl.w}}{2} + t_w \right)}{A_{sl.2.w}} = 38 \cdot mm$$

Eccentricity

$$e_{x.w} := \max\left(\left|x_{tp.sl.2} - x_{tp.sl.1}\right|, \left|x_{tp.sl.1} - \frac{t_w}{2}\right|\right) = 27.855\cdot mm$$

Moment of interia of contributing parts

$$I_{sl.1.w} := \frac{b_{tot.sl.1}\cdot t_w^{3}}{12} + b_{tot.sl.1}\cdot t_w\cdot\left(\frac{t_w}{2} - x_{tp.sl.1}\right)^2 + \frac{t_{sl.w}\cdot h_{sl.w}^{3}}{12} + t_{sl.w}\cdot h_{sl.w}\cdot\left(\frac{h_{sl.w}}{2} + t_w - x_{tp.sl.1}\right)^2 = 7.627\times 10^{-7}\,m^4$$

3.2 Shear buckling

Calculations for critical shear stress with the use of contributing width according to Figure 5.3 in EN1993-1-5

Contributing part above stiffener

$$b_{a.1} := \min\left(15\cdot\varepsilon\cdot t_w, h_{w.1}\right) = 89.76\cdot mm$$

Contributing part below stiffener

$$b_{a.2} := \min\left(15\cdot\varepsilon\cdot t_w, h_{w.2}\right) = 89.76\cdot mm$$

Total contributing part

$$b_{tot.sl.w} := t_{sl.w} + b_{a.1} + b_{a.2} = 189.52\cdot mm$$

Area of the contributing part

$$A_{sl.w.s} := b_{tot.sl.w}\cdot t_w + t_{sl.w}\cdot h_{sl.w} = 2.116\times 10^{3}\cdot mm^2$$

Center of gravity of the contributing part

$$x_{tp.sl.w} := \frac{t_{sl.w}\cdot h_{sl.w}\cdot\left(\frac{h_{sl.w}}{2} + t_w\right) + b_{tot.sl.w}\cdot\frac{t_w^{2}}{2}}{A_{sl.w.s}} = 13.64\cdot mm$$

Moment of intertia of the contributing part

$$I_{sl.w.s} := \frac{b_{tot.sl.w}\cdot t_w^{3}}{12} + b_{tot.sl.w}\cdot t_w\cdot\left(x_{tp.sl.w} - \frac{t_w}{2}\right)^2 + \frac{t_{sl.w}\cdot h_{sl.w}^{3}}{12} + t_{sl.w}\cdot h_{sl.w}\cdot\left(\frac{h_{sl.w}}{2} + t_w - x_{tp.sl.w}\right)^2 = 6.8503\times 10^{-7}\,m^4$$

3. Cross-section properties web stiffener

4. Slenderness for total stress field

4 SLENDERNESS FOR TOTAL STRESS FIELD: WEB

4.1 Critical normal stress

Calculations according to EN1993-1-5 Section A.2.

Limit for panel width

$$a_c := 4.33\cdot\sqrt[4]{\frac{I_{sl.1.w}\cdot h_{w.1}^{\,2}\cdot\left(h_w - h_{w.1}\right)^2}{t_w^{\,3}\cdot h_w}} = 2.59\,\text{m}$$

Critical stress in stiffener

$$\sigma_{cr.x.w} := \begin{cases} \dfrac{1.05\cdot E_s}{A_{sl.1.w}}\cdot\dfrac{\sqrt{I_{sl.1.w}\cdot t_w^{\,3}\cdot h_w}}{h_{w.1}\cdot\left(h_w - h_{w.1}\right)} & \text{if } a \geq a_c \\ \dfrac{\pi^2\cdot E_s\cdot I_{sl.1.w}}{A_{sl.1.w}\cdot a^2} + \dfrac{E_s\cdot t_w^{\,3}\cdot h_w\cdot a^2}{4\cdot\pi^2\cdot\left(1-\nu^2\right)\cdot A_{sl.1.w}\cdot h_{w.1}^{\,2}\cdot\left(h_w - h_{w.1}\right)^2} & \text{otherwise} \end{cases} = 235.14\cdot\text{MPa}$$

4.2 Critical shear stress

Calculations according to EN 1993-1-5 Section A.1 and A.3.

Critical stress for unstiffened plate

$$\sigma_{E.w} := \frac{\pi^2\cdot E_s\cdot t_w^{\,2}}{12\cdot\left(1-\nu^2\right)\cdot h_w^{\,2}} = 5.4\cdot\text{MPa}$$

Shear buckle coefficient

$$k_{\tau sl} := \max\left[9\cdot\left(\frac{h_w}{a}\right)^2\cdot\sqrt[4]{\left(\frac{I_{sl.w.s}}{t_w^{\,3}\cdot h_w}\right)^3}, \frac{2.1}{t_w}\cdot\sqrt[3]{\frac{I_{sl.w.s}}{h_w}}\right] = 8.26$$

$$k_{\tau.w} := \begin{cases} 5.34 + 4\cdot\left(\dfrac{h_w}{a}\right)^2 + k_{\tau sl} & \text{if } \dfrac{a}{h_w} \geq 3 \\ 4.1 + \dfrac{6.3 + 0.18\cdot\dfrac{I_{sl.w.s}}{t_w^{\,3}\cdot h_w}}{\left(\dfrac{a}{h_w}\right)^2} + 2.2\sqrt[3]{\dfrac{I_{sl.w.s}}{t_w^{\,3}\cdot h_w}} & \text{if } \dfrac{a}{h_w} < 3 \end{cases} = 12.68$$

Critical shear stress

$$\tau_{cr.w} := k_{\tau.w}\cdot\sigma_{E.w} = 68.45\cdot\text{MPa}$$

4.3 Slenderness

Normal stresses in z is not regarded, therefor the constant are set to the following

$$\sigma_{z.Ed.w} := 0MPa$$

$$\psi_{z.w} := 0$$

$$\rho_{z.w} := 1$$

$$\alpha_{cr.z.w} := 10^{10}$$

Calculations according to EN 1993-1-5 Chapter 10.

Design normal stress (x-dir.)

$$\sigma_{x.Ed.w} := \left|\min\left(\sigma_{w.T}, \sigma_{w.B}\right)\right| = 203.44 \cdot MPa$$

Design shear stress

$$\tau_{Ed} := \left|\max\left(\tau_t, \tau_b\right)\right| = 85.54 \cdot MPa$$

Stress ratio

$$\psi_{x.w} := \frac{\sigma_{w.B}}{\sigma_{w.T}} = -1.06$$

Minimum load amplifier (char. load)

$$\alpha_{ult.k.w} := \sqrt{\frac{1}{\left(\frac{\sigma_{x.Ed.w}}{f_y}\right)^2 + \left(\frac{\sigma_{z.Ed.w}}{f_y}\right)^2 - \left(\frac{\sigma_{x.Ed.w}}{f_y}\right)\cdot\left(\frac{\sigma_{z.Ed.w}}{f_y}\right) + 3\cdot\left(\frac{\tau_{Ed}}{f_y}\right)^2}} = 1.669$$

Minimum load amplifier (crit. load, x-dir)

$$\alpha_{cr.x.w} := \frac{\sigma_{cr.x.w}}{\max\left(\sigma_{x.Ed.w}, 0.001MPa\right)} = 1.156$$

Minimum load amplifier (crit. shear load)

$$\alpha_{cr.\tau.w} := \frac{\tau_{cr.w}}{\max\left(\tau_{Ed}, 0.001MPa\right)} = 0.8$$

Minimum load amplifier (crit. load, total stress field)

$$\alpha_{cr.h.w} := \frac{1}{\frac{1+\psi_{x.w}}{4\cdot\alpha_{cr.x.w}} + \frac{1+\psi_{z.w}}{4\cdot\alpha_{cr.z.w}} + \left[\left(\frac{1+\psi_{x.w}}{4\cdot\alpha_{cr.x.w}} + \frac{1+\psi_{z.w}}{4\cdot\alpha_{cr.z.w}}\right)^2 ... + \frac{1-\psi_{x.w}}{2\cdot\alpha_{cr.x.w}^2} + \frac{1-\psi_{z.w}}{2\cdot\alpha_{cr.z.w}^2} + \frac{1}{\alpha_{cr.\tau.w}^2}\right]^{\frac{1}{2}}} = 0.66$$

If a careful FE analysis is made the load amplifyer should overwrite the current calculated value.

Minimum load amplifier (crit. load, FE-analysis)

$$\alpha_{cr.FE.w} := 0.98$$

Minimum load amplifier (crit. load)

$$\alpha_{cr.w} := \text{if}\left(\alpha_{cr.FE.w} > 0, \alpha_{cr.FE.w}, \alpha_{cr.h.w}\right) = 0.98$$

Plate slenderness

$$\lambda_{p.w} := \sqrt{\frac{\alpha_{ult.k.w}}{\alpha_{cr.w}}} = 1.3$$

4. Slenderness for total stress field

5. Verification of panel

5 Verification of panel

All reductionsfacor are calculatied with respect to slenderness for the total stress field according to EN1993-1-5 Chapter 10. This slenderness is replacing the individual calculations of slenderness for respective stress component.

5.1 Reduction for normal stresses

Calculations according to 1993-1-5 Section 4.4.

Reduction factor plate buckling

$$\rho_w := \begin{cases} 1 & \text{if } \lambda_{p.w} \le 0.5 + \sqrt{0.085 - 0.055\psi_{x.w}} \\ \min\left(\frac{\lambda_{p.w} - 0.055\cdot\max\left(3 + \psi_{x.w}, 0\right)}{\lambda_{p.w}^{2}}, 1\right) & \text{otherwise} \end{cases} = 0.704$$

Control according to Section 10 (2) in EN1993-1-5

$$\text{if}\left(\rho_w\cdot\frac{\alpha_{ult.k.w}}{\gamma_{M1}} \ge 1, \text{"CSC3 characteristics assumed"}, \text{"Not ok"}\right) = \text{"CSC3 characteristics assumed"}$$

Calculations accroding to 1993-1-5 Section 4.5.3 and EN1993-1-1 section 6.3.1.2.

Parameter for open cross section (stiffener)

$$\alpha_w := 0.49$$

Radius of gyration for stiffener

$$i_w := \sqrt{\frac{I_{sl.1.w}}{A_{sl.1.w}}} = 0.015\,\text{m}$$

Parameter

$$\alpha_{e.w} := \alpha_w + \frac{0.09}{\frac{i_w}{e_{x.w}}} = 0.66$$

Parameter

$$\phi_w := 0.5\cdot\left[1 + \alpha_{e.w}\cdot\left(\lambda_{p.w} - 0.2\right) + \lambda_{p.w}^{2}\right] = 1.7$$

Reduction factor for column-like buckling

$$\chi_{c.w} := \frac{1}{\phi_w + \sqrt{\phi_w^{2} - \lambda_{p.w}^{2}}} = 0.35$$

Critical stress

$$\sigma_{cr.c.w} := \frac{\pi^{2}\cdot E_s\cdot I_{sl.1.w}}{A_{sl.1.w}\cdot a^{2}} = 211.66\cdot\text{MPa}$$

Parameter for weighting

$$\xi_w := \min\left(\max\left(0, \frac{\sigma_{cr.x.w}}{\sigma_{cr.c.w}} - 1\right), 1\right) = 0.11$$

Reduction factor interaction buckling

$$\rho_{x.w} := \left(\rho_w - \chi_{c.w}\right)\cdot\xi_w\cdot\left(2 - \xi_w\right) + \chi_{c.w} = 0.43$$

5.2 Reduction factor shear stress

Calculations according to 1993-1-5 avsnitt 4.4.

Stiff or not

$$\text{Stiff} := \text{"NO"}$$

Reduction factor shear buckling

$$\chi_{w.w} := \begin{cases} \eta & \text{if } \lambda_{p.w} < \frac{0.83}{\eta} \\ \frac{0.83}{\lambda_{p.w}} & \text{if } \frac{0.83}{\eta} \le \lambda_{p.w} < 1.08 \\ \text{if}\left(\text{Stiff} = \text{"YES"}, \frac{1.37}{0.7 + \lambda_{p.w}}, \frac{0.83}{\lambda_{p.w}}\right) & \text{if } \lambda_{p.w} \ge 1.08 \end{cases} = 0.64$$

5.3 Results

Calculations according to 1993-1-5 Chapter 10.

Utilisation factor, stresses in x-dir.

$$U_x := \frac{\sigma_{x.Ed.w}}{\frac{\rho_{x.w} \cdot f_y}{\gamma_{M1}}} = 113.34 \cdot \%$$

Utilisation factor, shear stresses

$$U_\tau := \frac{\tau_{Ed}}{\frac{\chi_{w.w} \cdot f_y}{\sqrt{3} \cdot \gamma_{M1}}} = 55.46 \cdot \%$$

Utilisation factor, method 1

$$U_{1.w} := \frac{\left[\left(\frac{\sigma_{x.Ed.w}}{\frac{f_y}{\gamma_{M1}}}\right)^2 + \left(\frac{\sigma_{z.Ed.w}}{\frac{f_y}{\gamma_{M1}}}\right)^2 - \left(\frac{\sigma_{x.Ed.w}}{\frac{f_y}{\gamma_{M1}}}\right) \cdot \left(\frac{\sigma_{z.Ed.w}}{\frac{f_y}{\gamma_{M1}}}\right) + 3 \cdot \left(\frac{\tau_{Ed}}{\frac{f_y}{\gamma_{M1}}}\right)^2\right]^{0.5}}{\min\left(\chi_{w.w}, \rho_{x.w}, \rho_{z.w}\right)} = 1.4$$

Utilisation factor, method 2

$$U_{2.w} := \left(\frac{\sigma_{x.Ed.w}}{\frac{\rho_{x.w} \cdot f_y}{\gamma_{M1}}}\right)^2 + \left(\frac{\sigma_{z.Ed.w}}{\frac{\rho_{z.w} \cdot f_y}{\gamma_{M1}}}\right)^2 - \left(\frac{\sigma_{x.Ed.w}}{\frac{\rho_{x.w} \cdot f_y}{\gamma_{M1}}}\right) \cdot \left(\frac{\sigma_{z.Ed.w}}{\frac{\rho_{z.w} \cdot f_y}{\gamma_{M1}}}\right) + 3 \cdot \left(\frac{\tau_{Ed}}{\frac{\chi_{w.w} \cdot f_y}{\gamma_{M1}}}\right)^2 = 1.59$$

Final utilisation

$$U_{max} := \max\left(U_x, U_\tau, \min\left(U_{1.w}, U_{2.w}\right)\right) = 1.4$$

5. Verification of panel

6. Cross-section properties of flange stiffeners

6 CROSS SECTION PROPERTIES FLANGE STIFFENER

6.1 Normal buckling

Contributing width according to EN 1993-1-5 Section 4.5.

Stress ratio $\psi_{f.1} := 1$

Stress ratio $\psi_{f.2} := 1$

Stress ratio $\psi_{f.3} := 1$

Normal stress buckling coefficient $k_\sigma := 4$

Width of plate contributing to stiffeners total gross cros.section according to EN1993-1-5 Section 4.5.

$b_{1.inf.f} := 0.5 b_{f.1} = 0.2\,m$

$b_{2.sup.f} := 0.5 \cdot b_{f.2} = 0.2\,m$

$b_{2.inf.f} := 0.5 \cdot b_{f.2} = 0.2\,m$

$b_{3.sup.f} := 0.5 \cdot b_{f.3} = 0.2\,m$

$b_{tot.sl.1.f} := b_{1.inf.f} + b_{2.sup.f} = 0.4\,m$

Gross area of stiffener including adjacent parts of plate

$$A_{sl.1.f} := b_{tot.sl.1.f} \cdot t_{f.t} + t_{sl.f} \cdot h_{sl.f} = 6.2 \times 10^3 \cdot mm^2$$

Area of stiffener

$$A_{sl.2.f} := t_{sl.f} \cdot h_{sl.f} = 600 \cdot mm^2$$

Combined center of gravity

$$y_{tp.sl.1.f} := \frac{h_{sl.f} \cdot t_{sl.f} \cdot \left(\frac{h_{sl.f}}{2}\right) + t_{f.t} \cdot b_{tot.sl.1.f} \frac{-t_{f.t}}{2}}{A_{sl.1.f}} = -3.42 \cdot mm$$

Center of gravity of the stiffener

$$y_{tp.sl.2.f} := \frac{h_{sl.f} \cdot t_{sl.f} \cdot \left(\frac{h_{sl.f}}{2}\right)}{A_{sl.2.f}} = 30 \cdot mm$$

Distance to combined center of gravity from flange's or stiffener's ytp

$$e_{x.f} := \max\left(\left|y_{tp.sl.2.f} - y_{tp.sl.1.f}\right|, \left|\frac{-t_{f.t}}{2} - y_{tp.sl.1.f}\right|\right) = 33.4 \cdot mm$$

Moment of inertia of contributing parts

$$I_{sl.1.f} := \frac{t_{f.t}^{3} \cdot b_{tot.sl.1.f}}{12} + b_{tot.sl.1.f} \cdot t_{f.t} \cdot \left(\frac{-t_{f.t}}{2} - y_{tp.sl.1.f} \right)^2 \dots = 1.013 \times 10^{-6}\ m^4$$
$$+ \frac{h_{sl.f}^{3} \cdot t_{sl.f}}{12} + t_{sl.f} \cdot h_{sl.f} \cdot \left(\frac{h_{sl.f}}{2} - y_{tp.sl.1.f} \right)^2$$

6. Cross-section properties of flange stiffeners

7. Slenderness of total stress field: Flange

7 SLENDERNESS FOR TOTAL STRESS FIELD: FLANGE

7.1 Normal buckling

Calculated according to EN1993-1-5 Section A.2.

Width from left edge of flange to critical buckling point according to Figure A.3

$$b_{1.f} := \begin{pmatrix} b_{f.1} \\ b_{f.2} \\ \frac{b_f}{2} \end{pmatrix} = \begin{pmatrix} 0.4 \\ 0.4 \\ 0.6 \end{pmatrix} \cdot m$$

Width from right edge of flange to critical buckling point according to Figure A.3

$$b_{2.f} := \begin{pmatrix} b_{f.2} \\ b_{f.3} \\ \frac{b_f}{2} \end{pmatrix} = \begin{pmatrix} 0.4 \\ 0.4 \\ 0.6 \end{pmatrix} \cdot m$$

Total buckling length according to Figure A.3

$$b_{flange} := b_{1.f} + b_{2.f} = \begin{pmatrix} 0.8 \\ 0.8 \\ 1.2 \end{pmatrix} m$$

Moment of inertia

$$I_{sl.1.f.p} := \begin{pmatrix} I_{sl.1.f} \\ I_{sl.1.f} \\ 2 \cdot I_{sl.1.f} \end{pmatrix} = \begin{pmatrix} 1.01 \times 10^{-6} \\ 1.01 \times 10^{-6} \\ 2.03 \times 10^{-6} \end{pmatrix} m^4$$

Area of stiffeners

$$A_{sl.1.f.p} := \begin{pmatrix} A_{sl.1.f} \\ A_{sl.1.f} \\ 2 \cdot A_{sl.1.f} \end{pmatrix} = \begin{pmatrix} 6.2 \times 10^{-3} \\ 6.2 \times 10^{-3} \\ 0.01 \end{pmatrix} m^2$$

Limit for panel width

$$a_{c.f} := \left| \begin{array}{l} \text{for } i \in 0..2 \\ \quad t_i \leftarrow 4.33 \cdot \sqrt[4]{\dfrac{I_{sl.1.f.p_i} \cdot \left(b_{1.f_i}\right)^2 \left(b_{2.f_i}\right)^2}{t_{f.t}^{\,3} \cdot b_{flange_i}}} \\ t \end{array} \right. = \begin{pmatrix} 1.43 \\ 1.43 \\ 2.3 \end{pmatrix} m$$

Critical stress in stiffener

$$\sigma_{cr.sl.x.f} := \left| \begin{array}{l} \text{for } i \in 0..2 \\ t_i \leftarrow \left| \begin{array}{ll} \dfrac{1.05 \cdot E_s}{A_{sl.1.f.p_i}} \cdot \dfrac{\sqrt{I_{sl.1.f.p_i} \cdot t_{f.t}^{\,3} \cdot b_{flange_i}}}{b_{1.f_i} \cdot b_{2.f_i}} & \text{if } a \geq a_{c.f_i} \\ \dfrac{\pi^2 \cdot E_s \cdot I_{sl.1.f.p_i}}{A_{sl.1.f.p_i} \cdot a^2} + \dfrac{E_s \cdot t_{f.t}^{\,3} \cdot b_{flange_i} \cdot a^2}{4 \cdot \pi^2 \cdot \left(1 - v^2\right) \cdot A_{sl.1.f.p_i} \cdot \left(b_{1.f_i}\right)^2 \cdot \left(b_{2.f_i}\right)^2} & \text{if } a < a_{c.f_i} \end{array} \right. \\ t \end{array} \right.$$

$$\sigma_{cr.sl.x.f} = \begin{pmatrix} 3.32 \times 10^8 \\ 3.32 \times 10^8 \\ 1.78 \times 10^8 \end{pmatrix} \text{Pa}$$

$$\sigma_{cr.x.f} := \min\left(\sigma_{cr.sl.x.f}\right) = 177.51 \cdot \text{MPa}$$

Critical stress in stiffener

7.2 Slenderness

Normal stresses in z is not regarded, therefor the constant are set to the following

$\sigma_{z.Ed.f} := 0\text{MPa}$

$\tau_{Ed} := 0\text{MPa}$

$\psi_{z.f} := 0$

$\rho_{z.f} := 1$

$\alpha_{cr.z.f} := 10^{10}$

Calculations according to EN 1993-1-5 Chapter 10.

Design normal stress (x-dir.)

$$\sigma_{x.Ed.f} := \left|\min\left(\sigma_{f.t}, \sigma_{f.b}\right)\right| = 205.4 \cdot \text{MPa}$$

Stress ratio

$$\psi_{x.f} := \frac{\sigma_{f.b}}{\sigma_{f.t}} = -1.06$$

Minimum load amplifier (char. load)

$$\alpha_{ult.k.f} := \sqrt{\frac{1}{\left(\frac{\sigma_{x.Ed.f}}{f_y}\right)^2 + \left(\frac{\sigma_{z.Ed.f}}{f_y}\right)^2 - \left(\frac{\sigma_{x.Ed.f}}{f_y}\right) \cdot \left(\frac{\sigma_{z.Ed.f}}{f_y}\right) + 3 \cdot \left(\frac{\tau_{Ed}}{f_y}\right)^2}} = 2.04$$

Minimum load amplifier (crit. load, x-dir)

$$\alpha_{cr.x.f} := \frac{\sigma_{cr.x.f}}{\max\left(\sigma_{x.Ed.f}, 0.001\text{MPa}\right)} = 0.86$$

Minimum load amplifier (crit. shear load)

$\alpha_{cr.\tau.f} := 10^{10}$

Minimum load amplifier (crit. load, total stress field)

$$\alpha_{cr.h.f} := \frac{1}{\frac{1+\psi_{x.f}}{4\cdot\alpha_{cr.x.f}} + \frac{1+\psi_{z.f}}{4\cdot\alpha_{cr.z.f}} + \left[\left(\frac{1+\psi_{x.f}}{4\cdot\alpha_{cr.x.f}} + \frac{1+\psi_{z.f}}{4\cdot\alpha_{cr.z.f}}\right)^2 + \frac{1-\psi_{x.f}}{2\cdot\alpha_{cr.x.f}^2} + \frac{1-\psi_{z.f}}{2\cdot\alpha_{cr.z.f}^2} + \frac{1}{\alpha_{cr.\tau.f}^2}\right]^{\frac{1}{2}}} = 0.8$$

If a careful FE analysis is made the load amplifyer should overwrite the current calculated value.

Minimum load amplifier (crit. load, FE-analysis) $\alpha_{cr.FE.f} := 1.22$

Minimum load amplifier (crit. load) $\alpha_{cr.f} := \text{if}\left(\alpha_{cr.FE.f} > 0, \alpha_{cr.FE.f}, \alpha_{cr.h.f}\right) = 1.22$

Plate slenderness $\lambda_{p.f} := \sqrt{\frac{\alpha_{ult.k.f}}{\alpha_{cr.f}}} = 1.29$

7. Slenderness of total stress field: Flange

8. Verification of panel

8 VERIFICATION OF PANEL

All reductionsfacor are calculatied with respect to slenderness for the total stress field according to EN1993-1-5 Chapter 10. This slenderness is replacing the individual calculations of slenderness for respective stress component.

8.1 Reduction for normal stresses

Calculations according to 1993-1-5 Section 4.4.

Reduction factor plate buckling

$$\rho_f := \begin{cases} 1 & \text{if } \lambda_{p.f} \le 0.5 + \sqrt{0.085 - 0.055\psi_{x.f}} \\ \min\left(\frac{\lambda_{p.f} - 0.055\cdot\max\left(3 + \psi_{x.f}, 0\right)}{\lambda_{p.f}^{\,2}}, 1\right) & \text{otherwise} \end{cases} = 0.71$$

Control according to Section 10 (2) in EN1993-1-5

$$\text{if}\left(\rho_{x.w}\cdot\frac{\alpha_{ult.k.w}}{\gamma_{M1}} \ge 1, \text{"CSC3 characteristics assumed"}, \text{"Not ok"}\right) = \text{"Not ok"}$$

Calculations according to 1993-1-5 avsnitt 4.5.3 samt EN1993-1-1 avsnitt 6.3.1.2.

Parameter for stiffeners with open cross-section

$$\alpha_f := 0.49$$

Radius of gyration for stiffener

$$i_f := \sqrt{\frac{I_{sl.1.f}}{A_{sl.1.f}}} = 0.01\,\text{m}$$

Parameter

$$\alpha_{e.f} := \alpha_f + \frac{0.09}{\frac{i_f}{e_{x.f}}} = 0.73$$

Parameter

$$\phi_f := 0.5\cdot\left[1 + \alpha_{e.f}\cdot\left(\lambda_{p.f} - 0.2\right) + \lambda_{p.f}^{\,2}\right] = 1.73$$

Reduction factor for column-like buckling

$$\chi_{c.f} := \frac{1}{\phi_f + \sqrt{\phi_f^{\,2} - \lambda_{p.f}^{\,2}}} = 0.35$$

Critical stress

$$\sigma_{cr.c.f} := \frac{\pi^2\cdot E_s\cdot I_{sl.1.f}}{A_{sl.1.f}\cdot a^2} = 150.56\cdot\text{MPa}$$

Parameter for weighting

$$\xi_f := \min\left(\max\left(0, \frac{\sigma_{cr.x.f}}{\sigma_{cr.c.f}} - 1\right), 1\right) = 0.18$$

Reduction factor plate buckling

$$\rho_{x.f} := \left(\rho_f - \chi_{c.f}\right)\cdot\xi_f\cdot\left(2 - \xi_f\right) + \chi_{c.f} = 0.46$$

8.2 Reduction factor for shear stress

Calculations according to 1993-1-5 Section 4.4.

Stiff or not

$\text{Stiff} := \text{"NO"}$

Reduction factor for shear buckling

$\chi_{f.s} := 1$

$a_{f.s} := 10^{10}$

8.3 Results

Calculations according to 1993-1-5 Chapter 10.

Utilisation factor, stresses in x-dir.

$$U_{x.f} := \frac{\sigma_{x.Ed.f}}{\frac{\rho_{x.f} \cdot f_y}{\gamma_{M1}}} = 1.05$$

Utilisation factor, shear stresses

$$U_{\tau.f} := \frac{\tau_{Ed}}{\frac{\chi_{f.s} \cdot f_y}{\sqrt{3} \cdot \gamma_{M1}}} = 0$$

Utilisation factor, method 1

$$U_{1.f} := \frac{\left[\left(\frac{\sigma_{x.Ed.f}}{\frac{f_y}{\gamma_{M1}}}\right)^2 + \left(\frac{\sigma_{z.Ed.f}}{\frac{f_y}{\gamma_{M1}}}\right)^2 - \left(\frac{\sigma_{x.Ed.f}}{\frac{f_y}{\gamma_{M1}}}\right) \cdot \left(\frac{\sigma_{z.Ed.f}}{\frac{f_y}{\gamma_{M1}}}\right) + 3 \cdot \left(\frac{\tau_{Ed}}{\frac{f_y}{\gamma_{M1}}}\right)^2\right]^{0.5}}{\min\left(\chi_{f.s}, \rho_{x.f}, \rho_{z.f}\right)} = 1.05$$

Utilisation factor, method 2

$$U_{2.f} := \left(\frac{\sigma_{x.Ed.f}}{\frac{\rho_{x.f} \cdot f_y}{\gamma_{M1}}}\right)^2 + \left(\frac{\sigma_{z.Ed.f}}{\frac{\rho_{z.f} \cdot f_y}{\gamma_{M1}}}\right)^2 - \left(\frac{\sigma_{x.Ed.f}}{\frac{\rho_{x.f} \cdot f_y}{\gamma_{M1}}}\right) \cdot \left(\frac{\sigma_{z.Ed.f}}{\frac{\rho_{z.f} \cdot f_y}{\gamma_{M1}}}\right) + 3 \cdot \left(\frac{\tau_{Ed}}{\frac{\chi_{f.s} \cdot f_y}{\gamma_{M1}}}\right)^2 = 1.11$$

Final utalisation ratio

$U_{max.f} := \max\left(U_{x.f}, U_{\tau.f}, \min\left(U_{1.f}, U_{2.f}\right)\right) = 1.($

8. Verification of panel

E

Python script for parametrisation of panel

This Appendix contains one of the Python scripts that is used to obtain the buckling mode, this script creates a web with a stiffener and applies the appropriate loads. This is also done for an unstiffened web, an unstiffened flange and a stiffened flange in a similar way with small modifications to the script.

```
from part import *
from material import *
from section import *
from assembly import *
from step import *
from interaction import *
from load import *
from mesh import *
from optimization import *
from job import *
from sketch import *
from visualization import *
from connectorBehavior import *
import csv

myElements = ['Web']
data_saver = []
# Creating a variable to save the data from the buckling modes and the corresponding geometry
data_saver.append('\n')
data_saver.append(myElements[0])

# Bending stresses in top flange
MaxBendingStresses=[256.74,240.11,234.38,256.74,223.43,213.60,244.68,223.43,191.78,262.40,
222.13,177.28,304.28,281.60,258.19,304.28,246.56,212.56,278.89,247.23,194.45,266.24,227.20,
194.45,304.28,281.60,266.49,304.28,247.23,222.74,278.89,247.23,194.45,266.24,227.20,194.45]      #MPa

# Bending stresses in bottom flange
Bending_bot=[273.12,258.51,255.51,273.12,242.96,236.12,262.08,242.96,216.14,283.49,244.74,
199.80,323.69,303.17,281.47,323.69,268.12,234.97,298.73,268.85,219.16,287.65,250.32,219.16,
323.69,303.17,290.52,323.69,268.85,246.23,298.73,268.85,219.16,287.65,250.32,219.16,] #MPa

# Shear stresses
MaxShearStresses=[106.9,106.9,106.9,106.9,82.4,82.4,82.4,82.4,57.8,46.3,46.3,46.3,84.0,84.0,84.0,
84.0,65.3,65.3,65.0,65.0,45.6,45.6,45.6,45.6,83.9,83.9,83.9,82.8,64.2,64.2,64.2,64.2,45.1,45.1,45.1,45.1]       #MPa

# Distances between transverse stiffeners
width_vary = [1500, 3000, 4500, 6000]
thickness_vary = {'Web': [8,6,4],
                  'Flange': [14,10,7]}    #Thickness of web and flange

counter = -1                        # LOOP CONSTANT

# -------FOR LOOP: TO LOOP HEIGHT AND THICKNESS--------------------------------
for Width in width_vary:
    for Thickness in thickness_vary['Web']:
        for Flange_thickness in range(3):
            counter += 1
            # -------MODEL-----------------------------------------------------------
            myModel_name = 'Stiffened_web'
            myModel = mdb.Model(modelType=STANDARD_EXPLICIT,
                                name=myModel_name)      # Creating the model
            myAssemble = myModel.rootAssembly

            # -------INPUT-----------------------------------------------------------
            myIntegration = {'num': 5, 'rule': SIMPSON}  # GAUSS SIMPSON

            # -------MATERIAL--------------------------------------------------------
            myMaterial = {'Material': 'Steel', 'E': 210E3,
                          'v': 0.3, 'f_y': 420}         # E = 210E3 MPa  f_y=420 MPa
            material = myModel.Material(name=myMaterial['Material'])
            material.Elastic(table=((myMaterial['E'], myMaterial['v']), ))
            epsilon = (235/myMaterial['f_y']) ** 0.5

            # -------WEB AND FLANGE DIMENSIONS---------------------------------------
            myPart = {
                'Web': {'Name': 'Web', 'Width': Width, 'Height': 1500, 'Thickness': Thickness},
                'Flange': {'Name': 'Flange', 'Width': Width, 'Height': 1200, 'Thickness': Thickness},
```

```
    'Stiffener': {'Name': 'Stiffener', 'Width': Width, 'Height': 60+Thickness/2, 'Thickness': 10},
}
c_t = myPart['Web']['Height']/myPart['Web']['Thickness']

# CHECK CSC
if c_t <= 124*epsilon:
    continue

# Appending the current geometry
data_saver.append('\n')
data_saver.append(str(myPart['Web']['Width'])+'x'+str(
    myPart['Web']['Thickness'])+'x'+str(thickness_vary['Flange'][Flange_thickness]))

# -------GEOMETRY----------------------------------------------------
# WEB/FLANGE
Sketch = myModel.ConstrainedSketch(
    name='__profile__', sheetSize=10000.0)
Sketch.rectangle(point1=(0.0, 0.0),
                 point2=(myPart['Web']['Width'], myPart['Web']['Height']))
part = myModel.Part(dimensionality=THREE_D,
                    name=myPart['Web']['Name'], type=DEFORMABLE_BODY)
part.BaseShell(sketch=myModel.sketches['__profile__'])
del myModel.sketches['__profile__']

# STIFFENER
myModel.ConstrainedSketch(name='__profile__', sheetSize=10000.0)
myModel.sketches['__profile__'].rectangle(point1=(0.0, 0.0),
                                          point2=(myPart['Stiffener']['Width'], myPart['Stiffener']['Height']))
myModel.Part(dimensionality=THREE_D,
             name=myPart['Stiffener']['Name'], type=DEFORMABLE_BODY)
myModel.Part(myPart['Stiffener']['Name']).BaseShell(
    sketch=myModel.sketches['__profile__'])
del myModel.sketches['__profile__']

# -------SECTION-----------------------------------------------------
section = myModel.HomogeneousShellSection(idealization=NO_IDEALIZATION,
                                          integrationRule=myIntegration['rule'], material=myMaterial['Material'],
                                          name=myPart['Web']['Name'], nodalThicknessField='', numIntPts=myIntegration['num'],
                                          poissonDefinition=DEFAULT, preIntegrate=OFF, temperature=GRADIENT,
                                          thickness=myPart['Web']['Thickness'], thicknessField='', thicknessModulus=None,
                                          thicknessType=UNIFORM, useDensity=OFF)

myAssemble.DatumCsysByDefault(CARTESIAN)
myAssemble.Instance(
    dependent=ON, name=myPart['Web']['Name'], part=myModel.parts['Web'])

# -------SECTION-----------------------------------------------------
# Placing the web stiffener at 80% of the height
myAssemble.Instance(dependent=ON, name='Stiffener-1',
                    part=myModel.parts[myPart['Stiffener']['Name']])
myAssemble.Instance(dependent=ON, name='Web-1',
                    part=myModel.parts[myPart['Web']['Name']])
myAssemble.rotate(angle=90.0, axisDirection=(-10.0,
0.0, 0.0), axisPoint=(Width, myPart['Stiffener']['Height'], 0.0), instanceList=('Stiffener-1', ))
myAssemble.translate(instanceList=('Stiffener-1', ), vector=(
    0.0, myPart['Web']['Height']*0.8-myPart['Stiffener']['Height'], 0.0))

myAssemble.InstanceFromBooleanMerge(domain=GEOMETRY, instances=(
    myAssemble.instances[myPart['Web']['Name']],
myAssemble.instances['Stiffener-1'],
myAssemble.instances['Web-1']), name='Web_with_stiffener',
originalInstances=SUPPRESS)

myModel.parts['Web_with_stiffener'].SectionAssignment(offset=0.0, offsetField='',
offsetType=MIDDLE_SURFACE, region=Region(
    faces=myModel.parts['Web_with_stiffener'].faces.getSequenceFromMask(
        mask=('[#7 ]', ), )), sectionName='Web', thicknessAssignment=FROM_SECTION)
```

```
# -------STEP----------------------------------------------------------
Stepname = {'i': 'Initial', 'b': 'Buckling',
          's': 'Static', 'NumEig': 15, 'MaxIter': 250}
myModel.StaticStep(name=Stepname['s'], previous=Stepname['i'])

myModel.BuckleStep(maxIterations=int(Stepname['MaxIter']), name=Stepname['b'],
                numEigen=int(Stepname['NumEig']), previous=Stepname['s'], vectors=18)
myModel.steps[Stepname['b']].setValues(blockSize=DEFAULT,
                                eigensolver=LANCZOS, maxBlocks=DEFAULT, minEigen=0.0)

# -------BOUNDARY CONDITIONS-------------------------------------------
BCset = {'free': UNSET, 'fixed': SET}

# Fixed in x direction
myModel.DisplacementBC(amplitude=UNSET, createStepName=Stepname['i'],
distributionType=UNIFORM, fieldName='', localCsys=None, name='left edge',
                region=Region(edges=myAssemble.instances[
                   'Web_with_stiffener-1'].edges.getSequenceFromMask(mask=('[#210 ]', ), )),
                u1=BCset['fixed'], u2=BCset['free'], u3=BCset['free'],
                ur1=BCset['free'], ur2=BCset['free'], ur3=BCset['free'])

# Fixed in y direction
myModel.DisplacementBC(amplitude=UNSET, createStepName=Stepname['i'],
distributionType=UNIFORM, fieldName='', localCsys=None, name='Origo point',
                region=Region(vertices=myAssemble.instances[
                   'Web_with_stiffener-1'].vertices.getSequenceFromMask(mask=('[#10 ]', ), )),
                u1=BCset['free'], u2=BCset['fixed'], u3=BCset['free'],
                ur1=BCset['free'], ur2=BCset['free'], ur3=BCset['free'])

# Fixed in z direction
myModel.DisplacementBC(amplitude=UNSET, createStepName=Stepname['i'],
distributionType=UNIFORM, fieldName='', localCsys=None,
   name='Out of plane restraint',region=Region(
      edges=myAssemble.instances['Web_with_stiffener-1'].edges.getSequenceFromMask(mask=(
      '[#3f0 ]', ), )), u1=BCset['free'], u2=BCset['free'], u3=BCset['fixed'],
       ur1=BCset['free'], ur2=BCset['free'], ur3=BCset['free'])

# -------MESH----------------------------------------------------------
Sizes = 45  # Mesh size chosen to 45 after convergance study

myAssemble.makeIndependent(instances=(
   myAssemble.instances['Web_with_stiffener-1'], ))
myAssemble.seedEdgeBySize(
   deviationFactor=0.1, edges=myAssemble.instances['Web_with_stiffener-1'].edges.getSequenceFromMask(
      ('[#3ff ]', ), ), size=Sizes)
myAssemble.setMeshControls(
   elemShape=QUAD, regions=myAssemble.instances['Web_with_stiffener-1'].faces.getSequenceFromMask(
      ('[#7 ]', ), ))
myAssemble.setElementType(elemTypes=(ElemType(elemCode=S4R, elemLibrary=STANDARD,
secondOrderAccuracy=OFF,
hourglassControl=DEFAULT),ElemType(elemCode=S3, elemLibrary=STANDARD)),
regions=(myAssemble.instances['Web_with_stiffener-1'].faces.getSequenceFromMask(
   ('[#7 ]', ), ), ))
myAssemble.generateMesh(
   regions=(myAssemble.instances['Web_with_stiffener-1'], ))

myAssemble.setElementType(elemTypes=(ElemType(
   elemCode=S8R, elemLibrary=STANDARD), ElemType(elemCode=STRI65,
                                    elemLibrary=STANDARD)), regions=(
   myAssemble.instances['Web_with_stiffener-1'].faces.getSequenceFromMask(
      ('[#7 ]', ), ), ))

# Different force variations, 80%/80%, 100%/0%, 0%/100%
bending_type = [0.8, 1, 0]
shear_type = [0.8, 0, 1]
for situation in range(2):
```

```
Force = {'M': MaxBendingStresses[counter]*myPart['Web']['Thickness']*bending_type[situation],
        'V': MaxShearStresses[counter]*myPart['Web']['Thickness']*shear_type[situation]}  # N/m

# If shear force is present, creating load for both static step and buckling step
if Force['V'] > 0:
    myModel.ShellEdgeLoad(createStepName=Stepname['b'], directionVector=((0.0, 0.0, 0.0), (1.0, 0.0, 0.0)),
    distributionType=UNIFORM, field='', localCsys=None, magnitude=-Force['V'], name='Shear_top_edge',
                        region=Region(
        side1Edges=myAssemble.instances['Web_with_stiffener-1'].edges.getSequenceFromMask(
            mask=('[#100 ]', ), )), traction=GENERAL)

    myModel.ShellEdgeLoad(createStepName=Stepname['b'], directionVector=((0.0, 0.0, 0.0), (1.0, 0.0, 0.0)),
    distributionType=UNIFORM, field='', localCsys=None, magnitude=Force['V'], name='Shear_bot_edge',
                        region=Region(
        side1Edges=myAssemble.instances['Web_with_stiffener-1'].edges.getSequenceFromMask(
            mask=('[#20 ]', ), )), traction=GENERAL)

    myModel.ShellEdgeLoad(createStepName=Stepname['b'], directionVector=((0.0, 0.0, 0.0), (0.0, 1.0, 0.0)),
    distributionType=UNIFORM, field='', localCsys=None, magnitude=Force['V'], name='Shear_left_edge',
                        region=Region(
        side1Edges=myAssemble.instances['Web_with_stiffener-1'].edges.getSequenceFromMask(
            mask=('[#210 ]', ), )), traction=GENERAL)

    myModel.ShellEdgeLoad(createStepName=Stepname['b'], directionVector=((0.0, 0.0, 0.0), (0.0, 1.0, 0.0)),
    distributionType=UNIFORM, field='', localCsys=None, magnitude=-Force['V'], name='Shear_right_edge',
                        region=Region(
        side1Edges=myAssemble.instances['Web_with_stiffener-1'].edges.getSequenceFromMask(
            mask=('[#c0 ]', ), )), traction=GENERAL)

    # STATIC
    myModel.ShellEdgeLoad(createStepName=Stepname['s'], directionVector=((0.0, 0.0, 0.0), (1.0, 0.0, 0.0)),
    distributionType=UNIFORM, field='', localCsys=None, magnitude=-Force['V'], name='Static_Shear_top_edge',
                        region=Region(
        side1Edges=myAssemble.instances['Web_with_stiffener-1'].edges.getSequenceFromMask(
            mask=('[#100 ]', ), )), traction=GENERAL)

    myModel.ShellEdgeLoad(createStepName=Stepname['s'], directionVector=((0.0, 0.0, 0.0), (1.0, 0.0, 0.0)),
    distributionType=UNIFORM, field='', localCsys=None, magnitude=Force['V'], name='Static_Shear_bot_edge',
                        region=Region(
        side1Edges=myAssemble.instances['Web_with_stiffener-1'].edges.getSequenceFromMask(
            mask=('[#20 ]', ), )), traction=GENERAL)

    myModel.ShellEdgeLoad(createStepName=Stepname['s'], directionVector=((0.0, 0.0, 0.0), (0.0, 1.0, 0.0)),
    distributionType=UNIFORM, field='', localCsys=None, magnitude=Force['V'], name='Static_Shear_left_edge',
                        region=Region(
        side1Edges=myAssemble.instances['Web_with_stiffener-1'].edges.getSequenceFromMask(
            mask=('[#210 ]', ), )), traction=GENERAL)

    myModel.ShellEdgeLoad(createStepName=Stepname['s'], directionVector=((0.0, 0.0, 0.0), (0.0, 1.0, 0.0)),
    distributionType=UNIFORM, field='', localCsys=None, magnitude=-Force['V'], name='Static_Shear_right_edge',
                        region=Region(
        side1Edges=myAssemble.instances['Web_with_stiffener-1'].edges.getSequenceFromMask(
            mask=('[#c0 ]', ), )), traction=GENERAL)
else:
    mdb.models['Stiffened_web'].loads.delete(('Shear_bot_edge',
                                    'Shear_left_edge', 'Shear_right_edge', 'Shear_top_edge',
                                    'Static_Shear_bot_edge', 'Static_Shear_left_edge',
                                    'Static_Shear_right_edge', 'Static_Shear_top_edge'))

# If moment is present, creating load for both static step and buckling step
if Force['M'] > 0:
    Forcename = {'M': 'Moment', 'V': 'Shear'}
    AppliedStress = {
        'sigma_top': -1, 'sigma_bot': Bending_bot[counter]/MaxBendingStresses[counter]}

    # Uniform compression
    if AppliedStress['sigma_top'] == AppliedStress['sigma_bot']:
```

```
        myModel.ShellEdgeLoad(createStepName=Stepname['b'], distributionType=UNIFORM, field='',
            localCsys=None,magnitude=Force['M'], name=Forcename['M'], region=Region(
            side1Edges=myAssemble.instances['Web_with_stiffener-1'].edges.getSequenceFromMask(
                mask=('[#c0 ]', ), )))

        myModel.ShellEdgeLoad(createStepName=Stepname['b'], distributionType=UNIFORM, field='',
            localCsys=None,magnitude=-MaxBendingStresses[counter]*myPart['Stiffener']['Thickness']*(1200-m)/k,
            name='stiffener_moment', region=Region(
            side1Edges=myAssemble.instances['Web_with_stiffener-1'].edges.getSequenceFromMask(
                mask=('[#2 ]', ), )))
        # static
        myModel.ShellEdgeLoad(createStepName=Stepname['s'], distributionType=UNIFORM, field='',
            localCsys=None,magnitude=Force['M'], name='static_moment', region=Region(
            side1Edges=myAssemble.instances['Web_with_stiffener-1'].edges.getSequenceFromMask(
                mask=('[#c0 ]', ), )))

        myModel.ShellEdgeLoad(createStepName=Stepname['s'], distributionType=UNIFORM, field='',
            localCsys=None,magnitude=Force['M'], name='static_moment_stiffener', region=Region(
            side1Edges=myAssemble.instances['Web_with_stiffener-1'].edges.getSequenceFromMask(
                mask=('[#2 ]', ), )))

    # Linearly varying moment
    else:
        k = (myPart['Web']['Height']-0) / \
            (AppliedStress['sigma_top'] -
             AppliedStress['sigma_bot'])
        m = -k*AppliedStress['sigma_top'] + \
            myPart['Web']['Height']
        myModel.ExpressionField(description='',
                        expression='(Y-m)/k', localCsys=None, name='Line Load')
        myModel.ShellEdgeLoad(createStepName=Stepname['b'], distributionType=FIELD, field='Line Load',
        localCsys=None, magnitude=-Force['M'], name=Forcename['M'], region=Region(
            side1Edges=myAssemble.instances['Web_with_stiffener-1'].edges.getSequenceFromMask(
                mask=('[#c0 ]', ), )))

        myModel.ShellEdgeLoad(createStepName=Stepname['b'], distributionType=UNIFORM, field='',
            localCsys=None,magnitude=-MaxBendingStresses[counter]*myPart['Stiffener']['Thickness']*(1200-m)/k,
             name='stiffener_moment', region=Region(
            side1Edges=myAssemble.instances['Web_with_stiffener-1'].edges.getSequenceFromMask(
                mask=('[#2 ]', ), )))

        # STATIC
        myModel.ShellEdgeLoad(createStepName=Stepname['s'], distributionType=FIELD, field='Line Load',
        localCsys=None, magnitude=-Force['M'], name='Static_Moment', region=Region(
            side1Edges=myAssemble.instances['Web_with_stiffener-1'].edges.getSequenceFromMask(
                mask=('[#c0 ]', ), )))

        myModel.ShellEdgeLoad(createStepName=Stepname['s'], distributionType=UNIFORM, field='',
            localCsys=None,magnitude=Force['M'], name='static_moment_stiffener', region=Region(
            side1Edges=myAssemble.instances['Web_with_stiffener-1'].edges.getSequenceFromMask(
                mask=('[#2 ]', ), )))


else:
    mdb.models['Stiffened_web'].loads.delete(
        ('Moment', 'stiffener_moment', 'Static_Moment', 'static_moment_stiffener'))

# -------JOB------------------------------------------------------------
myJob = mdb.Job(atTime=None, contactPrint=OFF, description='', echoPrint=OFF,
                explicitPrecision=SINGLE, getMemoryFromAnalysis=True, historyPrint=OFF,
                memory=90, memoryUnits=PERCENTAGE, model=myModel_name, modelPrint=OFF,
                multiprocessingMode=DEFAULT, name='Buckling_w_s', nodalOutputPrecision=SINGLE,
                numCpus=1, numGPUs=0, queue=None, resultsFormat=ODB, scratch='',
                type=ANALYSIS, userSubroutine='', waitHours=0, waitMinutes=0)

myModel.steps['Static'].suppress()
myJob.submit()
```

```
        # WAIT FOR COMPLETETION OF JOB
        try:
            myJob.waitForCompletion(6000)
        except AbaqusException, message:
            print "Job timed out", message

        # Obtaining the current buckling mode from odb file
        odb = openOdb(path='Z:\Master_thesis\Abaqus\Buckling_w_s.odb')
        odb.steps[Stepname['b']].frames[1].mode
        EV = odb.steps[Stepname['b']].frames[1].description
        data_saver.append(str(EV[29:]))
        odb.close()


# Enters all geometries and corresponding buckling modes to Excel
with open('Web_stiffened_buckling_combined.csv', 'w') as f1:
    wtr = csv.writer(f1, delimiter=',', quotechar=',',
        quoting=csv.QUOTE_MINIMAL, lineterminator='\n')
    wtr.writerow(data_saver)
```

DEPARTMENT OF ARCHITECTURE AND CIVIL ENGINEERING
CHALMERS UNIVERSITY OF TECHNOLOGY
Gothenburg, Sweden
www.chalmers.se

CHALMERS
UNIVERSITY OF TECHNOLOGY